BRNO UNIVERSITY OF TECHNOLOGY

VYSOKÉ UČENÍ TECHNICKÉ V BRNĚ

FACULTY OF MECHANICAL ENGINEERING

FAKULTA STROJNÍHO INŽENÝRSTVÍ

ENERGY INSTITUTE

ENERGETICKÝ ÚSTAV

DETERMINATION OF CLOTHING EVAPORATIVE RESISTANCE FOR -THERMO-PHYSIOLOGY MODELLING USING A THERMAL MANNEQUIN

ZJIŠŤOVÁNÍ VÝPARNÉHO ODPORU ODĚVU S VYUŽITÍM MANEKÝNA PRO VYUŽITÍ V SIMULAČNÍCH MODELECH TERMO-FYZIOLOGIE

DOCTORAL THESIS

DIZERTAČNÍ PRÁCE

AUTHOR — Ing. Róbert Toma

AUTOR PRÁCE

SUPERVISOR — prof. Ing. Miroslav Jícha, CSc.

ŠKOLITEL

BRNO 2023

ABSTRACT

Global warming and environmental changes are currently one of the main topics discussed around the world. As we could start to see the signs of climate changes, more attention needs to be placed on the protection of humans health, as the changing climate could have impact also in places, were it was not the case in the past. Many professions, especially the ones using some kind of protective clothing, could be in danger from heat stress. It is known that sweat evaporation is the main thermoregulatory feature for a heat dissipation from the human body to the environment and these protective clothing, with combination with higher metabolic rates during the work, could be potentially dangerous. These are the reason why heat stress prediction models and thermo-physiological models are being enhanced and used widely. One of the most problematic input data for these models are clothing properties - thermal insulation, clothing area factor and evaporative resistance, whose inaccuracy could have huge impact on the resultant physiological prediction. Although thermal insulation measurements on thermal manikins are well tested, precise and reliable, this cannot be said about measurement of evaporative resistance using manikins, including manikin NEWTON at Brno University of Technology.

Thus, the aim of this study was the development of the measurement procedure and calculation methods to determine clothing evaporative resistance using thermal manikin NEWTON at BUT. Measurement setup and methodology was successfully validated using dataset measured on manikin TORE at Lund University, with the results laying within 4 % of the mean values in all but two cases. The results shows that with strict measurement methodology, it is possible to achieve good reproducibility of the measurement, which was not the case in previous studies. Furthermore, the results shows that repeatability of the measurement is also within 4 % on both manikins, as same repeatability precision is set in the standards for thermal insulation measurements. Lastly, the mass loss method is essentially correct and closer to the physical nature of heat transfer by sweating, but with the current technical limitations, it is very challenging to obtain local evaporative resistance values from this method. Thus, heat loss method must be used to obtain these local values. Multiple corrections for the calculation of evaporative resistance values from the heat loss method were tested and verified. This could be of interest to engineers and researchers in the field of thermo-physiological modeling, as local values of clothing properties are essential to obtain precise physiological predictions. Finally, the possibility to obtain evaporative resistance values at BUT could potentially bring new opportunities for projects and cooperations.

Key words

Thermal insulation, clothing area factor, evaporative resistance, thermal manikin, thermo-physiological modeling, protective clothing,

ABSTRAKT

Globálne otepľovanie a klimatické zmeny sú aktuálne jednou z najdiskutovanejších tém na svete. Keďže začíname vidieť jasné známky klimatických zmien, je nutné sa čoraz viac zaoberať ochranou ľudského zdravia pred tepelnou záťažou aj na miestach sveta, kde táto téma nebola v minulosti aktuálna. Pracovníci vo viacerých profesiách, hlavne v tých ktoré využívajú špeciálne ochranné odevy, môžu byť potencionálne ohrozený vplyvom tepla. Je známe že vyparovanie potu z tela je hlavným termoregulačným prvkom ľudského tela a práve použitie takýchto ochranných odevov, obmedzujúcich toto vyparovanie, v kombinácií s vysokou aktivitou môže byť zdraviu nebezpečné. Z týchto dôvodov sa do popredia dostávajú termofyziologické modeli alebo predikčné modeli tepelnej záťaže, ktoré sú neustále vylepšované a aplikované v rôznych situáciách. Jednými z najproblematickejších vstupných dát takýchto modelov patria vlastnosti odevu – tepelná izolácia, faktor oblasti prekrytia oblečením a odpor odevu proti vyparovaniu, ktorých nepresné hodnoty môžu spôsobiť veľké nepresnosti vo finálny predikciách týchto modelov. Napriek tomu že meranie tepelnej izolácie odevu pomocou tepelných manekýnov je už zavedené, spoľahlivé a presné, to isté nie je možné povedať o meraní odporu odevu proti vyparovaniu, ktoré je stále vo svojich začiatkoch.

Cieľom tejto práce bolo vyvinúť a implementovať experimentálne zariadenie, procedúru merania a spôsob kalkulácie pre získanie odporu odevu proti vyparovaniu pomocou manekýna NEWTON-a na VUT v Brne. Výsledky merania boli validované na základe dát nameraných pomocou manekýna TORE na Univerzite v Lunde. Reprodukovateľnosť merania bola na úrovni do 4 % rozdielu od strednej hodnoty takmer vo všetkých prípadoch. Výsledky ukazujú že je možné dosiahnuť dobrej reprodukovateľnosti merania pri striktnom dodržaní metodológie merania. Výsledky taktiež ukázali dobru opakovateľnosť merania, kedy bol dosiahnutý výsledok opäť na úrovni 4 % na oboch manekýnoch, čo je zároveň aj požadovaná hranica určená v normách pre meranie tepelnej izolácie odevu. Ďalším bodom práce bola verifikácia samotnej kalkulácie výparného odporu. Aj keď mass loss metóda určuje priamo intenzitu prenosu hmoty vyparovaním a najbližšie opisuje samotný jav vyparovania potu z ľudského tela, nie je vhodná pre určenie lokálnych hodnôt odporu proti vyparovaniu odevov z dôvodu technických limitácií senzorov a tepelných manekýnov. Z tohto dôvodu je použitá heat loss metóda, ktorej výpočet však musí byť korigovaný. Súčasťou práce bolo testovanie a verifikácia viacerých korekcií tejto metódy, čo môže byť prínosom výskumných pracovníkov z oblasti termofyziológie, keďže tieto lokálne hodnoty vlastností odevov sú pre dosiahnutie presných predikcii priam nevyhnutné. Úspešná implementácia a validácia možnosti merania odporu odevu proti vyparovaniu na VUT v Brne pomocou tepelného manekýna prináša taktiež nové možnosti pre ďalšie projekty a kooperácie v rámci výskumnej ci komerčnej činnosti Univerzity.

Kľúčové slová

Tepelná izolácia odevu, faktor oblasti prekrytej oblečením, odpor odevu proti vyparovaniu, tepelný manekýn, modelovanie termofyziológie, ochranné odevy,

BIBLIOGRAPHIC CITATION

TOMA, Róbert. Determination of Clothing Evaporative Resistance for Thermo-Physiology Modelling using a Thermal Mannequin. Brno, 2023. Dizertační práce. Vysoké učení technické v Brně, Fakulta strojního inženýrství, Energetický ústav. Vedoucí práce Miroslav Jícha.

AFFIRMATION

I hereby declare that I have written the PhD thesis on my own according to advice of my supervisor prof. Ing. Miroslav Jícha, CSc. and supervisor specialist doc. Ing. Bc. Jan Fišer, Ph.D. and all the literary sources are quoted correctly and completely.

Date

Ing. Róbert Toma

ACKNOWLEDGMENTS

I would like to express my gratitude to all the people, who helped me and made it possible to finish this PhD thesis. Firstly, I would like to express my gratitude to prof. Ing. Miroslav Jicha CSc. and doc. Ing. Bc. Jan Fišer, Ph.D. for guidance and knowledge. Secondly, I would like to thank Assoc. Prof. Kalev Kuklane, Ph.D. for the opportunity to join his team for 6 months at Lund University and for all the knowledge and experience. I would also like to thank to all of my colleagues, both at BUT and Lund University, for their cooperation and support.

I am thankful for the financial support of Brno University of Technology and Lund University that made my scientific work possible. I would like to thank Ayming Slovensko for making it possible to finish my thesis.

Finally, I would like to express my deepest gratitude to my wife and daughter, parents, grandparents, and my brother and whole family for their love and invaluable support throughout my life.

Content

1 INTRODUCTION 13
2 EVAPORATIVE RESISTANCE 15
2.1 Determination of evaporative resistance 15
2.2 Sweating simulation on thermal manikins 16
2.2.1 Construction of water-filled sweating system 16
2.2.2 Construction of sweating system with water supply to the skin 17
2.2.3 Construction of pre-wetted sweating system 18
2.3 Measurement and calculation of total evaporative resistance 19
2.3.1 Calculation methods 20
2.3.2 Mass loss method 20
2.3.3 Heat loss method 21
2.3.4 Comparison of these methods 21
2.4 Different factors influencing Ret measurements and calculations 23
2.4.1 Effect of temperature difference 23
2.4.2 Effect of moisture content on apparent ´wet´ thermal insulation 26
2.4.3 Effect of clothing fit and size 27
2.4.4 Fabric thickness and material effect on apparent ´wet´ thermal resistance. 27
2.5 Proposed approach for Ret measurements 29
3 SUMMARY OF KNOWLEDGE GAP 33
4 AIM AND OBJECTIVES 35
4.1 Aim of the thesis 35
4.2 Scientific questions and original hypotheses 35
4.2.1 How do clothing properties affect the accuracy of thermo-physiological models? 35
4.2.2 Is it necessary to measure clothing properties? 35
4.2.3 Are the results of evaporative resistance measurements repeatable and reproducible? 35
4.2.4 Is it needed to use all proposed correction from the literature for evaporative resistance calculation? 35
4.3 Objectives 36
4.4 Structure of the thesis 36
4.5 The author's contribution to the papers 37
4.6 Other publications of the author related to the topic of the thesis 37
4.7 Other publications of the author 38
5 SUMMARY OF THE CONDUCTED WORK 39
5.1 Paper I (Objectives I and III): Verification of Fiala-based human thermo-physiological model and its application to protective clothing under high metabolic rates 39
5.1.1 Summary of main findings 39
5.2 Paper II (Objectives II, III and IV) Local clothing properties for thermo-physiological modelling: Comparison of methods and body positions 41
5.2.1 Summary of main findings 42

5.3 Paper III (Objectives V, VI and VII): Determination of evaporative resistance and thermal insulation by means of thermal manikin – comparison of methods 43
5.3.1 Methods used to obtain clothing properties 43
5.3.2 Testing scenarios 44
5.3.3 Data analysis and sensitivity study 44
5.3.4 Summary of the main findings 45
5.4 Paper IV (Objectives I and IV): Insulation and evaporative resistance values of clothing for sugarcane harvesters and chemical sprayers in Latin America, and their application in PHS model-based exposure predictions 47
5.4.1 Summary of main findings 47
5.5 Paper V (Objectives V, VI and VII): Reproducibility of evaporative resistance measurements and calculations using different thermal manikins (to be published) 50
5.5.1 Clothing ensembles 50
5.5.2 Measurement setup and equipment 51
5.5.3 Methods and Results 52
5.5.4 Summary of main findings 54
6 CONCLUSIONS 55
6.1 Future research 56
6.2 Limitations 56
7 REFERENCES 59
8 LIST OF FIGURES AND TABLES 63
9 LIST OF SYMBOLS 65
10 APPENDICES 67
10.1 Paper I 68
10.2 Paper II 82
10.3 Paper III 95
10.4 Paper IV 118

1 INTRODUCTION

As it is important to protect humans´ health, thermo-physiological modeling is often used to calculate maximum exposure time for which could humans stay in given environment without their endangerment. Many workers are exposed to heat stress that can be exacerbated by the type of clothing they wear. The resulted heat strain can lead to short or long-term heat-related disorders. Nowadays, more importance is given to this area of research as global warming and environmental changes are one of the most discussed issues around the world (Kjellstrom et al. 2009; Błażejczyk et al. 2010; Angelova 2017).

It is known that evaporation is the main thermoregulatory feature for a heat dissipation from the human body to the environment. Hot working environment is typical for physically demanding jobs (e.g. soldiers, firefighters, builders, miners) for which more and more protective clothing and equipment is used to protect the workers from the primary risks (e.g. protection from flames for firefighters). Consequently, wearing of these less permeable protective clothing could often result in reduction of sweat evaporation from human skin leading to an elevated skin temperature, core temperature or sweat rate (Holmer 2006; Wang et al. 2011b). This phenomenon could be also seen on protective clothing usage in cold environments with high metabolic activity (e.g. mountain rescuers, fishers, athletes) as the conductivity is low through the insulated clothing and evaporation is limited by less permeable layers. Those are the reasons why the heat stress prediction models (e.g. PHS (ISO 7933 2004)) and thermo-physiological predictive models (Fiala et al. 1999; Havenith et al. 2012) also contain clothing properties as ones of the most important input data, namely the thermal insulation (I_t), clothing area factor (f_{cl}) and the evaporative resistance (R_{et}).

Therefore, the clothing parameters should be obtained with highest precision and accuracy possible (Wang et al. 2011b; Ueno and Sawada 2012) to mitigate some errors in these predictions. Thermal manikins are the most realistic available option for measuring clothing parameters at the moment. Although thermal insulation measurements on non-sweating manikins are well tested, precise and reliable, this cannot be said about measurement of evaporative resistance on sweating thermal manikins where significant discrepancies between results from different laboratories were found (Fan and Chen 2002; Richards and McCullough 2005; Wang et al. 2014; Wang 2017). Effects on evaporative resistance measurement protocols and calculations have been thoroughly investigated in recent years.

The aim of this thesis is to identify and apply a reliable method and procedure for measurement of evaporative resistance using manikin NEWTON in laboratory conditions at Brno University of Technology. Secondly, the repeatability of the measurements is investigated and accuracy of the methodology conducted at BUT is verified with data measured at Lund University on manikin TORE using the same measurement procedures, as the measurement of evaporative resistance is already well established there. Lastly, the study contains analysis of formulas and already proposed corrections for evaporative resistance calculation for heat loss method (Wang et al. 2015; Wang 2017), which will be accommodated and verified for multiple clothing ensembles covering the whole range of thermal insulation scale from *0.5* to *3.2 clo*. This study will widen the range of applications of manikin NEWTON at BUT opening the possibilities for new projects and will also enhanced the knowledge about clothing properties needed for thermo-physiological modeling.

2 EVAPORATIVE RESISTANCE

Total thermal resistance (I_t) is the value of thermal insulation from the body surface to the environment (including all clothing, enclosed air layers and boundary air layer) under reference conditions in static state (ISO 9920 2007). It´s measurements by the means of a thermal manikin are well documented and are showing high accuracy and repeatability (Wang et al. 2017). For example, in the corresponding ISO standard (ISO 15831 2004) the difference between two independent measurements should not exceed *4 %*. Similarly, in the ASTM standard (ASTM F1291-16 2016) results of three replications should not vary by more than *10 %* from the mean value.

On the other hand, total evaporative resistance (R_{et}), which determines the amount of water vapor evaporation from a human body to an environment (including all clothing, enclosed air layers and boundary air layers) under reference condition in static state (ISO 9920 2007), is not well documented. Results from the previous interlaboratory studies on measurement of evaporative resistance (Richards et al. 2008; Mayor et al. 2012; Młynarczyk et al. 2018) shows that huge discrepancies of more than *50 %* were found between different institutions, mainly caused by sweating simulation systems, calculation methods of evaporative resistance (R_{et}), different test conditions etc. (Wang 2017). Although new ASTM standard (ASTM F1291-16 2016) is widely spread and used by many laboratories around the world, it does not define detailed requirements for the total evaporative resistance (R_{et}) measurements (Wang 2017). Thus, various changes in test protocols, types of sweating simulations and other effects, which might affect the value of evaporative resistance, has being investigated recently. In most comprehensive round robin study found (Wang et al. 2014), the difference from mean values where, in most of the cases, around *4 %*, but in some extremes cases, the difference from mean values were more than *10 %* (up to *30 %* in one case).

2.1 Determination of evaporative resistance

In praxis, three methods to determine evaporative resistance of clothing are used: sweating guarded hot plates, sweating thermal manikins or measurements on human subjects. Studies show (Ross 2005) that evaporative resistance values from a sweating thermal manikin for heat stress simulations are more realistic than those from sweating guarded hot plates. Sweating thermal manikins are in shape of a human body and it can be distinguish between different body parts. It is also possible to capture the effect of boundary air layers around the garment which cannot be done on the guarded hot plates as the air is pressed out by the hot plates. The last method - human subject measurements are costly, time consuming and it may raise an ethical concern (Caravello et al. 2008). Because of this, (Wang et al. 2011b) described sweating thermal manikins as a perfect intermediate tool between guarded hot plates and human subject testing. Recently, new interesting method using Permetest skin model is being studied and validated and it might bring good correlation with manikin testing (Fung et al. 2020).

Figure 1: Sweating guarded hot plates SGHP-8.2 and Sweating thermal manikin Newton from Thermetrics, Advanced Thermal Measurement Technology, Seattle, USA; test person from Santra Technology, UK website.

2.2 Sweating simulation on thermal manikins

In the previous chapter, it was decided that sweating thermal manikins are the best option for evaporative resistance measurement regarding the precision, accuracy, and the ability to imitate human body in real conditions. There are many types and options of these manikins available around the world, for instance: (Holmer 2004; Koelblen et al. 2017).

Manikins with water-filled body and skin from permeable waterproof material

- Water-filled manikin with a waterproof but vapor-permeable surface, e.g. "Walter" manikin from Hong Kong Polytechnic University, Hong Kong (Chen et al. 2003).
- Manikin with an inner skin spreading water superficially and an outer vapor-permeable skin, e.g. "Coppelius" (Varheenmaa 2014).

Manikins with water supply to tight-fitting fabric skin

- Manikin with a water supply to a fabric skin by means of sweating outlets on manikin´s surface, e.g. "SAM" manikin (Empa, Switzerland).
- "Newton" manikin (Thermetrics, Seattle, USA).
- "Adam" manikin (Thermetrics, Seattle, USA).

Manikins with pre-wetted tight-fitting fabric skin

- Pre-wetted tight fabric skin on a worn on a dry thermal manikin, e.g. "Tore" manikin from Lund University, Sweden (Wang et al. 2010).

2.2.1 Construction of water-filled sweating system

Body is suspended by a water pipe system projecting from the head, which also supplies manikin body with water. Manikin´s core temperature is controlled at *37 °C*. The weight of the filled body is around *100 kg*. Skin is made from special GORE-TEX material used for marine application, which is waterproof but permeable, thus the water is being held inside but vapor is

flowing through the material to the environment (Fan and Chen 2002). Although, this system has advantage in measuring evaporative resistance from mass loss rate, it has few major setbacks (Wang 2017):

- Manikin has only one segment, thus local values cannot be computed.
- Only insensible sweating can be simulated – no liquid is absorbed by clothing.
- Too low perspiration rate compared to water supply manikins.

Figure 2: Sweating manikin "Walter" from Hong Kong Polytechnic University with GORE-TEX skin, taken from (Fan and Chen 2002)

2.2.2 Construction of sweating system with water supply to the skin

The manikin is constructed using hard carbon-epoxy shell with embedded resistance wire heating and sensor wire elements. Software is used for controlling manikin´s surface temperature for different zones separately. Water is supply to the skin through the glands in the hard-shell body. It is also possible to control sweating rate by the software (Thermetrics, Seattle, USA). The evaporative resistance could be calculated both from sweat rate and heat loss of the manikin. Although, this type of manikin is the state-of-the-art equipment for clothing and environmental testing, it has some imperfections:

- Costly equipment.
- It is difficult to set a proper sweat rate to keep the skin wet but to prevent water dripping from it.
- Impossible to control manikin´s skin temperature to calculate evaporative resistance precisely.

Figure 3: Sweating ´Newton´ type manikin with water supply through pores made by Thermetrics, Seattle, USA

2.2.3 Construction of pre-wetted sweating system

The concept was originally proposed by Goldman (R. F. Goldman 2006) and is still in use with some modifications. Human body shaped dry manikin with hard-shell body is dressed in tight fitted knitted textile skin (Wang et al. 2011a; Ueno and Sawada 2012; Koelblen et al. 2017). This textile is pre-wetted by tap water in washing machine for about *5 min* and then centrifuged for about *5 s* to ensure no water dripping. Manikin´s surface is control at *34 °C* to simulate the average temperature of human skin. Whole manikin system could be placed on a weighing scale with high accuracy which enables mass loss rate measurement. This system got also some imperfections as did the previous systems:

- Costly equipment but much cheaper than the sweating manikin.
- impossible to control manikin´s skin temperature to calculate evaporative resistance precisely.
- pre-wetted skin tends to dry out after around *40-60 min* of testing.

Figure 4: Sweating manikin “Tore” from Lund University with pre-wetted skin on.

2.3 Measurement and calculation of total evaporative resistance

In general, there are three different conditions possible to measure evaporative resistance.

- Non-isothermal conditions *($T_a \neq T_r \neq T_{sk}$)*
- Isothermal conditions *($T_a = T_r = T_{sk}$)*
- So-called isothermal conditions *($T_a = T_r = T_{manikin}$)*

T_{sk}	*manikin´s skin temperature*	*[°C]*
T_a	*ambient temperature of the environment*	*[°C]*
T_r	*radiant temperature in environment*	*[°C]*
$T_{manikin}$	*manikin´s surface temperature*	*[°C]*

It was found that measurement of the evaporative resistance in non-isothermal conditions causes significant error. As clothing materials absorb moisture, their dry thermal insulation changes accordingly (Chen et al. 2003; ISO 9920 2007; Xiaohong et al. 2010). Thus, we can represent this statement by following equation.

$$R_{et} \neq \frac{\Delta p_{iso} * A}{H_e} \neq \frac{\Delta p_{iso} * A}{H_t - H_d} \quad (1)$$

R_{et}	*total clothing evaporative resistance*	*[kPa.m²/W]*
H_e	*calculated evaporative heat loss*	*[W]*
H_t	*total evaporative heat loss*	*[W]*
H_d	*dry evaporative heat loss*	*[W]*
Δp_{iso}	*water vapor pressure gradient between wet skin and environment*	*[kPa]*
A	*sweating surface area*	*[m²]*

Mentioned studies (Chen et al. 2004; Xiaohong et al. 2010) conclude that using non-isothermal conditions for measuring evaporative resistance is not recommended and isothermal conditions should be used.

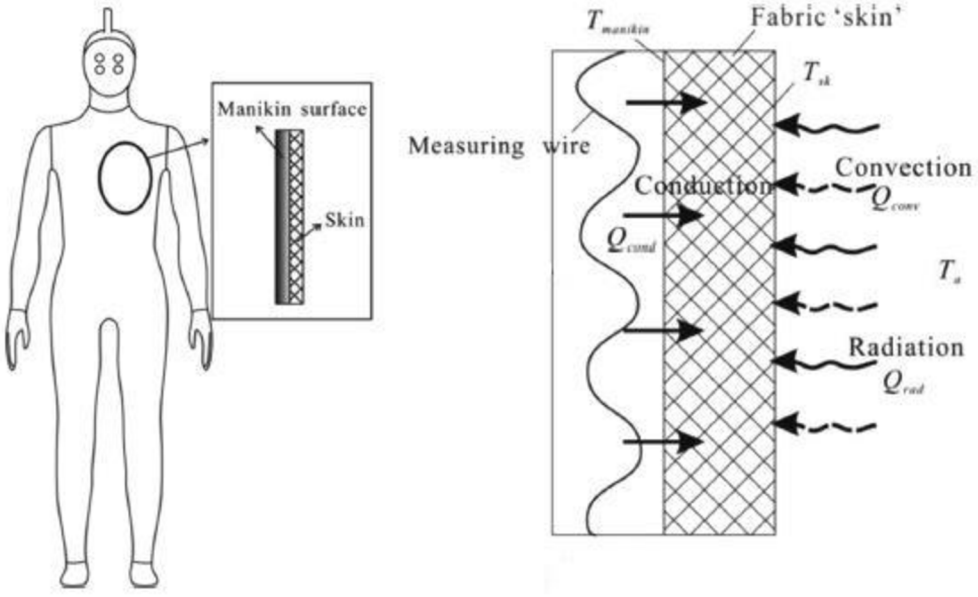

Figure 5: The heat transfer mechanism among the manikin surface, the wetted skin and the environment in a so-called isothermal conditions *($T_a = T_r = T_{manikin}$)* without clothing, adapted from (Wang et al. 2015)

However, it is not possible to setup isothermal conditions for current sweating manikins as we are only able to control manikin surface temperature, not the temperature of the wetted manikin´s skin (it is not yet technically possible due to sensor limitations). Thus, so-called isothermal must be used instead. As it can be seen from Figure 5, in so-called isothermal conditions, the heat transfer process is very complex. Previous studies (Wang et al. 2011b, 2016) have demonstrated that the fabric 'skin' and wet clothing spots will draw heat from the ambient in a so-called isothermal environment due to the negative temperature gradient between the uncontrolled fabric 'skin' and the ambient. Thus, the heating that is supplied to the manikin is not equal to the actual energy that is used for water evaporation occurring in the wet fabric 'skin'-clothing system. As the fabric 'skin' should be tightly fitted to the manikin body, there is no or minimal air gap between the fabric 'skin' and the manikin surface. For the nude scenario in the so-called isothermal conditions, the heat will be transferred from the manikin surface to the fabric 'skin' mainly through conduction. The fabric 'skin' is directly exposed to the ambient air so the heat will be transferred from the ambient environment in to the fabric 'skin' by convection and radiation. If clothing is worn on top of the fabric 'skin', the heat transfer process will become more complicated. First, the moisture contained in the fabric 'skin' may be wicked away by the tested clothing and some moisture evaporation is from the tested clothing on the inner or outer surface of the clothing. In the so-called isothermal condition, the energy used for moisture evaporation occurring in the wet fabric 'skin' clothing system can only be drawn from either the heated manikin or the ambient environment. Thus, the heat may be transferred from the ambient air to some evaporation locations in the tested clothing and further to the saturated fabric 'skin'. This heat transfer process may involve convection, radiation and conduction (Wang et al. 2015).

2.3.1 Calculation methods

There were two calculation methods for clothing evaporative resistance provided in ASTM standard from 2010 (ASTM F2370 - 10 2010) – mass loss method and heat loss method. Mass loss method was removed from new version of this standard (ASTM F2370-16 2016). The reason behind it is probably because it is challenging to use the mass loss method to calculate localized clothing evaporative resistance (Wang 2017) which were added in this new ASTM standard (ASTM F2370-16 2016). According to Wang (Wang 2017) exclusion of mass loss method was not the right decision as this method directly determining the intensity of mass transfer by evaporation and is closer to the physical nature of heat transfer by sweating.

2.3.2 Mass loss method

This method measures the mass loss rate and then converts it to the evaporative heat loss by multiplying the latent heat of vaporization of water.

$$R_{et,mass} = \frac{\Delta p_{iso} * A}{H_{e,mass}} = \frac{\Delta p_{iso} * A}{\lambda * \frac{dm}{dt}} \quad (2)$$

$R_{et,mass}$	*total clothing evaporative resistance calculated by mass loss method*	*[kPa.m²/W]*
$H_{e,mass}$	*calculated evaporative heat loss from mass loss rate*	*[W]*

Δp_{iso}	*water vapor pressure gradient between wet skin and environment*	*[kPa]*
A	*sweating surface area*	*[m²]*
λ	*vaporization heat of water at measured skin temperature*	*[W.h/g]*
dm/dt	*evaporation rate of moisture from the wet skin*	*[g/h]*

2.3.3 Heat loss method

Evaporative resistance is calculated from area-weighted heat loss observed from thermal manikin software.

$$R_{et,heat} = \frac{\Delta p_{iso} * A}{H_{e,heat}} \quad (3)$$

$R_{et,heat}$	*total clothing evaporative resistance calculated by heat loss method*	*[kPa.m²/W]*
$H_{e,heat}$	*evaporative heat loss from manikin´s surface*	*[W]*
Δp_{iso}	*water vapor pressure gradient between wet skin and environment*	*[kPa]*
A	*sweating surface area*	*[m²]*

2.3.4 Comparison of these methods

There are many studies comparing evaporative resistance calculated by these two methods. Firstly, nude manikin (manikin + wetted skin only) and five following clothing ensembles were measured on manikin ´Tore´: L - Light clothing, HV – high-visibility clothing, MIL – military clothing, CLM – climber overall, FIRE – firefighting clothing. Results can be seen on Figure 6. Significant differences can be seen between the values of $R_{et,heat}$ calculated from heat loss method and the $R_{et,mass}$, which were calculated from the mass loss obtained by a weighting scale system (Wang et al. 2011a).

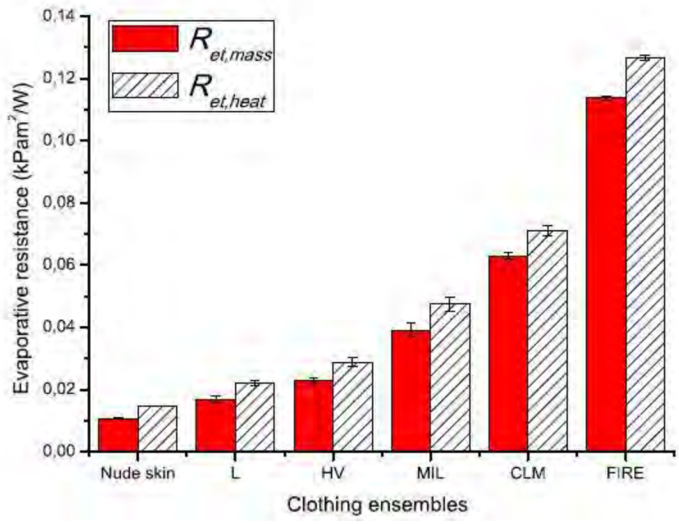

Figure 6: Comparison of values of total evaporative resistance calculated by heat loss and mass loss methods taken from (Wang et al. 2011a)

Secondly, similar results (Figure 7) were found by (Wang et al. 2009) in another study on ´Tore´ manikin where combinations of two wetted skin materials (C – knit cotton, G – Gore-Tex) and two clothing ensembles (U – knitted underwear, P – permeable coverall) were tested. Finally, three types of clothing ensembles (PERM – permeable, SEMI – semi permeable and IMP – impermeable) were tested by (Havenith et al. 2008a) on sweating ´Newton´ type manikin with water supply – Figure 8.

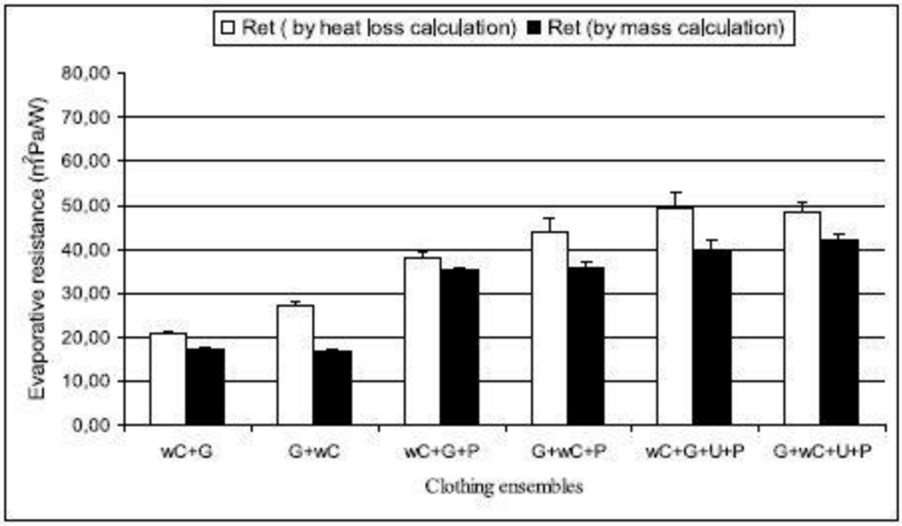

Figure 7: Comparison of values of total evaporative resistance calculated by heat loss and mass loss methods taken from (Wang et al. 2009)

It can be seen from Figures 6 and 7 that R_{et} values calculated from heat loss method are always significantly larger (more than *10 %)* as those calculated from mass loss method. This is caused by todays imperfection in sweating manikin design – inability to control wetted skin temperature. This constrain researchers to usage of a so-called isothermal conditions where the heat for evaporation is also taken from the environment. Thus, some corrections had to be made for evaluation of R_{et} by heat loss method to mitigate resulting errors as the mass loss method yields physically correct values.

2.4 Different factors influencing Ret measurements and calculations

There were many factors investigated throughout the years to identify the source of errors and mitigate their effects on evaporative resistance measurement and calculation:

- Temperature difference between controlled surface temperature of the manikin and its pre-wetted skin.
- Effect of moisture content on apparent ´wet´ thermal insulation.
- Fit and size of clothing.
- Fabric used for the pre-wetted skin.

2.4.1 Effect of temperature difference

As we mentioned, significant error was made by calculating evaporative resistance using manikin surface temperature (due to technical difficulties and complexity of sensor attachment on wetted skin) and not the temperature of pre-wetted skin as it should be according to ASTM standard (ASTM F2370 - 10 2010). In 2010, Wang (Wang et al. 2010) conducted experiment with aim to see how much error usage of manikin surface temperature causes and how he could possibly predict wetted skin temperature for further calculations. In first part of his study, he managed to test the temperature difference between inner and outer side of the wetted skin and he found it can be neglected. From nude "Tore" manikin (nude manikin + wetted skin) tests he derived equation (4) for prediction of manikin´s skin temperature for environmental temperature range between *25 °C* and *34 °C*.

$$T_{sk} = 34.00 - 0.0132 * HL \tag{4}$$

T_{sk}	*predicted manikin´s skin temperature*	*[°C]*
HL	*heat loss from manikin´s total sweating area – heat flux*	*[W/m²]*

Similar prediction was made by a thermal infrared camera (Havenith et al. 2008b). However, this equation was only done for temperature of *34 °C* on Newton type manikin.

$$T_{sk} = 34.13 - 0.012 * HL \tag{5}$$

T_{sk}	*predicted manikin´s skin temperature*	*[°C]*
HL	*heat loss from manikin´s total sweating area – heat flux*	*[W/m²]*

Six clothing ensembles (L - Light clothing, HV – high-visibility clothing, MIL – military clothing, CLM – climber overall, PERM – permeable clothing, IMP – impermeable clothing) were used for comparison of three temperatures – measured wetted skin temperature – t_{sk}, temperature predicted by equation (4) – t_{sk_p1} and temperature predicted by equation (5) – t_{sk_p2}. From statistical point of view using the root squared deviation method, predicted values from these two equations are not accurate enough on significance level of *0.95*. However, with consideration of temperature measurement precision of ± *0.3 °C*, agreement between observed data and predicted values can be always accepted within this precision level (Wang et al. 2010).

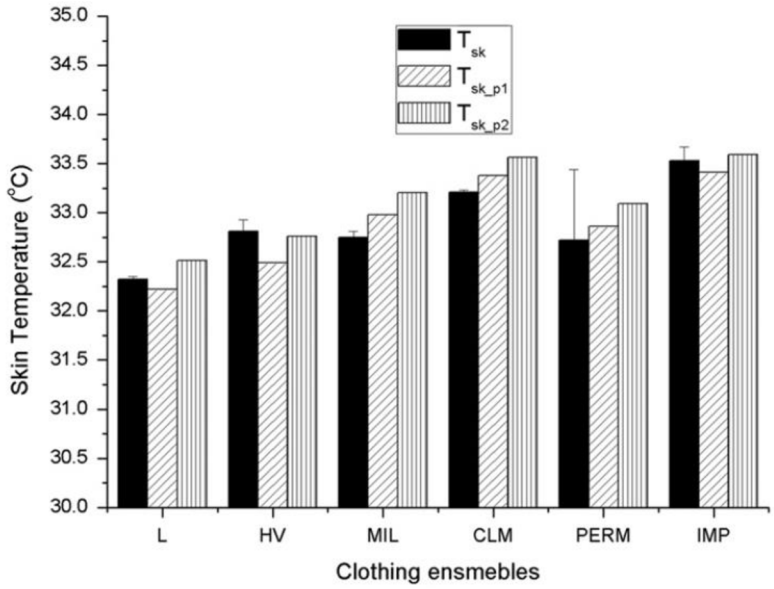

Figure 9: Comparison of temperature values measured t_{sk}, predicted by equation (4) – t_{sk_p1} , predicted by equation (5) – t_{sk_p2} taken from (Wang et al. 2010)

Next step in (Wang et al. 2010) was to determine total evaporative resistance of six previously mentioned clothing ensembles by using two predicted temperatures t_{sk_p1} (4) and t_{sk_p2} (5) and one measured temperature t_{sk} to see the difference between R_{et} values calculated from the manikin surface temperature, measured skin temperature and those calculated by predictive equations.

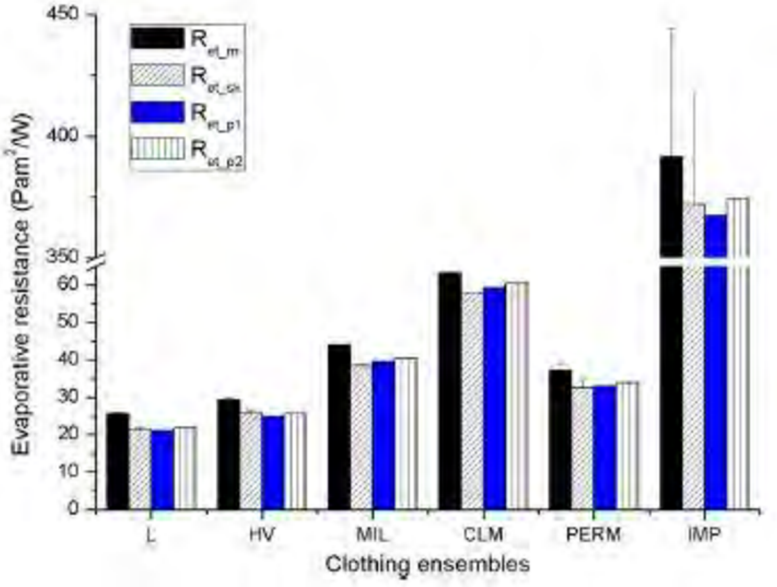

Figure 10: Comparison of R_{et} values calculated from prevailing mass loss method using manikin surface temperature – R_{et_m}, measured skin temperature – $R_{et\text{-}sk}$, predicted by equation (4) – $R_{et\text{-}p1}$, predicted by equation (5) – $R_{et\text{-}p2}$ taken from (Wang et al. 2010)

It can be clearly seen from the Figure 10 that values of R_{et} calculated from measured skin temperature, predicted temperature by equation (4) and (5) matching nicely. However, R_{et} values calculated by prevailing method – from the manikin surface temperature is significantly higher. Thus, these predictive equations enhance greatly the accuracy of clothing evaporative resistance measurements, especially for lower insulated and permeable clothing ensembles.

In the erratum of the following study (Wang et al. 2011b), the difference between prevailing method (using manikin surface temperature) and method from ASTM standard (using wetted skin temperature) was thoroughly investigated. Firstly, it was found that prevailing method overestimates the clothing evaporative resistance by up from *3.8* to *23.7 %*. Secondly, the error caused by prevailing method is more pronounced for permeable clothing ensembles due to their smaller intrinsic evaporative resistance - R_{ecl} (Wang et al. 2011b), which can be calculated from equation (6).

$$R_{et} = R_{ecl} + \frac{R_{ea}}{f_{cl}} \tag{6}$$

R_{et}	*clothing total evaporative resistance*	*[kPa.m²/W]*
R_{ecl}	*clothing intrinsic evaporative resistance*	*[kPa.m²/W]*
R_{ea}	*evaporative resistance of the boundary surface air layer and the skin*	*[kPa.m²/W]*
f_{cl}	*clothing area factor*	*[-]*

It is assumed that R_{ecl} is a constant and that the clothing total evaporative resistance measurement on a thermal manikin will not introduce further errors. Therefore, the error is introduced only by temperature difference between manikin surface and wetted skin. Finally, (Wang et al. 2011b) mentioned the importance of using the right equation for wetted skin temperature prediction made on the same type of thermal manikin.

Similar experiment was conducted by (Ueno and Sawada 2012) Predictive equations were proposed for five manikin body parts and one additional equation for whole body.

$T_{sk} = T_{manikin} - 0.0130 * HL$	(Arm)
$T_{sk} = T_{manikin} - 0.0089 * HL$	(Trunk)
$T_{sk} = T_{manikin} - 0.0115 * HL$	(Hip)
$T_{sk} = T_{manikin} - 0.0063 * HL$	(Thigh)
$T_{sk} = T_{manikin} - 0.0071 * HL$	(Calf)
$T_{sk} = T_{manikin} - 0.0092 * HL$	(Whole manikin)

T_{sk}	*predicted manikin´s skin temperature*	*[°C]*
HL	*heat loss from manikin´s associated sweating area – heat flux*	*[W/m²]*

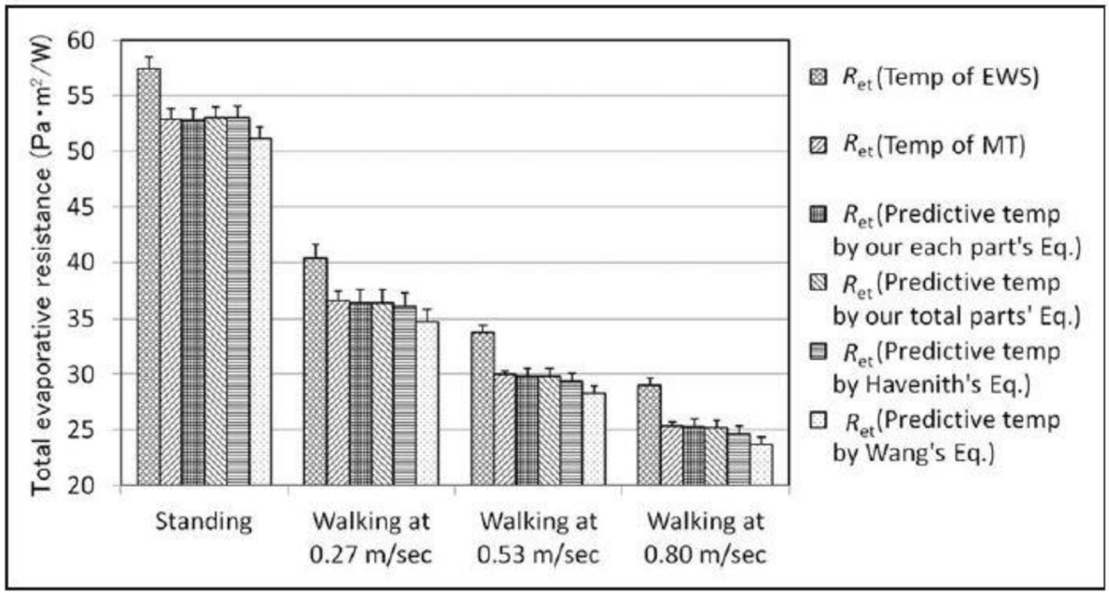

Figure 11: Comparison of R_{et} values calculated from prevailing heat loss method using manikin surface temperature – R_{et} (Temp of EWS), measured skin temperature – R_{et} (Temp of MT), predicted by equations for each part – R_{et} (Predictive temp by Ueno each part´s Eq), predicted by equation for whole manikin – R_{et} (Predictive temp by Ueno whole manikin Eq), predicted by Haveninth Eq. (Havenith et al. 2008b) and by Wang Eq. (Wang et al. 2010) taken from (Ueno and Sawada 2012)

These six equations were made from data on ´Newton´ type thermal manikin in four walking speeds – *0 ms^{-1}, 0.27 ms^{-1}, 0.53 ms^{-1}, 0.80 ms^{-1}*. Increasing walking speed increases both ventilation and mass transfer between the environment and manikin. In higher walking speeds, the manikin was not able to control the surface temperature $T_{manikin}$ at *34 °C* on some body parts due to increased effect of convection. Thus, for higher walking speeds, the predictive equations for wetted skin temperatures won't apply cause of the different manikin surface temperature $T_{manikin}$. This results confirms findings of the previous researchers (Havenith et al. 2008a; Wang et al. 2015). The differences between the (Wang et al. 2015; Wang 2017) prediction and other predictions (Figure 11) are probably due to usage of different manikin type and the smaller number of sensors attached on the wetted skin.

2.4.2 Effect of moisture content on apparent ´wet´ thermal insulation

Thermal insulation governs the possible amount of body heat dissipated to the environment. Two types of thermal insulation are recognized – dry thermal insulation measured on dry manikin (ISO 15831 2004) and ´wet´ thermal insulation when measured clothing is fully or partially wet. The ´wet´ thermal insulation in presence of moisture and/or air movement is often referred to as apparent ´wet´ thermal insulation (Lotens et al. 1995; Wang et al. 2016).

$$I_{t,apparent} = I_t * (1 - 1 * 10^{-9} * w_t^3 + 1.6 * 10^{-6} * w_t^2 - 1.004 * 10^{-3} * w_t) \quad (7)$$

$I_{t,apparent}$	*clothing apparent ´wet´ thermal insulation*	*[m².K/W]*
I_t	*clothing dry thermal insulation*	*[m².K/W]*
w_t	*the amount of moisture contained in the tested clothing* $0 < w_t < 800g$	*[g]*

Equation (7) describes the effect of moisture content on apparent ´wet´ thermal insulation. This equation was deduced from Figure 12 from Wang´s (Wang et al. 2016) dataset which correlates with data from Hall and Polte (Hall and Polte 1956). It is suggested to use this equation only for moisture content between 100 – 800g.

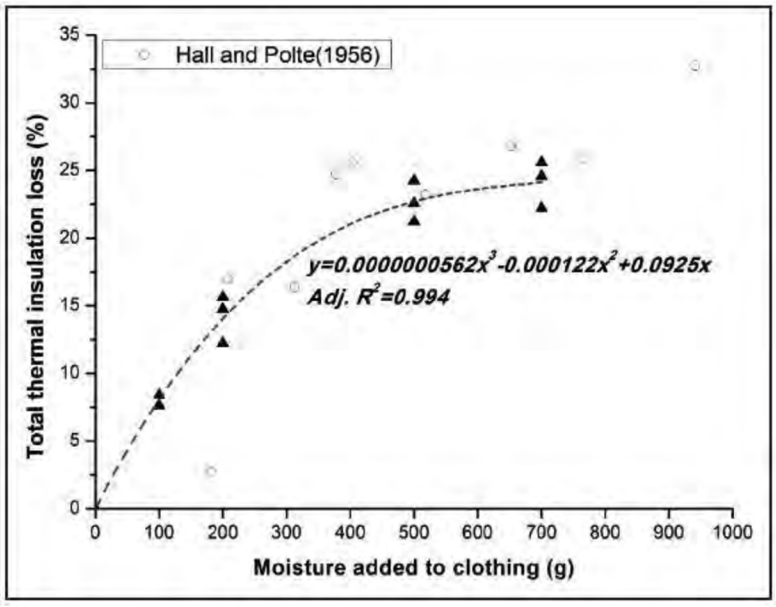

Figure 12: effect of moisture content added to clothing on total thermal insulation loss (circle are data from (Hall and Polte 1956), rest of the data and graph itself is taken from (Wang et al. 2016)

2.4.3 Effect of clothing fit and size

Previous study also investigated the effect of fit/size on the thermal insulation. It was found that dry insulation of clothing increases with the increasing clothing size and then decreases with still increasing clothing size (Wang et al. 2016). The decrease of thermal insulation is caused by natural air convection between clothing and manikin body as the air gap becomes thick enough, normally thicker than *8 – 11 mm* (Wang et al. 2016). These findings are in accordance with result from (Chen et al. 2004). Although, the clothing size/fit has impact on dry thermal insulation, the effect on apparent ´wet´ thermal insulation and evaporative resistance is minimal. However, it is suggested that the right size of clothing fitting the manikin should be used if possible.

2.4.4 Fabric thickness and material effect on apparent ´wet´ thermal resistance

The missing requirements for manikin´s skin material in new ASTM standard (ASTM F2370-16 2016) led to the investigation of the effect of different fabric materials and its thickness on thermal insulation and evaporative resistance by means of sweating thermal manikins. In (Wang et al. 2017) conducted experiment where seven pieces of highly stretchable single-jersey knitted cotton and polyester fabric ´skins´ (CO1, CO2, CO3, CO4, PES1, PES2, PES3) of different thicknesses were tested. New skin temperature predictive equations were made and the apparent ´wet´ thermal resistance was calculated using water content, thickness, and also the fabrics´ physical properties (e.g. mass per unit area, fabric conductivity, fiber density) for each of the seven samples.

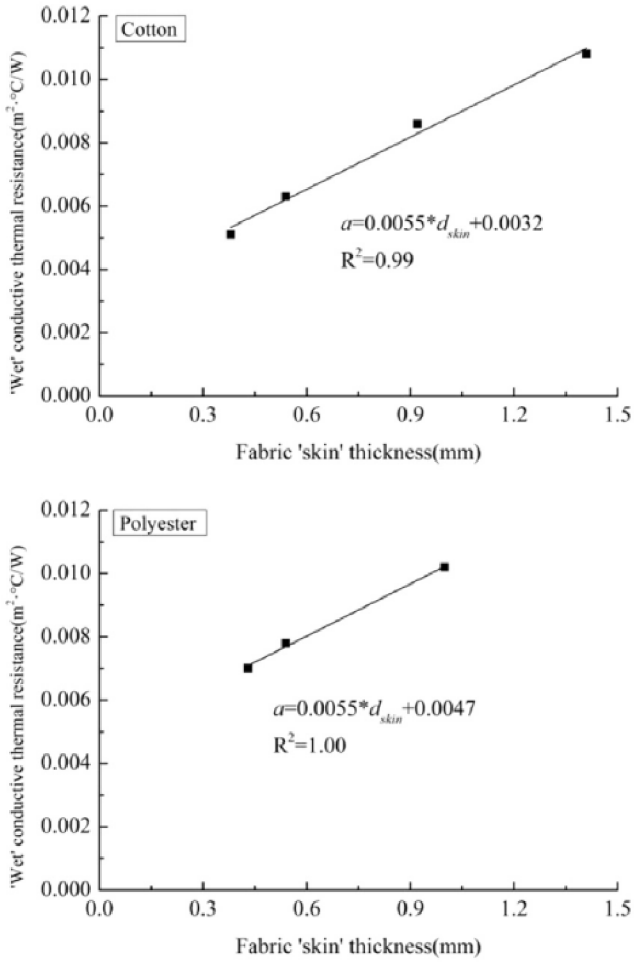

Figure 13: Effect of fabric thickness on the apparent ´wet´ thermal insulation of manikin´s sweating skins for both cotton and polyester material, taken from (Wang et al. 2017)

It can be clearly seen from Figure 13 that there is a linear relation between fabric thickness and its apparent ´wet´ thermal insulation for both cotton and polyester materials. Total evaporative resistance was measured on two clothing ensembles EN1 (cotton briefs, cotton pants and polyester T-shirt) and EN2 (cotton briefs, cotton long sleeve T-shirt and polyester trousers) to validate newly formed skin temperature predictive equations and to statistically compare different skin materials. For all scenarios (except CO4 and PES3 in EN2 ensemble) the total evaporative resistance calculated from the constant manikin surface temperature was significantly higher than those calculated from measured or predicted skin temperatures – Figure 14. This result is in great agreement with previous studies (Wang et al. 2011a, b; Ueno and Sawada 2012).

To conclude, both fabric material and thickness have impact on apparent ´wet´ thermal resistance and hence on total evaporative resistance. It is suggested that skin with thickness from *0.40 mm* to around *0.55 mm* should be used for evaporative resistance measurements. Also, cotton material was better in maintaining skin wetness for longer time and it should be used rather than polyester to avoid skin´s drying during the test procedure especially on sweating manikins with no water supply.

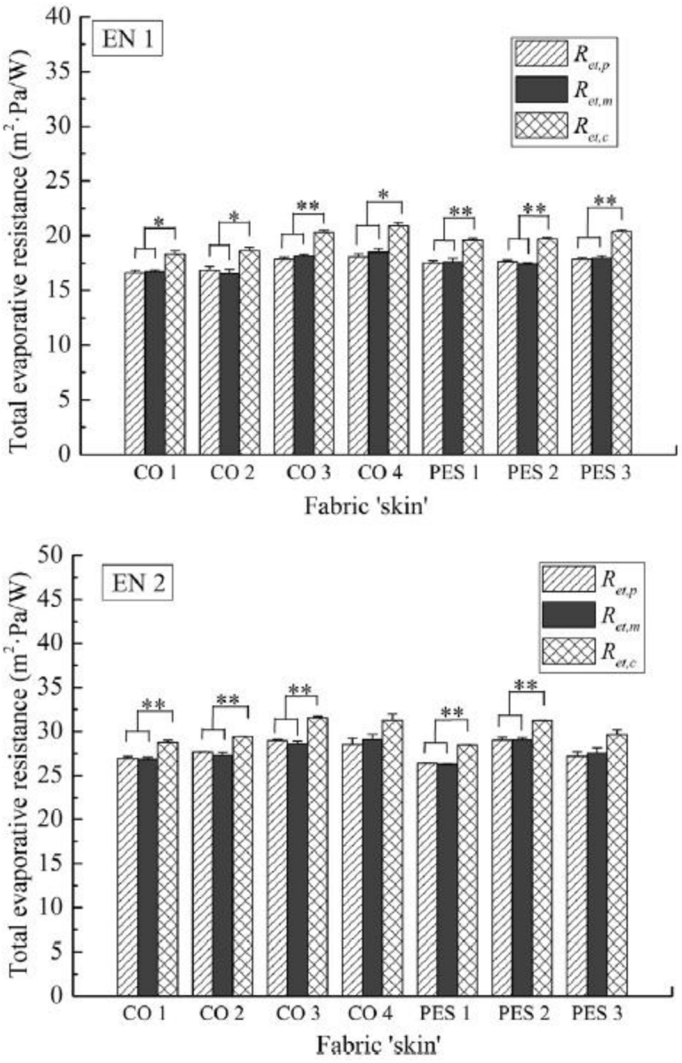

Figure 14: Comparison of total evaporative resistance values on two ensembles EN1 and EN2 calculated from predicted skin temperatures for each ´skin´ material option – $R_{et,p}$, from measured skin temperature – $R_{et,m}$ and from prevailing method (manikin surface temperature) – $R_{et,c}$, taken from (Wang et al. 2017)

In another study (Koelblen et al. 2017) the cotton material with around *0.50 mm* thickness was also labeled as the best option for making sweating simulation skin for thermal manikins.

2.5 Proposed approach for Ret measurements

Results from previous years were summarized to overview article about evaporative resistance measurement (Wang 2017). Evaporative resistance measured in non-isothermal conditions is always referred to as apparent evaporative resistance – AR_{et}. Determined values will be referred to as real evaporative resistance – $R_{et,real}$ when measured in so-called isothermal conditions. Although, no dry thermal insulation tests are needed for calculation of the $R_{er,real}$ because the observed heat loss from the manikin in so-called isothermal conditions represents the evaporative heat loss, some corrections must be used (Wang et al. 2011a; Wang 2017). It is suggested to follow this scheme when calculating real evaporative resistance measured in so-called isothermal conditions.

Apparent ´wet´ thermal fabric insulation calculation including skin fabric properties. Derivation of this equation can be found in overview article as appendix (Wang 2017).

$$AI_{wet} = \frac{(d_{fabric} * \rho_w)^2}{d_{fabric} * \rho_w{}^2 * k_{fiber} + (k_w - k_{fiber}) * w_c * m_{fabric} * (\rho_w + \rho_{fiber} * w_c)} \quad (8)$$

AI_{wet}	*apparent ´wet´ thermal insulation of the fabric*	*[m².K/W]*
d_{fabric}	*fabric thickness*	*[mm]*
ρ_{fiber}	*fiber density*	*[kg/m³]*
ρ_w	*water density*	*[kg/m³]*
k_{fiber}	*fiber thermal conductivity*	*[W/m.K]*
k_w	*water thermal conductivity*	*[W/m.K]*
m_{fabric}	*fabric´s mass per unit area*	*[g/m²]*
w_c	*water content in fabric*	*[% g/g]*

Apparent ´wet´ thermal insulation is then used for skin temperature prediction to mitigate the error in evaporative resistance calculation caused by using manikin surface temperature (prevailing method) and not manikin´s skin temperature as stated in standard (ASTM F2370-16 2016).

$$T_{sk} = T_{manikin} - AI_{wet} * HL \quad (9)$$

T_{sk}	*predicted manikin´s skin temperature*	*[°C]*
$T_{manikin}$	*manikin´s surface temperature*	*[°C]*
AI_{wet}	*apparent ´wet´ thermal insulation of the fabric*	*[m².K/W]*
HL	*heat loss from manikin´s total sweating area – heat flux*	*[W/m²]*

This predicted temperature is then used to correct heat loss for evaporation as part of it is taken from environment and the other part from thermal manikin. The effect of moisture content on clothing is also accommodated to this calculation as equation (7) from section 1.4. The final equation for corrected evaporative heat loss – Q_{evap} is as followed: (Wang et al. 2015; Lu et al. 2016).

$$Q_{evap} = H_{e,heat} + \frac{(T_a - T_{manikin}) + AI_{wet} * HL}{I_t * (1 - 1 * 10^{-9} * w_t^3 + 1.6 * 10^{-6} * w_t^2 - 1.004 * 10^{-3} * w_t)} \quad (10)$$

It can be easily deduced from equation (10) that the energy used for moisture evaporation during wet test in so-called isothermal conditions is always greater than the heating power supplied to the manikin. Finally, the Q_{evap} value can now be used for calculation the real evaporative resistance by heat loss method and should yield similar results to those from mass loss method.

Heat loss method

$$R_{et,heat} = \frac{(p_{sk} - p_a) * A}{H_{e,heat}}$$

Corrected heat loss method

$$R_{et,heat,corr} = \frac{(p_{sk} - p_a) * A}{Q_{evap}}$$

Mass loss method

$$R_{et,mass} = \frac{\Delta p_{iso} * A}{H_{e,mass}} = \frac{(p_{sk} - p_a) * A}{\lambda * \frac{dm}{dt}}$$

Where the saturated skin vapor pressure and ambient air vapor pressure can be calculated as follows.

$$p_{sk} = 0.1333 * exp(18.6686 - \frac{4030.183}{t_{sk}+235}) \quad (11)$$

$$p_a = 0.1333 * exp\left(18.6686 - \frac{4030.183}{t_a+235}\right) * RH_a \quad (12)$$

RH_a	*relative humidity of ambient air*	*[%]*
P_a	*ambient air vapor pressure*	*[kPa]*
P_{sk}	*saturated skin vapor pressure*	*[kPa]*

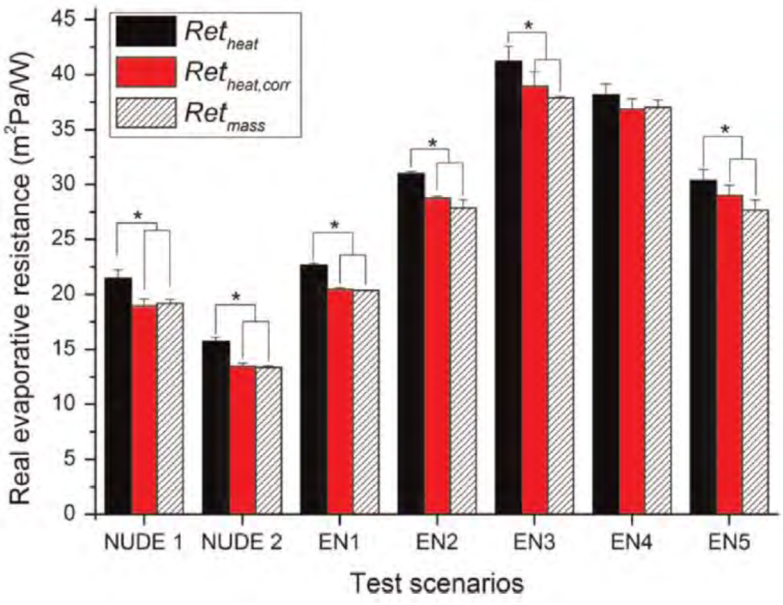

Figure 15: Comparison of real evaporative resistance values on 5 ensembles and two nude cases calculated from prevailing method (manikin surface temperature) – $R_{et,heat}$, from mass loss method – $R_{et,mass}$ and from corrected heat loss method – $R_{et,heat,corr}$, taken from (Wang et al. 2015).

It is clear from Figure 15 that correction for heat loss method improved the accuracy of real evaporative resistance by heat loss method and that there is no significant difference between $Ret_{heat,corr}$ and Ret_{mass}. In ensemble EN4, there is no significant difference between neither of

the three methods as only small amount of heat (around *3.6 %*) was drawn from the ambient due to high insulation and impermeable layers of the clothing. To simplify the calculation, it is suggested that the heat loss method may be directly used for calculating clothing real evaporative resistance with no corrections for high insulation clothing (e.g., higher than *2.0 clo*). For low insulation and vapor permeable clothing, the heat loss method must be corrected before calculating clothing real evaporative resistance (Wang et al. 2015).

3 SUMMARY OF KNOWLEDGE GAP

Although the knowledge in the field of measuring thermal insulation (I_t) and clothing area factor by means of thermal manikin are extensive, the measurement of evaporative resistance (R_{et}) is not documented too well. It is known that the repeatability of the thermal insulation measurement is within the *4 %* difference when the correct methodology from standards (ISO 9920 2007) is used. This is not the case for evaporative resistance measurement. As multiple sweating simulations systems for manikin with different methodology and calculations methods are used around the world, it is very challenging to compare any results and the reproducibility its uncertain. As the round robin study (Wang et al. 2014) shows the difference from mean values of measurements from multiple laboratories around *10 %* (in extreme case *30 %* difference), the aim is to accommodate the evaporative resistance measurement using manikin NEWTON at BUT and reach the values within *10 %* from the results from manikin TORE at Lund University. This level of precision would validate the methodology of the measurement at BUT, as well as confirm the reproducibility of the measurement between different laboratories using same methodology.

Secondly, the mass loss is closer to the physical nature of heat transfer by sweating while accommodation of heat loss method is more challenging. The global aim is to find the right measuring methodology and calculation methods for evaporative resistance using heat loss method, which would allow to calculate also local evaporative resistance values for different body parts for use in physiological modeling. Multiple corrections were proposed in the literature for heat loss method, but they are not verified on bigger sample of clothing ensembles (usually done on 2 or 3 ensembles in the study). Thus, it is unknown to what extend should the proposed corrections be used for ensembles with different insulation or for protective clothing etc.

4 AIM AND OBJECTIVES

4.1 Aim of the thesis

Development and integration of the measurement procedure and calculation methods to determine clothing evaporative resistance using thermal manikin Newton and to validate the precision, repeatability and reproducibility of the measurement.

4.2 Scientific questions and original hypotheses

4.2.1 How do clothing properties affect the accuracy of thermo-physiological models?

Clothing properties (thermal insulation, clothing area factor and evaporative resistance) are used as an input data for prediction models and are considered as one of the most problematic areas. To obtain the most precise prediction possible, it is vital that the clothing properties input data should define the properties of real clothing as realistically as possible.

4.2.2 Is it necessary to measure clothing properties?

As it is not always possible to measure clothing properties of real clothing ensembles used, multiple equations and models to predict clothing properties were proposed, but studies show that results are not always precise enough. Multiple methods for measuring clothing properties are also used, but the best way to obtain the most realistic results are the methods using thermal manikins, as the simulation of the shape of human body, with air gaps present in the clothing, is vital to obtain realistic results.

4.2.3 Are the results of evaporative resistance measurements repeatable and reproducible?

The repeatability and reproducibility of thermal insulation measurements is well study and should be within *4 %* while using same measurement setup according to the standards. For evaporative resistance measurements, the repeatability and reproducibility should be achievable in similar fashion, if the measurement setup, methods and calculations kept the same, for example, if the sweating system of the manikin is not changed. We believe that the difference should be within *10 %* as it was achieved in most cases in comparison study (Wang et al. 2014).

4.2.4 Is it needed to use all proposed correction from the literature for evaporative resistance calculation?

As the measurements are done in so-called isothermal conditions because we are unable to control manikin´s skin temperature, the correctio for the manikin skin temperature should be used for both mass loss and heat loss method, as it is not correct from the physical point of view to calculate the evaporative resistance from the manikin´s surface temperature. Our hypothesis is that the usage of other types of corrections are highly dependent on specific clothing ensembles and it do not in general enhance the precision of the measurements any further.

4.3 Objectives

To support all scientific questions, a set of specific objectives have been formulated:

I. Analyze the importance of obtaining precise clothing parameters for thermos-physiogical modeling.
II. Analyze multiple methods to obtain clothing properties and confirm the importance of manikin measurements.
III. Identify the impact of local values for different body zones on thermo-physiological models.
IV. Study the influence of body posture and body movement on clothing properties.
V. Verify the evaporative resistance measurement methodology and calculations including all proposed corrections to obtain most precise values.
VI. Implement the evaporative measurements methodology in BUT including equipment and calculation methods.
VII. Verify the reproducibility of the evaporative resistance measurement between two laboratories.

4.4 Structure of the thesis

The aim and objectives have been addressed in four stand-alone peer-review journal papers and one soon to be published paper. The number of citations taken from ScienceDirect and Google scholar, excluding auto citation as of July 2023 is given in brackets:

POKORNÝ, J.; FIŠER, J.; FOJTLÍN, M.; KOPEČKOVÁ, B.; **TOMA, R**.; SLABOTINSKÝ, J.; JÍCHA, M. Verification of Fiala-based human thermophysiological model and its application to protective clothing under high metabolic rates. BUILDING AND ENVIRONMENT, 2017, vol. 126, no. 2017, p. 13-26. ISSN: 0360-1323. **(16)**

FOJTLÍN, M.; PSIKUTA, A.; FIŠER, J.; **TOMA, R**.; ANNAHEIM, S.; JÍCHA, M. Local clothing properties for thermo-physiological modelling: Comparison of methods and body positions. BUILDING AND ENVIRONMENT, 2019, vol. 2019, no. 155, p. 376-388. ISSN: 0360-1323. **(14)**

TOMA, R.; KUKLANE, K.; FOJTLÍN, M.; FIŠER, J.; JÍCHA, M. Using a thermal manikin to determine evaporative resistance and thermal insulation – A comparison of methods. Journal of Industrial Textiles, 2020, vol. 2020, no. 1, p. 1-23. ISSN: 1530-8057. **(5)**

KUKLANE, K.; **TOMA, R**.; A. I. LUCAS, R. Insulation and Evaporative Resistance of Clothing for Sugercane Harvesters and Chemical Sprayers, and Their Application in PHS Model-Based Exposure Predictions. International Journal of Environmental Research and Public Health (printed), 2020, vol. 17, no. 9, p. 1-12. ISSN: 1661-7827. **(8)**

TOMA, R.; KUKLANE, K.; FOJTLÍN, M.; FIŠER, J.; JÍCHA, M. Reproducibility of evaporative resistance measurements and calculations using different thermal manikins. (to be published)

4.5 The author's contribution to the papers

I. Conducted part of literature survey, part of data analysis and correcting of the manuscript

II. Conducted part of experimental work, part of literature survey and correcting of the manuscript

III. Conducted all of experimental work, literature survey, data analysis and writing of the manuscript

IV. Conducted majority of experimental work, part of the literature survey, part of data analysis and correcting of the manuscript

V. Conducted all of experimental work and numerical work, literature survey, data analysis and writing of the manuscript

4.6 Other publications of the author related to the topic of the thesis

Three peer-review journal papers, which were co-authored during PhD studies closely connected with the topic of the dissertation but were not discussed in detail due to brevity. All papers are focused on clothing properties measurements using thermal manikin. The results of this thesis were presented at multiple international conferences.

KUKLANE, K.; **TOMA, R**. Common clothing area factor estimation equations are inaccurate for highly insulating (Icl>2 clo) and non-western loose-fitting clothing ensembles. INDUSTRIAL HEALTH, 2020, vol. 59, no. 2, p. 107-116. ISSN: 0019-8366. **(4)**

ŠVECOVÁ, J.; STROHMANDL, J.; FIŠER, J.; **TOMA, R**.; HAJNA, P.; HAVELKA, A. A comparison of methods for measuring thermal insulation of military clothing. Journal of Industrial Textiles, 2019, vol. 2019, no. 1, p. 1-17. ISSN: 1530-8057. **(3)**

KUKLANE, K.; **TOMA, R**. Validation of ISO 9920 clothing item insulation summation method based on an ambulance personnel clothing system. INDUSTRIAL HEALTH, 2021, vol. 59, no. 1, p. 27-33. ISSN: 0019-8366. **(5)**

POKORNÝ, J.; KOPEČKOVÁ, B.; FIŠER, J.; **TOMA, R**.; JÍCHA, M. Využití termofyziologického modelu na určení tepelné zátěže člověka v ochranných oděvech. In HAZMAT PROTECT 2018, 3. ročník odborné konference o ochraně proti CBRN látkám SBORNÍK ABSTRAKTU + DVD s celými články. SÚJCHBO, v. v. i., Kamenná, Česká republika. 2018. s. 1-10. ISBN: 978-80-270-4852-6.

Róbert Toma, Kalev Kuklane, Jan Fišer, Miroslav Jícha. CLOTHING EVAPORATIVE RESISTANCE MEASUREMENT USING THERMAL MANIKINS. In HAZMAT PROTECT 2018 - BOOK OF ABSTRACTS. 2018. p. 56-56. ISBN: 978-80-270-4852-6.

TOMA, R.; FIŠER, J.; FOJTLÍN, M.; JÍCHA, M. Estimation of thermal sensation based on human´s physiological parameters in indoor environment. 2017. p. 215-215.

TOMA, R.; HRUBANOVÁ, K.; FIŠER, J.; JÍCHA, M. Determination of clothing heat transfer coefficients for use in the iHVAC system. 2018. p. 1-2.

4.7 Other publications of the author

During PhD studies, the author contributed to several ongoing researches in the thermal comfort laboratory and collaborated with foreign research teams. Peer-review journal papers and international conference contributions are listed below.

FOJTLÍN, M.; PSIKUTA, A.; **TOMA, R**.; FIŠER, J.; JÍCHA, M. Determination of car seat contact area for personalised thermal sensation modelling. PLOS ONE, 2018, vol. 13, no. 12, p. 1-16. ISSN: 1932-6203. **(13)**

FOJTLÍN, M.; POKORNÝ, J.; FIŠER, J.; **TOMA, R**.; TUHOVČÁK, J. Impact of measurable physical phenomena on contact thermal comfort. EPJ Web of Conferences, 2017, vol. 143, no. 1, p. 1-4. ISSN: 2100-014X. **(5)**

FOJTLÍN, M.; PSIKUTA, A.; FIŠER, J.; POKORNÝ, J.; **TOMA, R**.; ANNAHEIM, S.; JÍCHA, M.; ROSSI, R. Thermal model of an unconditioned, heated and ventilated seat to predict human thermo-physiological response and local thermal sensation. BUILDING AND ENVIRONMENT, 2019, vol. 169, no. 2020, p. 1-15. ISSN: 0360-1323. **(6)**

FIŠER, J.; POKORNÝ, J.; FOJTLÍN, M.; **TOMA, R**. An innovative HVAC control system: Comparison of the system outputs to comfort votes. Kobe, Japonsko: International Society for Environmental Ergonomics., 2017. p. 39-39.

FIŠER, J.; POKORNÝ, J.; FOJTLÍN, M.; **TOMA, R**. Car cabin thermal comfort measurement under real traffic conditions. The 17th International Conference on Environmental Ergonomics ICEE2017 - book of abstracts. Kobe, Japonsko: International Society for Environmental Ergonomics., 2017. p. 190-190.

FIŠER, J.; POKORNÝ, J.; FOJTLÍN, M.; **TOMA, R**.; JÍCHA, M. Equivalent temperature calculation: The issue of total thermal resistance for Face and Scalp parts measured by thermal manikin. 12th International Manikin and Modelling Meeting (12i3m), 29-31 Aug 2018, St. Gallen, Switzerland: 2018.

POKORNÝ, J.; FIŠER, J.; **TOMA, R**.; FOJTLÍN, M.; JÍCHA, M. Visualisation of temperatures and heat fluxes in contact area of automotive seat. 12th International Manikin and Modelling Meeting (12i3m), 29-31 Aug 2018, St. Gallen, Switzerland: 2018.

5 SUMMARY OF THE CONDUCTED WORK

5.1 Paper I (Objectives I and III): Verification of Fiala-based human thermo-physiological model and its application to protective clothing under high metabolic rates

In this paper, a theory of how to predict thermal comfort and predict human heat stress in various conditions was studied. Although, fast and well established indices expressing heat stress, such as: PHS (Predicted Heat Strain) (ISO 7933 2004) , WBGT (Wet Bulb Globe Temperature) - ISO 7243 (Budd 2008), and thermal sensation and comfort PMV/PPD (Predicted Mean Vote/Predicted Percentage of Dissatisfied) - ISO 7730 (ČSN ISO 7730 1997) could be used, more detailed models should be used for prediction of heat stress in complex environments (Havenith and Fiala 2015). On one hand, complex models provide detailed results about human thermal state; on the other hand, they require rather detailed input data. Study (Katić et al. 2016) states that "Even though sophisticated models were developed…the accuracy of the inputs has to be assured in order to incorporate models in the design process of buildings and daily applications of thermal comfort". In practical applications, this means that a precise determination of environmental and personal parameters is essential to obtain satisfactory results. From authors perspective, the two most problematic parameters are metabolic rate and clothing properties, which was one of the factors behind the decision to conduct the research on the topic of this dissertation thesis to be able to obtain precise clothing data. Thus, clothing properties will be discussed more thoroughly.

Thermal and evaporative resistance of clothing can be determined, for example, according to ISO 9920 (ISO 9920 2007) and also directly measured using a guarded hot plate - ISO 11092 (ISO 11092 2014) or a thermal manikin - ISO 15831 (ISO 15831 2004). The thermal manikin has a human body shape which predetermines it as a suitable tool for the exact measurement of heat transfer coefficients at human body surface, as was described in (de Dear et al. 1997; Fojtlín et al. 2016). However, to obtain a detailed specification of clothing properties for each individual is rather problematic.

Fiala-based thermo-physiological model (FMTK model) was implemented and verified for protective clothing applications. The verification was carried out in three steps: validity of passive and active systems and correlation of the model with experimental data. Details about the verification methods and experimental setup are presented in chapter 2. Methods in Paper I.

5.1.1 Summary of main findings

The passive system of the FMTK model was successfully verified and compared to Theseus-FE model, reaching an average error of local skin temperature of *0.07 °C* through all 49 sectors. A comparison of active system with Theseus-FE model was conducted and the agreement was very good in all transient test cases (in the ambient temperature range from *5 to 48 °C*). Although small differences were found in the simulation of higher metabolic rates, the FMTK model was successfully verified. Detailed results can be found in the chapter 3. Results in Paper I.

The second part of this paper presented the application of the FMTK model to the chemical protective clothing in warm/hot environmental conditions. The model successfully predicted exposure time for three different garments in various conditions. Results show the demand for deeper verification of the Fiala-based model for protective clothing applications. Validation of

the model should be not only for the mean skin temperatures, but also for local temperatures. Several disadvantages were noticed with such a complex model, from which the proper definition of input data needed for the model is the most problematic one. Although we verified that the FMTK model itself is well constructed, a more attention should be paid to the complexity of the clothing model. The most of the inaccuracies stem from the estimation of local insulation parameters (both thermal and evaporative resistance) of clothing and from the effect of walking on the treadmill during the experiments. Thus, it is needed to find the best possible way of how to obtain precise clothing parameters used in the models.

5.2 Paper II (Objectives II, III and IV) Local clothing properties for thermo-physiological modelling: Comparison of methods and body positions

Paper II explores various methods for determining the clothing properties, with the aim of the study to explore possibilities to obtain local clothing parameters for better use in physiological modelling. The aim of the study was to explore various methods and compared them with the results of thermal manikin measurements, which is presently the most accurate method, but also requires expensive equipment, such as thermal manikins and a climatic chamber. Therefore, the researchers aim to find an alternative solution that can provide comparable accuracy to the state-of-the-art methods. The differences between standing and sitting body posture and effect of used method to obtain local clothing parameters on physiological modelling are also examine in the paper.

Table 1 summarizes the different scenarios examined, arranged in descending order of sophistication. The selected methods include manikin measurements, analytical heat transfer modeling (Psikuta et al. 2018; Joshi et al. 2019) regression modeling (Veselá et al. 2018), empirical modeling (e.g. the UTCI model (Havenith et al. 2012)), and ISO based approaches (Nelson et al. 2005; ISO 9920 2007). For a comprehensive understanding, refer to Paper II, Sections 2.3 – 2.9, where detailed descriptions of the cases are provided. Furthermore, the study delves into a thorough investigation of the discrepancies in local clothing values between sitting and standing body positions.

Case	f_{cl} (-)	I_{cl} ($m^2K.W^{-1}$)	$R_{e,cl}$ ($m^2Pa.W^{-1}$)	Position	Segments
1	3D scanning	Manikin heat loss	Manikin heat loss	sitting	13
2	Photography	Manikin heat loss	Manikin heat loss	standing	13
3	Physical model	Physical model	Physical model	sitting	8
4	Physical model	Physical model	Physical model	standing	10
5	Regression model	Regression model	Physical model	standing	11
6	ISO based model	ISO based model	ISO based model	standing	3
7	ISO Database	UTCI model	ISO Database	standing	7
8	ISO Database	ISO Database	ISO Database	standing	1

Table 1: Summary of the examined scenarios

In Case 1, the reference case, state-of-the-art methods were employed. To determine the f_{cl} (clothing area factor), a highly realistic three-dimensional (3D) scanning method was used. A specialized scanner was utilized to digitize the surface of both the nude and clothed body of a sitting manikin. Further information about the equipment used could be found in (Mert et al. 2017). For the determination of I_{cl} (thermal insulation) and $R_{e,cl}$ (evaporative resistance), a 34-zone Western Newton-type manikin (Thermetrics, Seattle, USA) was utilized. The manikin was seated on an adjustable perforated plastic chair inside a climatic chamber. Detailed descriptions of the chamber and the manikin could be found in (Fojtlín et al. 2016). The experimental conditions were set in accordance with ISO 15831:2004 (ISO 15831 2004). The $R_{e,cl}$ was determined using a pre-wetted tightly fitting, long sleeve overall, following the methods described in (Richards et al. 2008; Wang et al. 2011a). The measurement was conducted under isothermal conditions at *34 °C* (skin temperature equal to ambient temperature), with a relative humidity of *18 %* (partial water vapor pressure of *957 Pa*), and an air speed of 0.1 ± 0.05 *m/s*. The calculation of evaporative resistance was performed using the heat loss method described in ASTM F2370 (ASTM F2370-16 2016).

5.2.1 Summary of main findings

The results of this study showed substantial variation among the methods for all examined clothing parameters, ranging from *13 – 43 %* in f_{cl}, *35 – 198 %* in I_{cl}, and *53 – 233 %* in $R_{e,cl}$ of the reference value (Case 1).

Changing the body position from standing to sitting results in a reorientation of various body parts and a redistribution of air gaps. Consequently, all three clothing thermal parameters are affected. Although the global thermal and evaporative resistances exhibited only minor changes (Yu et al. 2011), the local parameters displayed significantly higher error margins (up to *31 %* for f_{cl}, *80 %* for I_{cl} and *92 %* for $R_{e,cl}$).

The local thermo-physiological responses were clearly affected by the variation of the local clothing inputs. The error induced by clothing inputs, in this case, has no critical medical relevance such as un-compensated heat storage or dehydration. However, in thermal sensation and comfort studies, error in the local clothing input can cause substantial error in the thermal sensation modelling. A sensitivity study revealed a dominant influence of the thermal insulation on the predicted thermo-physiological parameters (f_{cl} and $R_{e,cl}$ had lower impact). Therefore, to get a high-quality prediction of physiological responses, it is crucial to always choose the most reliable method to determine the local clothing properties, respecting the body position.

It is worth noting, that there were huge discrepancies found on some body parts between independent tests measuring $R_{e,cl}$ while using thermal manikin in Case 1 and Case 2. Similar discrepancies were showed in previous studies (Richards et al. 2008; Młynarczyk et al. 2018), even for global values for the whole body. Even though clothing properties measurements using thermal manikin are the state-of-the art methods, repeatability of evaporative resistance measurement between independent tests, and also between independent laboratories should be studied to guarantee the best possible input data for models.

5.3 Paper III (Objectives V, VI and VII): Determination of evaporative resistance and thermal insulation by means of thermal manikin – comparison of methods

The focus of Paper III was to determine three most important clothing properties for thermo-physiological modelling - clothing area factor, thermal insulation, and evaporative resistance, by means of a non-sweating thermal manikin using pre-wetted skin. The aim of this study was to identify, and possibly enhance, reliable and applicable methods to obtain protective clothing parameters using thermal manikin. As it could be seen from the results of Paper I and Paper II, the posture of the manikin and its movement is not to be neglected, so verification of multiple equations (EN 342 2004; ISO 9920 2007), used for predicting resultant total thermal insulation (I_{tr}) from total thermal insulation (I_t) was conducted. Secondly, multiple methods to measure and calculate evaporative resistance (ASTM F2370 - 10 2010) were examined, including various calculations and corrections (Wang et al. 2010, 2011b, 2015). According to the conclusions from Paper II, the repeatability of independent tests was also examined for evaporative resistance measurement. Finally, PHS simulations were conducted and a sensitivity analyses was done to observe the impact of the clothing properties, obtained by the different equations and corrections, on the workers' maximum exposure time.

5.3.1 Methods used to obtain clothing properties

All measurements and calculations were conducted on thermal manikin TORE (Kuklane et al. 2006) using two clothing ensembles used by agricultural workers in Latin America - sugarcane cutters (SC) and pesticide sprayers (PS). Only total values for the whole body were calculated in this study.

The clothing area factor (f_{cl}) was determined by the photographic method. This method provides high degree of accuracy without the need for specialized equipment. While in the early use of this method up to 6 photographs were taken from different sides and angles, an acceptable accuracy could also be achieved using photographs from only two positions: 0° - front side of the standing manikin and 90° - right/left side of the standing manikin (Havenith et al. 2015).

The widely used heat loss method was used to determine both the total thermal insulation (I_t) and the resultant total thermal insulation (I_{tr}) according to ISO 9920 (ISO 9920 2007). The walking stand for the manikin was used to simulate walking speed of approximately *3.5 km/h* (step rate set at *90 steps/min*). Multiple equations (Table 2) were used to predict the resultant total thermal insulation (I_{tr}) and the results were compared to the measured values.

	Equation label	Area of application	
Standard ISO 9920	(32)	light or normal clothing	$0.6 < I_{cl} < 1.4$ clo
	(33)	no clothing	$I_{cl} = 0$ clo
	(34)	low insulated clothing	$0 < I_{cl} < 0.6$ clo
	(35)	specialized or high insulated clothing	$I_{cl} > 1.4$ clo
	(36)	very low wind activity	
Standard EN 342	(EN342)	cold protective clothing	

Table 2: Overview of multiple investigated equations from standards for predicting resultant thermal insulation from total thermal insulation values.

Two calculations methods to determine evaporative resistance provided by (ASTM F2370 - 10 2010) were used – the mass loss method and the heat loss method (Havenith et al. 2008b). Both of the methods are presented in detail in chapter 2 of this thesis. Two corrections, namely for the skin temperature of the manikin (Wang et al. 2010, 2011b) and for the heat gains from the environment (Wang et al. 2015) were also used and evaluated.

A detailed description of the used equipment, tested clothing and used methodology including detailed equations are provided in Paper III, Chapter 2.

5.3.2 Testing scenarios

Non-sweating thermal manikin was placed in the climate chamber in an upright posture with the arms hanging freely as this posture is typically reported in the studies. The manikin´s arms and legs were connected to an articulated stand to enable measurement of the resultant total thermal insulation under walking conditions (I_{tr}). Both clothing sets were tested twice in the static and walking posture. The manikin was also measured naked to determine the thermal insulation of the air layer (I_a). The total thermal insulation (I_t) of the manikin´s skin, which was used for the evaporative resistance calculation was also measured.

For the evaporative resistance measurements, the manikin was placed in the chamber in the same posture and on the same place as for thermal insulation measurements, with the whole setup placed on the scale to measure mass loss. The mass loss measurement was conducted once for each test only, due to the unavailability of the extra equipment needed. The heat loss method using pre-wetted skin was measured three times for each clothing ensemble. The air velocity was raised compared to the thermal insulation tests, to *0.54 ±0.16 m/s* to ensure even humidity distribution inside the climatic chamber. Evaporative resistance was only measured in static conditions as the measurement setup (with the scale) did not allow for the use of a walking stand.

5.3.3 Data analysis and sensitivity study

All thermal insulation values presented in this study are the averaged values of two independent measurements with a difference lower than *4 %* between them as required by the ISO 9920 standard (ISO 9920 2007). For the evaporative resistance measurements, the values presented, including standard deviation from the heat loss method, were calculated as an average of three independent measurements. However, the mass loss method was measured only once for each clothing ensemble as a control measurement; therefore, no standard deviation could be presented.

PHS simulations were performed as part of sensitivity analyses to assess how variations in clothing properties, obtained through different equations and corrections, would impact the maximum exposure time for workers. The assessment of maximum exposure time was conducted based on two distinct criteria:

- D_Tre, representing the time it took for an average worker to reach a core temperature limit of *38 °C* (occupational exposure limit).
- Dwl_50, indicating the time it took for an average worker to reach the limit for water (sweat) loss.

With the exception of the measured clothing parameters resultant intrinsic thermal insulation (I_{clr}), and moisture permeability index (i_m), derived from measured thermal insulation and evaporative resistance), all parameters for the PHS simulations remained constant and aligned with the environmental conditions during lunchtime in the sugarcane fields of Latin America.

5.3.4 Summary of the main findings

The difference between measured values of the resultant intrinsic thermal insulation and those calculated according to equation (32) in ISO 9920 (ISO 9920 2007) ranged from *-0.6 to -3.6 %*. The accuracy of the equation (32) is sufficient and the difference decreased with the rising total thermal insulation for the ensemble. Bigger differences were found comparing the measured values with the prediction from equation (35) (*-27.9 %* for SC and *-27.3 %* for PS) and from equation used in EN 342 (EN 342 2004) (*-16.3 %* for SC and *-18.8 %* for PS). The issues is to choose the correct equation for clothing ensemble as it is not clear in some cases. From the perspective of thermal insulation, equation (32) from ISO 9920 (ISO 9920 2007) was the best fit for our clothing ensembles. On the other hand, equation (35) is meant to be applied to specialized clothing with impermeable layers, which was also true for used clothing sets. Equation from EN 342 (EN 342 2004) for cold protective clothing yields better results than equation (35) as it also takes into consideration impermeable layers, but used ensembles are not cold protective clothes. Although, it is possible to use these predictive equations to enhance the precision of thermophysiological modelling in some cases, were it is clear which equation should be used, more versatile and robust equation should be developed on bigger database of clothing ensembles in the future.

For the evaporative resistance measurements, the mass loss and heat loss methods were firstly compared. For the SC ensemble, same results were obtained from both methods ($R_{et,h\_manikin}$ = $R_{et,m}$ = *26.7* m^2Pa/W). For the PS set, the difference was slightly higher, amounting to *4,4 %* ($R_{et,h\_manikin}$ = *83.7* m^2Pa/W and $R_{et,m}$ = *87.4* m^2Pa/W). Secondly, the discrepancies caused by the use of multiple corrections were investigated. In the mass loss method, the differences between values calculated from the manikin´s surface temperature and from the manikin´s skin temperature were *13.2 %* for the SC ensemble and *4.4 %* for the PS ensemble. Similarly, the heat loss method involved differences of *13.7 %* and *8.6 %* for SC and PS respectively. Moreover, when the correction for gains from the environment was used in the heat loss method, the differences compared to the raw values (calculated from the manikin´s surface temperature) were even higher *21.2 %* for SC and *8.7 %* for PS. We could see that the percentage differences between both the mass loss and the heat loss method are not significant when the same temperature (either the surface temperature or the skin temperature of the manikin) is used for their calculation. However, calculations based on the manikin´s surface temperature should not be used as this is not correct from a physical point of view. Water evaporates from the manikin's skin and not its surface, thus the vapor pressure of saturated skin needs to be used in the calculations.

The outcomes obtained through sensitivity analyses substantiate our observations regarding the utilization of the manikin's surface temperature. In the context of the SC ensemble, the criteria for core temperature were not met when the manikin's surface temperature was used in either the mass loss or heat loss approach. Conversely, when the projected skin temperature was adopted in both methods, the maximum exposure time was limited to approximately *55 minutes*. This discrepancy is substantial and holds the potential to introduce significant inaccuracies in PHS predictions, which could, in turn, have adverse implications for the well-being of sugarcane workers. When PS ensemble was used, the presence of multiple impermeable layers in the ensemble led to the minimal heat transfer between the skin and the

environment, causing the mentioned corrections to exert minimal influence on calculated evaporative resistance values. This observation was further confirmed by the findings from the sensitivity analysis, where there were no disparities in exposure time based on water loss criteria and the core temperature limit was promptly reached (approximately within 30 minutes) across all scenarios.

Three independent measurements of evaporative resistance using heat loss method were conducted for the both sets. For SC ensemble, the standard deviation of three measurements was 0.90 and the values were within *4 %* (from *-3.74 %* to *2.15 %*) from their mean value. For the PS set, the standard deviation of three measurements was *2.76* and the values were also within *4 %* (from *-3.63 %* to *2,36 %*) from their mean value. These results shows very good repeatability of the measurements in the area of required precision of thermal insulation measurements stated in ISO 9920 (ISO 9920 2007).

Results from this study show the need to correct for the pre-wetted skin temperature in the calculations of both methods in order for them to be physically correct. Other corrections should not be needed as they do not improve the results any further. Although, the correction for the pre-wetted skin temperature can be omitted when impermeable and high insulated clothing is used (in conformity with Wang (Wang et al. 2015)), it has minimal impact on evaporative resistance values or heat stress predictions when high insulated and impermeable clothing is used, therefore, they can be used in all cases for simplicity.

5.4 Paper IV (Objectives I and IV): Insulation and evaporative resistance values of clothing for sugarcane harvesters and chemical sprayers in Latin America, and their application in PHS model-based exposure predictions

This study measured the clothing properties used in sugarcane fields in Latin America and utilized them in a standard tool for heat strain prediction - PHS. The aim of the study was to use the clothing parameters obtained during the manikin measurements used also for Paper III to obtain a heat strain prediction for advanced planning of a workday and for possible preparation of preventive measures against heat stress for sugarcane workers. Although more sophisticated prediction models could be used, the fairly simple PHS model was chosen for this study, as this model is easily available for everybody through web tool, has a low cost and has been validated in a wide range of hot conditions. The goal is to see of this model is capable of predicting heat strain for this kind of applications, for which the more sophisticated models might be too expensive to use. Exposure characteristics were calculated as the limit values of the core temperature and water loss based on an hour-by-hour approach under the extreme weather conditions of a hot day (with ambient temperature ranging from *18.6 °C* to *36.4 °C* and ground temperature ranging from *20.5 °C* to *52.1 °C*). This analysis encompassed various combinations of activity levels. Predictions were made for each hour separately and did not reflect the physiological status of the previous hour, thus there might be some overestimations or underestimations of the duration limited exposure (DLE).

For manikin testing, local values of total (I_t) and resultant (I_{tr}) thermal insulation were presented to analyze the impact of the movement on thermal insulation for different parts of the body. For evaporative resistance measurements, the local values were also presented to see the difference between body parts, which is important for use in more sophisticated thermos-physiological models.

5.4.1 Summary of main findings

Firstly, the impact of walking simulation was analyze. The whole body total thermal insulation (I_t) and resultant thermal insulation were compared for both sugarcane cutters (SC) and chemical sprayers (CP), reaching the difference of *25.3 %* and *26.8 %* respectively. These values are comparable with the prediction equation 32 from ISO 9920 (ISO 9920 2007), which is in the agreement with the results from Paper III. However, local thermal insulation in different manikin zones (body part) may vary from *0 %* (on Head) to *-48 %* (right hand) when SC ensemble was used and from *-2 %* (Head) o *-39 %* (Upper arms) when CP ensemble was used. The results clearly show the effect of body parts' swinging radius or being rigidly fixed in the walking manikin tests, where the biggest changes are for hands and feet, followed by arms and legs, then torso zones and finally the head, which is basically stationary during the test. For technical measurements and various model evaluations, we need to consider what differences between the zones do not match the reality. This may be built in the established correction equations in the future, e.g., for walking. There is also possibility of applying a higher air velocity during the measurements to offset for these differences, which might be very challenging as the differences are not similar for each zones.

Secondly, the local values and differences between different body parts were studied also for evaporative resistance data and as expected, huge differences were observed. When SC set was used, the values varied from *6.0 m^2 Pa/W* (right hand) to *65.6 m^2 Pa/W* (feet with protective boots). Similarly for CP set, the values varied from *20.4 m^2 Pa/W* (head) to above *500 m^2 Pa/W* (belly), where two tight impermeable layers were used on top of each other. This study utilized

only the values for the complete ensembles in a standard occupational heat strain model PHS. However, it could be seen from the huge differences between body parts, why it is important to use sophisticated models with local values as input data for complex and more detailed purposes, for example in the area of protective clothing design development.

Lastly, measured clothing properties were used in the PHS model to predict heat train on hour-by-hour bases for workers on sugarcane fields in Nicaragua.

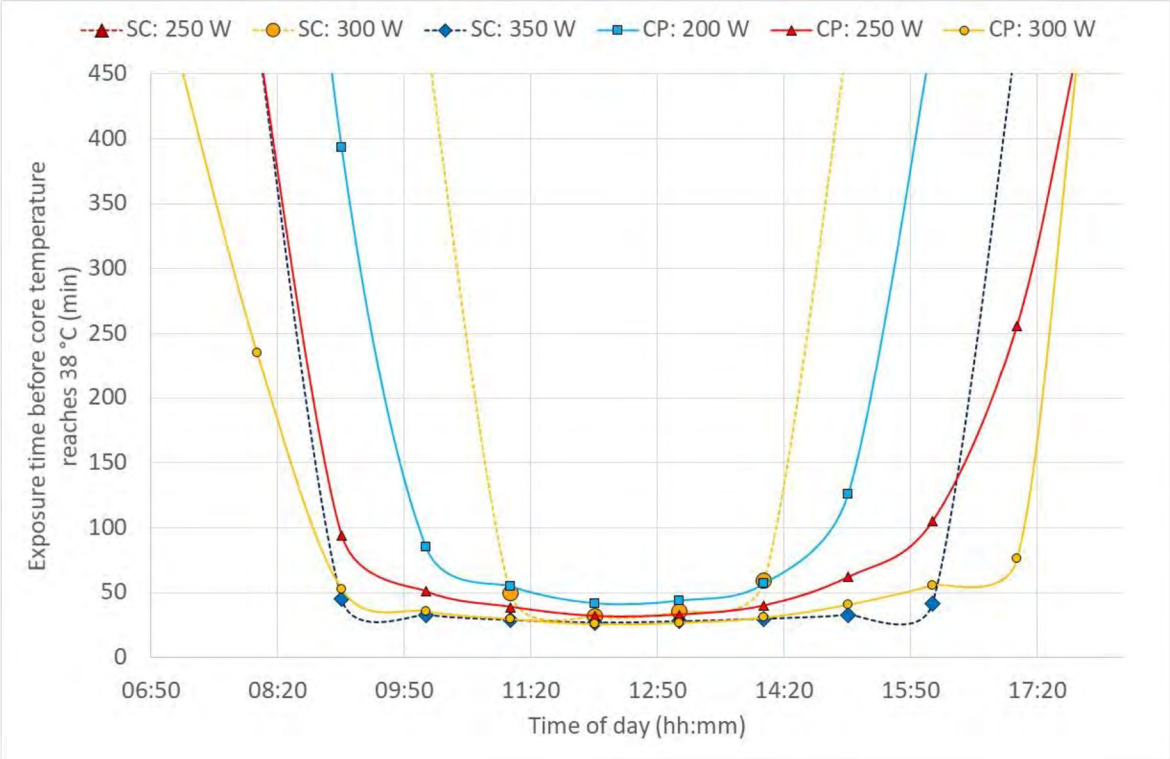

Figure 16: Expected daily duration limited exposure for sugarcane cutters (SC) and chemical sprayers (CP) at various activity levels based on core temperature (criterion Trec < *38 °C*). At the lowest activity for sugarcane cutters (SC: *250 W*), the duration limited exposure (DLE) was above *8 h (480 min),* and therefore, the line cannot be seen in this diagram.

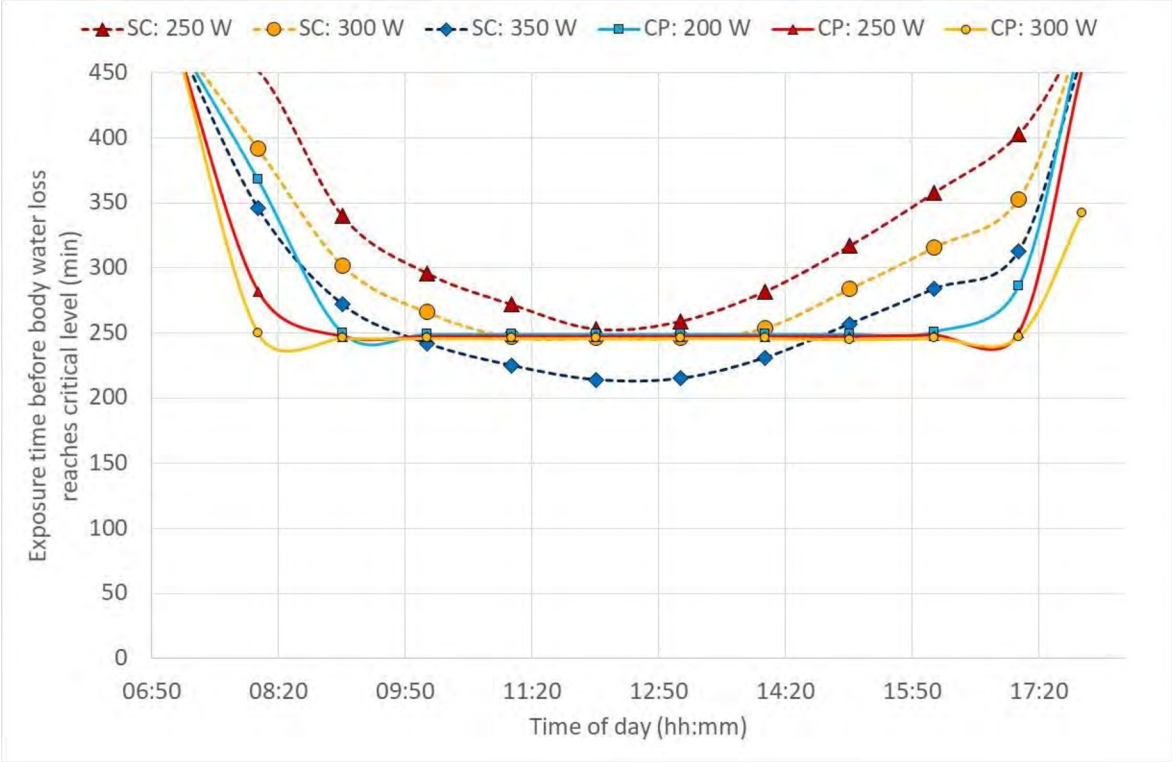

Figure 17: Expected daily duration limited exposure for sugarcane cutters (SC) and chemical sprayers (CP) at various activity levels based on water loss (criterion Dwl,lim < *5 %*).

The impact of heat exposure on workers wearing chemical protective clothing (CP) was significantly constrained by the rising core temperature, as indicated in Figure 16. In oppose, for sugarcane cutters (SC), core temperatures surpassed *38 °C* only during the most vigorous activities and the hottest periods of the day. In such instances, it is recommended that continuous exposure should not exceed *50 minutes*, and it becomes essential to incorporate regular breaks for rest and hydration. The findings strongly reinforce the established suggestion to incorporate extended recovery/lunch breaks (*>2 hours*) in shaded, well-ventilated areas during the peak heat of the day, along with adequate fluid replacement. While the sensation of thirst might not hold as much significance (Figure 17) compared to the increase in core temperature, dehydration can easily go unnoticed subconsciously (Parsons 2014). The results from the current study strongly recommend that more or less frequent drinking rest breaks should be enforced. By utilizing the PHS model to calculate water loss, recommendations for both the quantity and frequency of fluid intake can be approximated. Additionally, the PHS data offers insights into exposure duration and the optimal frequency of rest breaks, all based on core temperature calculations. This enables the evaluation of work situations, risk assessments and planning of the work/rest schedules. Although PHS model is very simple and have fair amount of limitations, it is fairly fast and easy to use tool to predict heat strain for specific environments and activities, which might be more useful in everyday situations than more sophisticated thermo-physiological models.

5.5 Paper V (Objectives V, VI and VII): Reproducibility of evaporative resistance measurements and calculations using different thermal manikins (to be published)

The aim of the final paper is to verify the reproducibility of the evaporative resistance measurements comparing the result from two different manikins measured in two different laboratories – Manikin TORE at Lund University and manikin NEWTON at BUT. The aim is to replicate the measurement scenario as much as possible and to compare the differences between the values obtained. Secondly, the goal is to accommodate all of the corrections for calculation of evaporative resistance from heat loss method proposed in the chapter 2.5 of this thesis and to analyze the impact of the corrections on the results. All corrections will be compared to the results of mass loss measurements using manikin´s skin temperature correction, as this values closer to the physical nature of heat transfer by sweating. As it is not possible to use mass loss method to obtain local evaporative resistance for different body parts, it is important to find the best possible calculation method for heat loss method, as it is crucial to obtain precise local values of clothing properties for thermo-physiological modelling. The study was conducted on 14 clothing ensembles covering the whole spectrum of thermal insulation from *0.5 clo to 3.2 clo* as described below.

5.5.1 Clothing ensembles

For the purpose of this study, *27* items from Taiga AB (Sweden) ambulance clothing system were tested individually on the thermal manikin Tore at Lund University according to ISO 15831 (ISO 15831 2004) following ISO 9920 (ISO 9920 2007) recommendations and basic insulation (I_{cl}) of each garment was calculated. More than *100* realistic clothing combinations were compiled and basic insulation was calculated according to the summation equation from ISO 9920 (ISO 9920 2007). Finally, *14* clothing ensembles were selected for this study from over *100* options to evenly cover values from *0.5 to 3.2 clo*. More information about used garments and detailed summation method research, calculation and validation could be found in (KUKLANE and TOMA 2021a).

Figure 18: 14 clothing ensembles from Taiga AB (Sweden) with basic thermal insulation from *0.5 to 3.2 clo* chosen for the study.

The clothing area factor (f_{cl}) of these ensembles were also measured using photographic method (same as Paper III.) for both manikins TORE and NEWTON. The f_{cl} estimation and calculation analysis for these particular clothing sets on manikin TORE is described in detail in a separate paper (KUKLANE and TOMA 2021b). For the NEWTON manikin, the same method was used. It could be seen that the values for NEWTON manikin are slightly higher (in average by *4,6 %*), which is probably caused by slightly bigger dimensions of the NEWTON manikin and small differences in the shape of some body parts.

Thermal insulation of chosen clothing ensembles (Table 3) were measured on manikin TORE at Lund University and were used in the calculation for evaporative resistance for both manikins, as there was no significant difference when measuring thermal insulation between the manikins.

	manikin TORE				***manikin NEWTON***			
Ensemble	f_{cl}	I_t	I_{cl}	I_{cl}	f_{cl}	I_t	I_{cl}	I_{cl}
	(-)	(m^2K/W)	(m^2K/W)	(clo)	(-)	(m^2K/W)	(m^2K/W)	(clo)
T1	1.15	0.164	0.082	0.53	1.22	0.164	0.087	0.56
T2	1.18	0.197	0.118	0.76	1.23	0.197	0.121	0.78
T3	1.27	0.277	0.204	1.31	1.34	0.277	0.208	1.34
T4	1.29	0.290	0.218	1.40	1.36	0.290	0.222	1.43
T5	1.39	0.336	0.269	1.74	1.41	0.336	0.270	1.74
T6	1.38	0.380	0.312	2.01	1.44	0.380	0.315	2.03
T7	1.28	0.298	0.226	1.45	1.36	0.298	0.230	1.48
T8	1.44	0.431	0.366	2.36	1.49	0.431	0.368	2.38
T9	1.40	0.386	0.319	2.06	1.47	0.386	0.322	2.08
T10	1.44	0.430	0.365	2.35	1.53	0.430	0.369	2.38
T11	1.41	0.440	0.373	2.41	1.48	0.440	0.377	2.43
T12	1.49	0.546	0.484	3.12	1.53	0.546	0.485	3.13
T13	1.49	0.557	0.495	3.19	1.53	0.557	0.496	3.20
T14	1.45	0.525	0.460	2.97	1.52	0.525	0.464	2.99

Table 3: Insulation and clothing are factor of selected clothing combinations for both TORE and NEWTON manikin.

5.5.2 Measurement setup and equipment

As it was mentioned already, manikin TORE (Kuklane et al. 2006) and manikin NEWTON (Thermetrics, Seattle, USA) (Fojtlín et al. 2016) were used for the purpose of the study. Both manikins are dry manikins with no water supply and sweating simulation was done using pre-wetted tight-fitting skin from the same material (thickness *d= 0.9 mm*, *95 %* cotton, *5 %* elastane). Measurements using manikin TORE were conducted in the climatic chamber at Lund University, with dimensions height × width × length: *2 400×2 360×3 200 mm* (detailed information in Paper III). The manikin was placed in upright posture with the arms hanging freely with the air flowing to the manikin´s back. The whole setup was put on the scale (Mettler Toledo K240) to measure mass loss. The whole setup was identical to the measurements from Paper III. For the manikin NEWTON measurements, the climate chamber in BUT (Fojtlín et al. 2016) was used, with dimensions height × width × length: *3 800×5 000×8 850 mm*. The setup was as close as possible to the measurements with manikin TORE - NEWTON was placed

in the upright posture with the arms hanging freely with the air flowing to the manikin´s back and the whole stand was placed on the scale (Lesak 1T6060-LN/060kg) with the same precision as the Mettler scale used at Lund University. It was possible to setup the same conditions in both climate chambers with air temperature of *34 ±0.2 °C*, air humidity of *40 ±5 %* and air velocity of around *0.45 ±0.1 m/s* measured in three different heights one meter from the back of the manikin. Both manikins had the skin temperature of *34 ±0.2 °C* set and controlled.

5.5.3 Methods and Results

All 14 ensembles were measured twice on both manikins. The results were calculated as an average value from the two measurements on each manikin. Only the correction for manikin´s skin temperature was used while analyzing the reproducibility of the measurement.

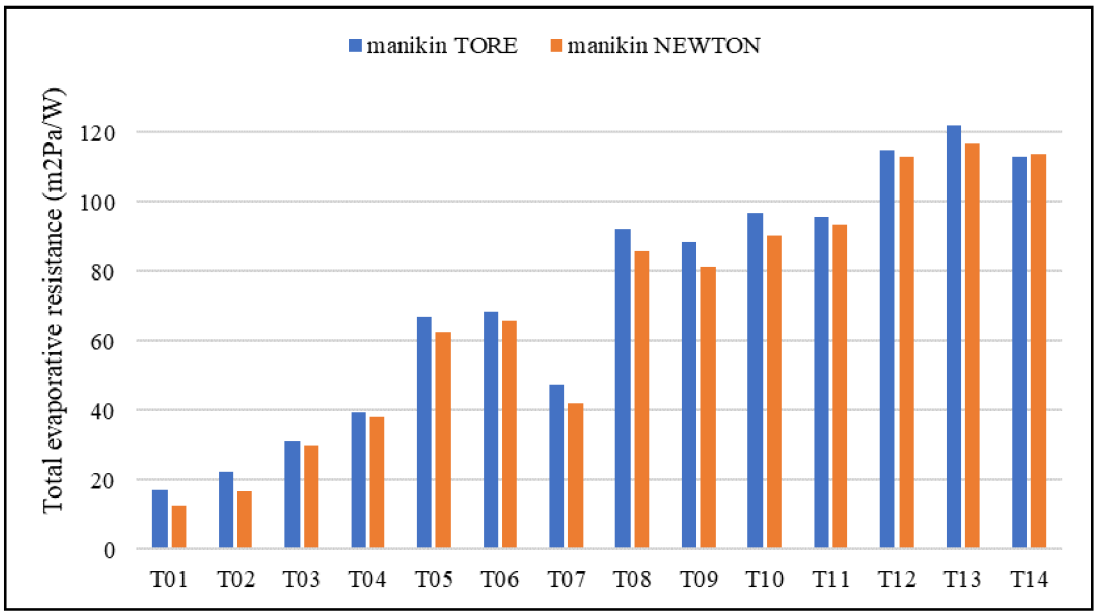

Figure 19: Comparison of total evaporative resistance values including correction for manikin´s skin temperature measured on both manikins calculated as an average of two measurements.

Paired two-tailed T-test was used to see if there is a difference between the total evaporative resistance (R_{et}) values obtain from different manikins. The p-value calculated from the T-test was *0.0000515* which means that there is enough evidence to suggest that there is a significant difference between these values. The same T-test was conducted for intrinsic evaporative resistance values (R_{ecl}) which takes into consideration slightly different shapes of the manikins´ bodies in form of clothing area factor (f_{cl}) for each ensemble. In this case, the p-value was *0.042*, which is very close to the significance level of *5 %* (*0.05*). For better visualization of the difference, the Bland-Altman graph was plotted from intrinsic evaporative resistance values (R_{ecl}). The limits of agreement (mean difference *±1.96* * standard deviation of differences) represent the range within which the differences between two measurements on different manikins are expected to fall with a level of confidence of *0.05*.

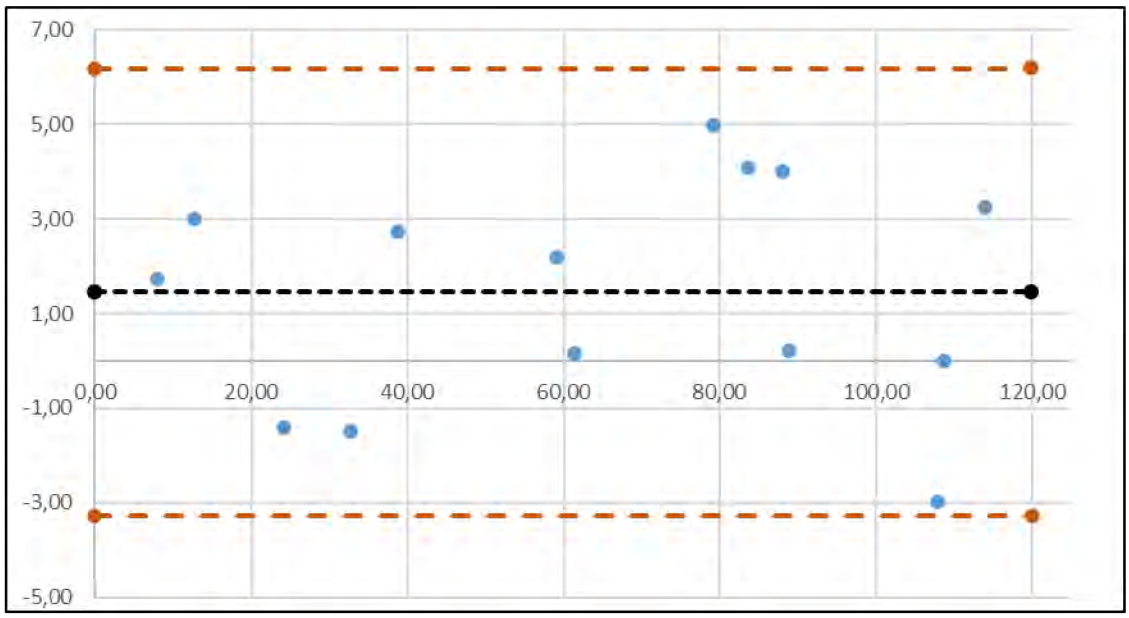

Figure 20: Bland-Altman plot for intrinsic evaporative resistance values (R_{ecl}) with level lower of agreement of *-3.26* and upper level of agreement of *6.18*.

As mentioned earlier, mass loss method directly determining the intensity of mass transfer by evaporation, with the correction for manikin´s skin temperature (as we are only able to control manikin surface temperature) calculated as $\boldsymbol{R_{et,mass}} = \frac{\Delta p_{iso} * A}{H_{e,mass}} = \frac{(p_{sk} - p_a) * A}{\lambda * \frac{dm}{dt}}$ is closer to the physical nature of heat transfer by sweating, it was taken as the etalon calculation for evaluation of all corrections for heat loss method. All of the corrections for heat loss method are descripted in detail in chapters 2.4 and 2.5 of this thesis and were all calculated for each clothing ensemble. Average values for each clothing set were calculated from all measurements (two measurements on TORE and two on NEWTON) for each correction. Paired two-tailed T-test was used to evaluate and compare the calculated total evaporative resistance (R_{et}) values from different corrections with the etalon value obtained from mass loss method using skin temperature ($R_{et\_Tskin\_mass\_loss}$). The same analysis was also done for intrinsic evaporative resistance (R_{ecl}) calculated using clothing area factors (f_{cl}). For the purposes of the correction evaluation, the *14* clothing ensembles were also divided into two groups and the corrections were tested in the same way using T-test for specific insulation groups – from *0.5 to 2.0 clo* and from *2.0 clo* to *3.2 clo*. The aim was to analyze the impact of the ensemble insulation on the calculated values through different corrections, as it was mentioned before that the corrections might be not needed for higher insulated clothing ensembles. Table 4 shows calculated p-values from T-test for all of the corrections. The p-values below level of significance of *0.05* shows that there is a significant difference between comparing values, which is not desirable as the aim is to get as close as possible to the values obtained from the mass loss method with manikin´s skin temperature correction applied.

Total evaporative resistance (R_{et})			
$R_{et\_Tskin\_mass\_loss}$	vs.	R_{et_Tskin}	**0.503**
		$R_{et\_Tskin\_Envi}$	0.000
		$R_{et\_Tskin\_Envi\_Itwet}$	0.000
		$R_{et\_Tskin\_fabric}$	0.000
		$R_{et\_Tskin\_fabric\_Envi}$	**0.749**
		$R_{et\_Tskin\_fabric\_Envi\_Itwet}$	**0.428**

Intrinsic evaporative resistance (R_{ecl})			
$R_{ecl\_Tskin\_mass\_loss}$	vs.	R_{ecl_Tskin}	**0.503**
		$R_{ecl\_Tskin\_Envi}$	0.003
		$R_{ecl\_Tskin\_Envi\_Itwet}$	0.000
		$R_{ecl\_Tskin\_fabric}$	0.080
		$R_{ecl\_Tskin\_fabric\_Envi}$	**0.346**
		$R_{ecl\_Tskin\_fabric\_Envi\_Itwet}$	**0.111**

Table 4: p-values from T-test comparing values calculated from different proposed corrections with the value calculated from mass loss method using correction for manikin´s skin temperature. Results showed both for total and intrinsic evaporative resistance.

5.5.4 Summary of main findings

According to the results of statistical analysis, there is significant difference between the measurements on the manikin TORE and manikin NEWTON. These differences could be caused by size of the chamber with different air flow. The air velocity was control near the manikins in both chambers as stated above, but the air flow in the rest of the chamber is impossible to measure and thus, it may cause some differences. Another cause of the difference could be slightly different shape of the manikin´s bodies. It is important to compare the intrinsic evaporative resistance values, as those are calculated using clothing area factor (f_{cl}) and takes into consideration the shape of the manikin and fitting of the clothes. When comparing the intrinsic values, the results of statistical analysis was very close to the level of significance of *5 %*. As stated in chapter 2 of this thesis, the replications of thermal insulations measurements should not vary by more than *10 %* from the mean value according to the ASTM standard (ASTM F1291-16 2016) and we set similar level of desired repeatability in our hypothesis also for evaporative resistance measurements. This was achieved in all but two clothing ensembles with lowest insulation – for ensemble T01, the difference from mean value was *10.89 %* and for ensemble T02 it was *11.96 %*. This could be caused by drying of some parts of the manikin (especially parts not covered with clothing) during the test, as it is complicated to ensure wetness of the manikin´s skin when the evaporation is high while avoiding water dripping from the manikin. For the rest of the ensembles , the difference from the mean value was within *4 %,* which is similar to the thermal insulation tests according to the ISO 9920 (ISO 9920 2007).

As mentioned earlier, the correction for manikin´s skin temperature should be implemented in both measuring methods to be correct from the physical point of view. The mass loss method was used as etalon. According to our statistical analysis, it is needed to use the correction for manikin´s skin temperature for both methods. Corrections for the gains from the environment and moisture content in the clothing did not show good correlation with etalon values, unless there were used together with the correction for manikin´s skin fabric. Integration of this correction is very problematic, as it requires lot of input data about manikin´s skin, which are difficult to obtain and there is a risk of importing error to the calculation via this input data.
According to our measurements, there are no should be no differences in calculations for ensembles with different insulation. The statistical analysis showed the same results for ensembles below and also above *2 clo*. Thus, the results suggest that using of the correction for manikin´s skin temperature for heat loss method should be enough to obtain the evaporative resistance values with sufficient precision for thermo-physiological modeling.

6 CONCLUSIONS

This PhD thesis showed the importance of obtaining precise clothing properties for the purpose of thermo-physiological modeling, methods to determine the thermal insulation (I_t), clothing area factor (f_{cl}) and most importantly, the development and integration of the measurement procedure and calculation methods to determine clothing evaporative resistance (R_{et}) using thermal manikin NEWTON at Brno University of Technology, including the precision validation and repeatability of the measurement.

The summary of the main conclusions from individual studies is as follows:

- Successful verification of the FMTK model, highlighting the importance to obtain precise clothing parameters as estimation is not sufficient.
- Estimation of clothing properties shows huge variations – the state-of-the-art methods to obtain clothing properties are using thermal manikin.
- It is necessary to use local values of clothing properties in thermo-physiological modeling to obtain precise predictions.
- Changing the body position results in a reorientation of various body parts and a redistribution of air gaps – it is important to obtain resultant clothing properties (I_{tr}).
- It is possible to calculate resultant thermal insulation (I_{tr}) from total thermal insulation (I_t) using equations in standards although one robust equation for all types of clothing would be beneficial.
- Methods to obtain thermal insulation (I_t) and clothing area factor (f_{cl}) are well documented and validated compared to methods to obtain and calculate evaporative resistance.
- Mass loss method is essentially correct, but it is currently not possible to obtain local values from this method due to technical limitations of the measurement equipment – heat loss method needs to be used to obtain local values..
- Correction for manikin´s skin temperature should be used in both mass loss and heat loss methods, as it is correct from physical point of view – we are only able to control manikin´s surface temperature, not pre-wetted skin temperature.
- Corrections for the gains from the environment and moisture content in the clothing should be used only in combination with the correction for manikin´s skin fabric.
- Correction for manikin´s skin fabric is complicated because multiple input data needed about manikin´s skin – risk of importing errors to calculation and not enhancing the results any further.
- Usage of heat loss method correction is not dependable on clothing´s insulation – corrections should be used for all ensembles even above *2 clo*.
- Using only the correction for manikin´s skin temperature is sufficient.
- Important to measure intrinsic evaporative resistance (R_{ecl}) – takes into account manikin´s shape and fitting to the clothing.
- Evaporative resistance (R_{et}) measurement and calculation successfully accommodate on manikin NEWTON at BUT.
- In all but two cases (*10.89 %* and *11.96 %),* the results are within *4 %* from the mean values, which is significantly better than *10 %* set in our hypothesis.

The evaporative resistance measurements were successfully accommodated and performed on manikin NEWTON at BUT. Methodology and calculation methods were compared and validated with the data from manikin TORE, as the manikin and laboratory at Lund University are participating also in round robin studies for standards and the evaporative resistance

measurements are well established there. The differences between measured values were in most cases within *4 %* which exceeded our expectations. In some case, similarly to the results published, the differences were higher (up to *12 %*) and occurred on the least insulated clothing ensembles, with some body parts not covered with clothing (see Figure 18 ensembles with shorts and short sleeves). The reason behind higher differences in lower insulated ensembles might be the different size of climate chambers (and thus different air flows in the chambers) at both Universities.

6.1 Future research

There are multiple areas which could be studied further in the field of evaporative resistance measurements.

- Heat loss method and its corrections were proposed and studied because it is very challenging, with current technical limitations, to obtain local values from the mass loss method, which is essentially correct and is closer to the physical essence of heat transfer by sweating. In this thesis, only the repeatability of the total evaporative resistance values were studied, thus it would be beneficial to study the repeatability of the measurements also for local values, as it was showed that local values are necessary to obtain precise thermo-physiological predictions.

- As it was showed in the thesis, the body posture can influence the orientation of various body parts and a redistribution of air gaps. Multiple equations for prediction resultant thermal insulation values are proposed and were studied in this thesis. It is important to note that these predictions are also made only for total values and not for local values. One robust equation would be beneficial to cover local values prediction for all types of clothing. Most importantly, there are no equations for calculation of resultant evaporative resistance. This is another huge area of knowledge gap, were it is necessary to either measure resultant evaporative resistance values (using movement simulation of the manikin) or to propose equation for its prediction from the static values.

- As the manikin measurements are complicated and require expensive equipment, it would be beneficial to find an alternative way to obtain or predict clothing properties. This is especially difficult for special and protective clothing with specific garments and impermeable layers.

6.2 Limitations

The sweat evaporation from the human body a clothing properties blocking this evaporation is such a complex process, that it is impossible to capture all its features with current technical equipment and methodology. For example, the sweat simulation on thermal manikin is even on all body parts and manikin´s surface temperature is also controlled on the same value, which is not the case in real situations. Another examples could be movement of the person wearing the clothes, moisture content stuck in the clothes from the previous activity, changing level of activity (sweating and cooling), changing air gaps or environmental conditions, such as changing temperature, air humidity or raining wetting the clothes from outside. Each of these effects plays a considerable role in the evaporation of the sweat and thus, in the thermoregulation of the person.

Further limitations are linked with the laboratory approach itself as several aspects presented in the real-life applications had to be omitted. For example, constant air flow, humidity and temperature in the climate chamber of the manikin or pre-set level of sweating.

7 REFERENCES

Angelova RA (2017) Working in Cold Environment: Clothing and Thermophysiological Comfort. In: Korhan O (ed) Occupational Health. IntechOpen, Rijeka

ASTM F1291-16 (2016) Standard Test Method for Measuring the Thermal Insulation of Clothing Using a Heated Manikin. West Conshohocken, PA

ASTM F2370 - 10 (2010) Standard Test Method for Measuring the Evaporative Resistance of Clothing Using a Sweating Manikin. West Conshohocken, PA

ASTM F2370-16 (2016) Standard Test Method for Measuring the Evaporative Resistance of Clothing Using a Sweating Manikin. West Conshohocken, PA

Błażejczyk K, Broede P, Fiala D, et al (2010) Principles of the New Universal Thermal Climate Index (UTCI) and its Application to Bioclimatic Research in European Scale. Miscellanea Geographica 14:91–102. https://doi.org/doi:10.2478/mgrsd-2010-0009

Budd GM (2008) Wet-bulb globe temperature (WBGT)—its history and its limitations. J Sci Med Sport 11:20–32. https://doi.org/10.1016/J.JSAMS.2007.07.003

Caravello V, McCullough EA, Ashley CD, Bernard TE (2008) Apparent evaporative resistance at critical conditions for five clothing ensembles. Eur J Appl Physiol 104:361–367. https://doi.org/10.1007/s00421-007-0655-9

Chen YS, Fan JT, Qian X, Zhang W (2004) Effect of garment fit on thermal insulation and evaporative resistance. TEXTILE RESEARCH JOURNAL 74:742–748. https://doi.org/10.1177/004051750407400814

Chen YS, Fan JT, Zhang W (2003) Clothing thermal insulation during sweating. Textile Research Journal 73:152–157. https://doi.org/10.1177/004051750307300210

ČSN ISO 7730 (1997) Mírné tepelné prostředí - Stanovení ukazatelů PMV a PPD a popis podmínek tepelné pohody. Český normalizační institut

de Dear RJ, Arens E, Hui Z, Oguro M (1997) Convective and radiative heat transfer coefficients for individual human body segments. Int J Biometeorol 40:141–156. https://doi.org/10.1007/s004840050035

EN 342 (2004) Protective clothing - ensembles and garments for protection against cold. Brussels, Belgium

Fan JT, Chen YS (2002) Measurement of clothing thermal insulation and moisture vapour resistance using a novel perspiring fabric thermal manikin. Meas Sci Technol 13:1115–1123. https://doi.org/10.1088/0957-0233/13/7/320

Fiala D, Lomas KJ, Stohrer M (1999) A computer model of human thermoregulation for a wide range of environmental conditions: the passive system. J Appl Physiol 87:1957–1972

Fojtlín M, Fišer J, Jícha M (2016) Determination of convective and radiative heat transfer coefficients using 34-zones thermal manikin: Uncertainty and reproducibility evaluation. Exp Therm Fluid Sci 77:257–264. https://doi.org/https://doi.org/10.1016/j.expthermflusci.2016.04.015

Fung F, Gao C, Hes L, Bajzik V (2020) Water vapor resistance measured on sweating thermal manikin and Permetest skin model in the vertical orientation . Communications in Development and Assembling of Textile Products 1:65–73. https://doi.org/10.25367/cdatp.2020.1.p65-73

Hall JF, Polte JW (1956) EFFECT OF WATER CONTENT AND COMPRESSION ON CLOTHING INSULATION. J Appl Physiol 8:539–545

Havenith G, Fiala D (2015) Thermal Indices and Thermophysiological Modeling for Heat Stress. In: Comprehensive Physiology. John Wiley & Sons, Ltd, pp 255–302

Havenith G, Fiala D, Błazejczyk K, et al (2012) The UTCI-clothing model. Int J Biometeorol 56:461–470. https://doi.org/10.1007/s00484-011-0451-4

Havenith G, Kuklane K, Fan J, et al (2015) A Database of Static Clothing Thermal Insulation and Vapor Permeability Values of Non-Western Ensembles for Use in ASHRAE Standard 55, ISO 7730 and ISO 9920. ASHRAE Trans 121:197–215

Havenith G, Richards MG, Wang XX, et al (2008a) Use of clothing vapor restistance values derived from manikin mass losses or isothermal heat losses may cause severe under and over estimation of heat stress. Proceedings of the 7th International Thermal Manikin and Modeling Meeting (7i3m) 1–2

Havenith G, Richards MG, Wang XX, et al (2008b) Apparent latent heat of evaporation from clothing: attenuation and “heat pipe” effects. J Appl Physiol 104:142–149. https://doi.org/10.1152/japplphysiol.00612.2007

Holmer I (2006) Protective clothing in hot environments. Ind Health 44:404–413. https://doi.org/10.2486/indhealth.44.404

Holmer I (2004) Thermal manikin history and applications. Eur J Appl Physiol 92:614–618. https://doi.org/10.1007/s00421-004-1135-0

ISO 7933 (2004) Ergonomics of the thermal environment - Analytical determination and interpretetion of heat stress using calculation of the predicted heat strain. Geneva, Switzerland

ISO 9920 (2007) Ergonomics of the thermal environment - Estimation of thermal insulation and water vapour resistance of a clothing ensemble. Geneva, Switzerland

ISO 11092 (2014) Textiles—Physiological Effects—Measurement of Thermal and Water-Vapour Resistance under Steady-State Conditions (Sweating Guarded-Hotplate Test). International Organization for Standardization (ISO), Geneva 0 grad-15 grad-30 grad 0 grad-15 grad-30 grad

ISO 15831 (2004) Clothing - Physiological effects - Measurement of thermal insulation by means of a thermal manikin. Geneva, Switzerland

Joshi A, Psikuta A, Bueno MA, et al (2019) Analytical clothing model for sensible heat transfer considering spatial heterogeneity. International Journal of Thermal Sciences 145:105949. https://doi.org/10.1016/J.IJTHERMALSCI.2019.05.005

Katić K, Li R, Zeiler W (2016) Thermophysiological models and their applications: A review. Build Environ 106:286–300. https://doi.org/10.1016/J.BUILDENV.2016.06.031

Kjellstrom T, Gabrysch S, Lemke B, Dear K (2009) The ‘Hothaps’ programme for assessing climate change impacts on occupational health and productivity: an invitation to carry out field studies. Glob Health Action 2:2082. https://doi.org/10.3402/gha.v2i0.2082

Koelblen B, Psikuta A, Bogdan A, et al (2017) Comparison of fabric skins for the simulation of sweating on thermal manikins. Int J Biometeorol 61:1519–1529. https://doi.org/10.1007/s00484-017-1331-3

Kuklane K, Heidmets S, Johansson T (2006) Improving thermal comfort in an orthopaedic aid: better boston brace for scoliosis patients. 343–351

KUKLANE K, TOMA R (2021a) Validation of ISO 9920 clothing item insulation summation method based on an ambulance personnel clothing system. Ind Health 59:27–33. https://doi.org/10.2486/indhealth.2020-0208

KUKLANE K, TOMA R (2021b) Common clothing area factor estimation equations are inaccurate for highly insulating (I_{cl}>2 clo) and non-western loose-fitting clothing ensembles. Ind Health 59:107–116. https://doi.org/10.2486/indhealth.2020-0209

Lotens WA, Vandelinde FJG, Havenith G (1995) EFFECTS OF CONDENSATION IN CLOTHING ON HEAT-TRANSFER. Ergonomics 38:1114–1131. https://doi.org/10.1080/00140139508925177

Lu Y, Wang F, Peng H (2016) Effect of two sweating simulation methods on clothing evaporative resistance in a so-called isothermal condition. Int J Biometeorol 60:1041–1049. https://doi.org/10.1007/s00484-015-1095-6

Mayor T, Wang F, Léonard J, Ribeiro M (2012) An interlaboratory study on measurements of clothing evaporative resistance with thermal manikins. In: The 5th European Conference on Protective Clothing and NOKOBETEF 10 (ECPC). pp 29–31

Mert E, Psikuta A, Bueno M-A, Rossi RM (2017) The effect of body postures on the distribution of air gap thickness and contact area. Int J Biometeorol 61:363–375. https://doi.org/10.1007/s00484-016-1217-9

Młynarczyk M, Havenith G, Léonard J, et al (2018) Inter-laboratory proficiency tests in measuring thermal insulation and evaporative resistance of clothing using the Newton-type thermal manikin. Textile Research Journal 88:453–466. https://doi.org/10.1177/0040517516681957

Nelson DA, Curlee JS, Curran AR, et al (2005) Determining localized garment insulation values from manikin studies: computational method and results. Eur J Appl Physiol 95:464–473. https://doi.org/10.1007/s00421-005-0033-4

Parsons K (2014) Human Thermal Environments: The Effects of Hot, Moderate, and Cold Environments on Human Health, Comfort, and Performance, 3rd edn. CRC Press, Inc., Boca Raton, FL, USA

Psikuta A, Mert E, Annaheim S, Rossi RM (2018) Local air gap thickness and contact area models for realistic simulation of human thermo-physiological response. Int J Biometeorol 62:1121–1134. https://doi.org/10.1007/s00484-018-1515-5

R. F. Goldman (2006) Thermal Manikins, Their Origins and Role,". In: SIXTH INTERNATIONAL THERMAL MANIKIN AND MODELLING MEETING (6I3M). pp 3–17

Richards MGM, McCullough EA (2005) Revised interlaboratory study of sweating thermal manikins including results from the sweating agile thermal manikin. Performance of Protective Clothing: Global Needs and Emerging Markets: 8th Symposium 27–39. https://doi.org/10.1520/stp12595s

Richards MGM, Rossi R, Meinander H, et al (2008) Dry and wet heat transfer through clothing dependent on the clothing properties under cold conditions. International Journal of Occupational Safety and Ergonomics 14:69–76. https://doi.org/10.1080/10803548.2008.11076750

Ross KA (2005) Evaluation of an Instrumented Sweating Manikin for Predicting Heat Stress in Firefighters' Turnout Ensembles. Master dissertation, North Carolina State University, NC

Ueno S, Sawada S (2012) Correction of the evaporative resistance of clothing by the temperature of skin fabric on a sweating and walking thermal manikin. Textile Research Journal 82:1143–1156. https://doi.org/10.1177/0040517511427966

Varheenmaa M (2014) A new generation sweating thermal manikin for the evaluation of the thermoregulation properties of protective clothing. proceedings of the 10th International Meeting on Thermal Manikin and Modelling (10i3m), Tampere, Finland 1–5

Veselá S, Psikuta A, Frijns AJH (2018) Local clothing thermal properties of typical office ensembles under realistic static and dynamic conditions. Int J Biometeorol 62:2215–2229. https://doi.org/10.1007/s00484-018-1625-0

Wang F, Havenith G, Mayor TS, et al (2014) Clothing real evaporative resistance determined by means of a sweating thermal manikin: a new round-robin study. In: Ambience14 & 10I3M, Scientific conference for Smart and functional textiles, Well-Being, Thermal comfort in clothing, Design, Thermal Manikins and Modelling

Wang FM (2017) Measurements of clothing evaporative resistance using a sweating thermal manikin: an overview. Ind Health 55:473–484

Wang FM, Gao CS, Kuklane K, Holmer I (2011a) Determination of Clothing Evaporative Resistance on a Sweating Thermal Manikin in an Isothermal Condition: Heat Loss Method or Mass Loss Method? Annals of Occupational Hygiene 55:775–783. https://doi.org/10.1093/annhyg/mer034

Wang FM, Gao CS, Kuklane K, Holmer I (2009) A Study on Evaporative Resistances of Two Skins Designed for Thermal Manikin Tore under Different Environmental Conditions. Textile Bioengineering and Informatics Symposium Proceedings, Vols 1 and 2 211–215. https://doi.org/10.3993/tbis2009039

Wang FM, Kuklane K, Gao C, Holmer I (2010) Development and validity of a universal empirical equation to predict skin surface temperature on thermal manikins. J Therm Biol 35:197–203. https://doi.org/10.1016/j.jtherbio.2010.03.004

Wang FM, Kuklane K, Gao CS, Holmer I (2011b) Effect of temperature difference between manikin and wet fabric skin surfaces on clothing evaporative resistance: how much error is there? (vol 56, pg 177, 2012). Int J Biometeorol 57:817. https://doi.org/10.1007/s00484-011-0512-8

Wang FM, Lai DD, Shi W, Fu M (2017) Effects of fabric thickness and material on apparent "wet" conductive thermal resistance of knitted fabric "skin" on sweating manikins. J Therm Biol 70:69–76. https://doi.org/10.1016/j.jtherbio.2017.03.004

Wang FM, Shi W, Lu YH, et al (2016) Effects of moisture content and clothing fit on clothing apparent "wet'' thermal insulation: A thermal manikin study." Textile Research Journal 86:57–63. https://doi.org/10.1177/0040517515580527

Wang FM, Zhang CJ, Lu YH (2015) Correction of the heat loss method for calculating clothing real evaporative resistance. J Therm Biol 52:45–51. https://doi.org/10.1016/j.jtherbio.2015.05.004

Xiaohong Z, Chunqin Z, Yingming Q, et al (2010) The thermal insulation difference of clothing ensembles on the dry and perspiration manikins. Meas Sci Technol 21:85203

Yu W, Wu YS, Fan JT (2011) Effect of posture positions on the evaporative resistance and thermal insulation of clothing. Ergonomics 54:301–313. https://doi.org/10.1080/00140139.2010.547604

8 LIST OF FIGURES AND TABLES

Figure 1: Sweating guarded hot plates SGHP-8.2 and Sweating thermal manikin Newton from Thermetrics, Advanced Thermal Measurement Technology, Seattle, USA; test person from Santra Technology, UK website.

Figure 2: Sweating manikin "Walter" from Hong Kong Polytechnic University with GORE-TEX skin, taken from (Fan and Chen 2002)

Figure 3: Sweating ´Newton´ type manikin with water supply through pores made by Thermetrics, Seattle, USA

Figure 4: Sweating manikin "Tore" from Lund University with pre-wetted skin on

Figure 5: The heat transfer mechanism among the manikin surface, the wetted skin and the environment in a so-called isothermal condition ($T_a = T_r = T_{manikin}$), adapted from (Wang et al. 2015)

Figure 6: Comparison of values of total evaporative resistance calculated by heat loss and mass loss methods taken from (Wang et al. 2011a)

Figure 7: Comparison of values of total evaporative resistance calculated by heat loss and mass loss methods taken from (Wang et al. 2009)

Figure 8: Comparison of values of total evaporative resistance calculated by heat loss and mass loss methods for three different clothing ensembles – permeable (PEM), semi-permeable (SEMI) and impermeable (IMP) taken from (Havenith et al. 2008a)

Figure 9: Comparison of temperature values measured t_{sk}, predicted by equation (4) – t_{sk_p1} , predicted by equation (5) – t_{sk_p2} taken from (Wang et al. 2010)

Figure 10: Comparison of R_{et} values calculated from prevailing mass loss method using manikin surface temperature – R_{et_m}, measured skin temperature – $R_{et\text{-}sk}$, predicted by equation (4) – $R_{et\text{-}p1}$, predicted by equation (5) – $R_{et\text{-}p2}$ taken from (Wang et al. 2010)

Figure 11: Comparison of R_{et} values calculated from prevailing heat loss method using manikin surface temperature – R_{et} (Temp of EWS), measured skin temperature – R_{et} (Temp of MT), predicted by equations for each part – R_{et} (Predictive temp by Ueno each part´s Eq), predicted by equation for whole manikin – R_{et} (Predictive temp by Ueno whole manikin Eq), predicted by Haveninth Eq. (Havenith et al. 2008b) and by Wang Eq. (Wang et al. 2010) taken from (Ueno and Sawada 2012)

Figure 12: effect of moisture content added to clothing on total thermal insulation loss (circle are data from (Hall and Polte 1956), rest of the data and graph itself is taken from (Lu et al. 2016)

Figure 13: Effect of fabric thickness on the apparent ´wet´ thermal insulation of manikin´s sweating skins for both cotton and polyester material, taken from (Wang 2017)

Figure 14: Comparison of total evaporative resistance values on two ensembles EN1 and EN2 calculated from prevailing method (manikin surface temperature) – $R_{et,c}$, from measured skin temperature – $R_{et,m}$ and from predicted skin temperatures for each ´skin´ material option – $R_{et,p}$, taken from (Wang 2017)

Figure 15: Comparison of real evaporative resistance values on 5 ensembles and two nude cases calculated from prevailing method (manikin surface temperature) – $R_{et,heat}$, from mass loss method – $R_{et,mass}$ and from corrected heat loss method – $R_{et,heat,corr}$, taken from (Wang et al. 2015)

Figure 16: Expected daily duration limited exposure for sugarcane cutters (SC) and chemical sprayers (CP) at various activity levels based on core temperature (criterion $T_{rec} < 38$ °C). At the lowest activity for sugarcane cutters (SC: *250 W*), the duration limited exposure (DLE) was above 8 h (480 min), and therefore, the line cannot be seen in this diagram.

Figure 17: Expected daily duration limited exposure for sugarcane cutters (SC) and chemical sprayers (CP) at various activity levels based on water loss (criterion $D_{wl,lim} < 5$ %).

Figure 18: 14 clothing ensembles from Taiga AB (Sweden) with basic thermal insulation from *0.5 to 3.2 clo* chosen for the study.

Figure 19: Comparison of total evaporative resistance values including correction for manikin´s skin temperature measured on both manikins calculated as an average of two measurements..

Figure 20: Bland-Altman plot for intrinsic evaporative resistance values (R_{ecl}) with level lower of agreement of *-3.26* and upper level of agreement of *6.18*.

Table 1: Summary of the examined scenarios

Table 2: Overview of multiple investigated equations from standards for predicting resultant thermal insulation from total thermal insulation values.

Table 3: Insulation and clothing are factor of selected clothing combinations for both TORE and NEWTON manikin.

Table 4: P-values from T-test comparing values calculated from different proposed corrections with the value calculated from mass loss method using correction for manikin´s skin temperature. Results showed both for total and intrinsic evaporative resistance.

9 LIST OF SYMBOLS

T_{skin}	manikin´s skin temperature	[°C]
T_a	ambient temperature of the environment	[°C]
T_r	radiant temperature in environment	[°C]
$T_{manikin}$	manikin´s surface temperature	[°C]
R_{et}	total clothing evaporative resistance	[kPa.m2/W]
H_e	calculated evaporative heat loss	[W]
H_t	total evaporative heat loss	[W]
H_d	dry evaporative heat loss	[W]
Δp_{iso}	water vapor pressure gradient between wet skin and manikin surface	[kPa]
$R_{et,mass}$	total clothing evaporative resistance calculated by mass loss method	[kPa.m2/W]
$H_{e,mass}$	calculated evaporative heat loss from mass loss rate	[W]
Δp_{iso}	water vapor pressure gradient between wet skin and manikin surface	[kPa]
A	sweating surface area	[m2]
λ	vaporization heat of water at measured skin temperature	[W.h/g]
dm/dt	evaporation rate of moisture from the wet skin	[g/h]
$R_{et,heat}$	total clothing evaporative resistance calculated by heat loss method	[kPa.m2/W]
$H_{e,heat}$	evaporative heat loss from manikin´s surface	[W]
T_{sk}	predicted manikin´s skin temperature	[°C]
HL	heat loss from manikin´s total sweating area – heat flux	[W/m2]
R_{ecl}	clothing intrinsic evaporative resistance	[kPa.m^2/W]
R_{ea}	evaporative resistance of the boundary surface air layer	[kPa.m^2/W]
f_{cl}	clothing area factor	[-]
$I_{t,apparent}$	clothing apparent ´wet´ thermal insulation	[m^2.K/W]
I_t	clothing dry thermal insulation	[m^2.K/W]
I_c	intrinsic clothing insulation	[m^2.K/W]

I_{tr}	resultant clothing insulation	[m^2.K/W]
w_t	the amount of moisture contained in the tested clothing $0 < w_t <$ 800g	[g]
AR_{et}	apparent evaporative resistance	[kPa.m^2/W]
$R_{et,real}$	real evaporative resistance	[kPa.m^2/W]
AI_{wet}	apparent ´wet´ thermal insulation of the fabric	[m^2.K/W]
d_{fabric}	fabric thickness	[mm]
ρ_{fiber}	fiber density	[kg/m^3]
ρ_w	water density	[kg/m^3]
k_{fiber}	fiber thermal conductivity	[W/m.K]
k_w	water thermal conductivity	[W/m.K]
m_{fabric}	fabric´s mass per unit area	[g/m^2]
w_c	water content in fabric	[% g/g]
Q_{evap}	corrected heat loss for moisture evaporation	[W]
$R_{et,heat,corr}$	total real evaporative resistance calculated by corrected heat loss method	[kPa.m2/W]
RH_a	relative humidity of ambient air	[%]
P_a	ambient air vapor pressure	[kPa]
P_{sk}	saturated skin vapor pressure	[kPa]

10 APPENDICES

Building and Environment 126 (2017) 13–26

Contents lists available at ScienceDirect

Building and Environment

journal homepage: www.elsevier.com/locate/buildenv

Verification of Fiala-based human thermophysiological model and its application to protective clothing under high metabolic rates

Jan Pokorný [a, *], Jan Fišer [a], Miloš Fojtlín [a], Barbora Kopečková [a], Róbert Toma [a], Jiří Slabotínský [b], Miroslav Jícha [a]

[a] Brno University of Technology, Faculty of Mechanical Engineering, Energy Institute, Technická 2896/2, Brno, Czech Republic
[b] National Institute for Nuclear, Chemical and Biological Protection, Kpt. Jaroše 1924/5, Brno, Czech Republic

ARTICLE INFO

Article history:
Received 15 June 2017
Received in revised form
3 August 2017
Accepted 8 August 2017
Available online 10 August 2017

Keywords:
Thermophysiological model
Protective clothing
NBC suit
Thermal comfort
Heat stress
Matlab

ABSTRACT

In the past years, a theory of how to predict human heat stress and thermal comfort using advanced thermo-physiological models has been broadly extended. These models are more complex than the well-established overall indices of the heat stress (ISO 7933) and thermal comfort (ISO 7730) and they allow to simulate the effects of metabolism, thermoregulation, and clothing on human thermal state in greater detail. However, the most discussed issue is a validity of such complex models. The validation process of multi-segment thermophysiological models has to be focused not only on the overall parameters, but also on the local ones. The aim of this study is to verify our implementation of Fiala-based model with similar models and measurements. To conclude with, the results were in a good agreement with the original Fiala model with respect to the simulation of the passive system, the active system, and the DTS index (Dynamical Thermal Sensation) for a wide range of ambient temperatures (from 5 °C to 48 °C). Further, the study covers testing of protective clothing, such as Tychem-F and military NBC (nuclear, biological, chemical) suit FOP M2000 including the Klimatex underwear. The mean absolute deviations (MAD) of rectal temperature, mean skin temperature, and local skin temperatures, valid for protective clothing in a range from 25 °C to 40 °C and metabolic rates up to 4.3 met, were 0.20 °C, 0.78 °C and 1.25 °C respectively.

1. Introduction

The interaction with ambient thermal environments is everyday experience of human beings. Mostly, it is not wittingly perceived and people respond to the stimulus subconsciously, especially when the conditions are comfortable. In uncomfortable environments (hot or cold), people tend to acclimatize themselves by altering their clothing, posture, activity or HVAC setting (Heating, Ventilation & Air-conditioning). If this is not applicable, the exposure to an inappropriate thermal load is perceived as a thermal stress, which can lead, in extreme situations, to hypothermia or hyperthermia. To reduce these risks, mainly under challenging environmental conditions, a well-designed and correctly used protective clothing is needed. A special category of protective clothing is a chemical protective clothing that prevents contamination of human skin and respiratory system with hazardous materials. Fabrics used to produce protective suits are typically less permeable compared to standard materials, or even impermeable. This directly influences sweat evaporation, moisture transport, and reduces effective cooling power of moisture evaporation, which may cause a severe heat stress under warm/hot conditions or at higher metabolic rates. In extreme situations, an uncompensable heat stress manifested by uncontrolled body temperature rise is life threatening. To prevent hazards of heat stroke, the design of chemical protective clothing plays an essential role with respect to its protective abilities and permeability properties. Moreover, there is also a need to test the already commercially available ensembles and reveal their performance under typical conditions of operation. In the case of environmental conditions with a fixed metabolic rate according to Fletcher et al. [1], the exposure is considered safe until the deep body temperature exceeds 38.5 °C.

For the fast screening of the effect of environmental conditions on a human, it is possible to use well established indices expressing the heat stress, such as: PHS (Predicted Heat Strain) - ISO 7933 [2], WBGT (Wet Bulb Globe Temperature) - ISO 7243 [3], and thermal

* Corresponding author.
E-mail address: pokorny.j@fme.vutbr.cz (J. Pokorný).

https://doi.org/10.1016/j.buildenv.2017.08.017
0360-1323/

sensation and comfort PMV/PPD (Predicted Mean Vote/Predicted Percentage of Dissatisfied) - ISO 7730 [4]. PHS and PMV indices are based on the overall heat balance of the human body and require a small amount of input data to quickly yield reasonably accurate results.

On the other hand, in some cases, these results have a rather coarse character and need to be taken carefully. Mainly in the case of the protective clothing and higher metabolic rates, the more complex thermophysiological models are recommended to be used instead: "*It should be noted that WBGT is rough screening index, and for screening such as simplification may be acceptable. For detailed analysis of protective clothing effects, more complex models would be needed though*" [5]. In the cited paper by Havenith & Fiala, a variety of problems regarding heat stress indices and thermophysiological modelling are discussed along with their limitations and recent development.

Thermophysiological models simulate human physiological responses in a complex way describing the heat transfer phenomena inside the body, and also the heat exchange with the ambient environment. Generally, these types of models are able to take into account: (1) the body constitution (weight, height, fat percentage, etc.), thermoregulation and cardiovascular system; (2) environmental conditions (air temperature, air speed, relative humidity, and mean radiant temperature); (3) personal factors (activity level, clothing insulation – thermal resistance and water vapour permeability).

One of the first and major motivations to develop human thermophysiological models was the evaluation of heat stress under various environmental conditions. Attempts to compose numerical models started in the 60's of 20th century as a part of medical research for military purposes. Such models were aimed to simulate the physical characteristics of the human thermal regulatory system in transient conditions including a simulation of blood vessel system (for detailed description see Wissler's 225-nodes model [6]). A later 25-node model by Stolwijk [7] was used for NASA to monitor the performance of Apollo astronauts. The main improvement of the model was an incorporation of thermoregulatory mathematical model. The development of the multi-segment models continued with the Fiala [8] and Tanabe [9] models designed also for thermal comfort applications. Their motivation was to extend the capability of the approach to deal with the asymmetric transient environmental conditions, which is not possible with the whole-body thermal comfort models based on the heat balance principle, e.g. Fanger [10] and Gagge [11]. Until now this issue has not been solved completely and there is a need for reliable thermal sensation/comfort predictions that are capable to capture non-uniform transient conditions, with a potential to become a basis for ISO standard [12].

Today, except for the original codes by Wissler et al. [6,13] and Fiala [8,14], there are other Fiala-based models either for scientific purposes (e.g. ThermoSEM [15,16]) or codes implemented in commercial software (e.g. Theseus-FE [17], Radtherm [18]). Certain models allow for personalization of the input parameters, namely body weight, percentage of body fat, etc. Although the theory behind the Fiala model is well described and documented, the model is mostly a part of commercial software and the source code is proprietary.

The reliability of the Fiala physiological model was the motivation to derive the Universal Thermal Climate Index (UTCI) [19], which was proved to be a more complex indicator of human thermal stress than the previous individual heat stress indices [20]. Also, a combination of Fiala-based model as the virtual manikin with the real thermal manikin was investigated by Hepokoski et al. [18]. In recent years, a virtual manikin has been incorporated and coupled with the advance simulation tools dealing with the complex simulation of heat transfer using the CFD (Computational Fluid Dynamics). This opens a new space for virtual thermal comfort engineering to directly investigate the local effects of the environment on the human using thermophysiological models for a detailed design and case studies [21–23].

The research in the field of thermoregulation models lasts for more than 60 years and the development of advanced models was also influenced by the rise of computational power. The introduction of the UTCI index was one of the first achievements that contribute to a higher acceptability of thermophysiological models by the community in environmental ergonomics. Yet, there are still many challenges with regards to special applications of the model, e.g. the area of protective clothing, thermal comfort predictions, and exploitation of physical or virtual thermal manikins.

Apart from plentiful opportunities, every simulation has its disadvantages which stem mainly from its complexity. On one hand, complex models provide detailed results about human thermal state; on the other hand, they require rather detailed input data. Katić [24] states that "*Even though sophisticated models were developed … the accuracy of the inputs has to be assured in order to incorporate models in the design process of buildings and daily applications of thermal comfort*". In practical applications, this means that a precise determination of environmental and personal parameters is essential to obtain satisfactory results. Moreover, the equipment required to do so might be available only in laboratory conditions. From the authors' experience, the problematical part is a precise specification of the metabolic rate. Even more uncertainty lies in identification of local insulation and permeability properties of clothing. Both mentioned parameters are defined as follows.

Metabolic rate can be specified by ISO 8996 [25]. "*The direct measurement of oxygen consumption provides the most accurate estimate of metabolic heat production. However, it is difficult to measure oxygen uptake in the field … These limitations make other, simpler, metabolic rate evaluation methods more practical for field measurements. Other methods to assess heat production are direct and indirect calorimetry methods and simpler indirect methods based on heart-rate measurements*" [26].

Thermal and evaporative resistance of clothing can be determined according to ISO 9920 [27] and also directly measured using a guarded hot plate - ISO 11092 [28] or a thermal manikin - ISO 15831 [29]. The thermal manikin has a human body shape which predetermines it as a suitable tool for the exact measurement of heat transfer coefficients at human body surface as was described in Refs. [30,31]. However, a detailed specification of clothing properties for each individual is rather problematic. The main problem is a dressing procedure specific for each person, which implies hardly predicable air gaps and openings. Also, permeability of membranes and thermal resistance of garments depend on the treatment with this specific piece of clothing over time (washing, etc.). Another fact to consider is that the data in ISO 9920 are mostly measured on a stationary manikin while in the field the actual thermal resistance is typically lower than in laboratory conditions. Namely, the human body motion inflicts the boundary layer at the clothing surface, and even the air flow through the clothing layers and in the air gaps is more intensive.

1.1. Motivation

A wide acceptability of the Fiala model is mainly because of its extensive validation by different laboratories. Martinéz et al. [32] verified the latest version of the original Fiala model (FPCm5.3) against experimental data. The root-mean-square deviations (rmsd) of core, mean skin and local skin temperatures were 0.26 °C, 0.92 °C and 1.32 °C respectively.

These results correspond with findings of Psikuta: "*In particular,*

good agreement for the mean skin temperature (typically < 1°C deviations, rmsd of 1.3°C) was shown for the Tanabe and UTCI-Fiala model". In the case of deep body core temperature *"differences between Tanabe model and reported data of 0.6 °C and for the UTCI-Fiala model of 0.2°C on average"* [33]. In this study the Fiala model was tested for 59 exposures to cold, moderate, warm and heat-stress environmental conditions. However, only four tests no. 11, 12 (Mekjavic, unpublished) and no. 22, 23 (Gonzalez [34]) were performed for protective clothing in warm/hot environment in combination with higher metabolic rates, which is a typical issue to deal with when the chemical protective clothing is worn. In the first pair of tests, the prediction was the most problematic among all validation cases, and in the latter case, even the information on the skin temperatures were missing and not evaluated at all. Thus, more studies related to chemical protective clothing in warm/hot conditions are demanded mainly due to the prediction of heat stress caused by restricted moisture transport.

Interest in prediction of thermal comfort using thermophysiological models led us to implement the Tanabe-based model with a counter current heat exchange of blood. This was done firstly in Dymola and later in the Matlab environment [35,36]. Further demands for more precise predictions were followed by implementation of the Fiala-based model [37], called FMTK (as a direct translation from Czech language - Physiological Model of Thermal Comfort). The model was built from the literature sources [8,17,38] and implemented again in Matlab.

In this paper, the final version of our Fiala-based human thermophysiological model FMTK is presented along with its evaluation based on literature and also the experimental data relating to the evaluation of chemical protective clothing.

2. Methods

The FMTK model describes an average man as it was originally defined in Fiala [8]. The model was modified and implemented in Matlab with resolution of 19 segments: 1_Head, 2_Face, 3_Neck, 4,5_Shoulders, 6_Thorax, 7_Abdomen, 8–11_Arms, 12,13_Hands, 14–17_Legs, 18–19_Feet with altogether 49 sectors see Fig. 1, right and Table 1. Below, there is a list of adopted modifications correspond to Theseus-FE model developed by P+Z engineering [17].

- Extended number of segments from 15 to 19 – Arms and Legs are split to upper and lower parts.
- Shoulders are considered without counter-current heat exchange of blood flow.

Additionally, the FMTK model differs in discretization.

- Thorax-Inferior, Abdomen-Inferior sectors and Shoulders segments are each split into two parts
- Each tissue layer is divided into 6 nodes – it is especially needed in case of Head to precisely calculate hypothalamus temperature.
- The Crank-Nicolson discretization scheme was used for solving the tissue temperatures in time, the central blood pool temperature was calculated implicitly as in Ref. [8] and the surface temperatures of clothing were calculated explicitly.

Finally, a simple graphical user interface (Fig. 1, left) was created that allows us to define boundary conditions and the specific clothing properties. Boundary conditions can be prescribed as uniform or specific for each of the 49 sectors including the properties of clothing as thermal resistance, evaporative resistance, and clothing area factor.

2.1. Verification of FMTK model

Implementation and verification of a thermophysiological model is usually carried out in three steps. Firstly, validity of the passive system is verified in simple environmental conditions. For this purpose, it is possible to use less complex tools, e.g. Fanger's PMV model [4] without heat accumulation and heat transfer in tissue. Secondly, validation of the active system is crucial in transient conditions to reveal the dynamic aspects of human

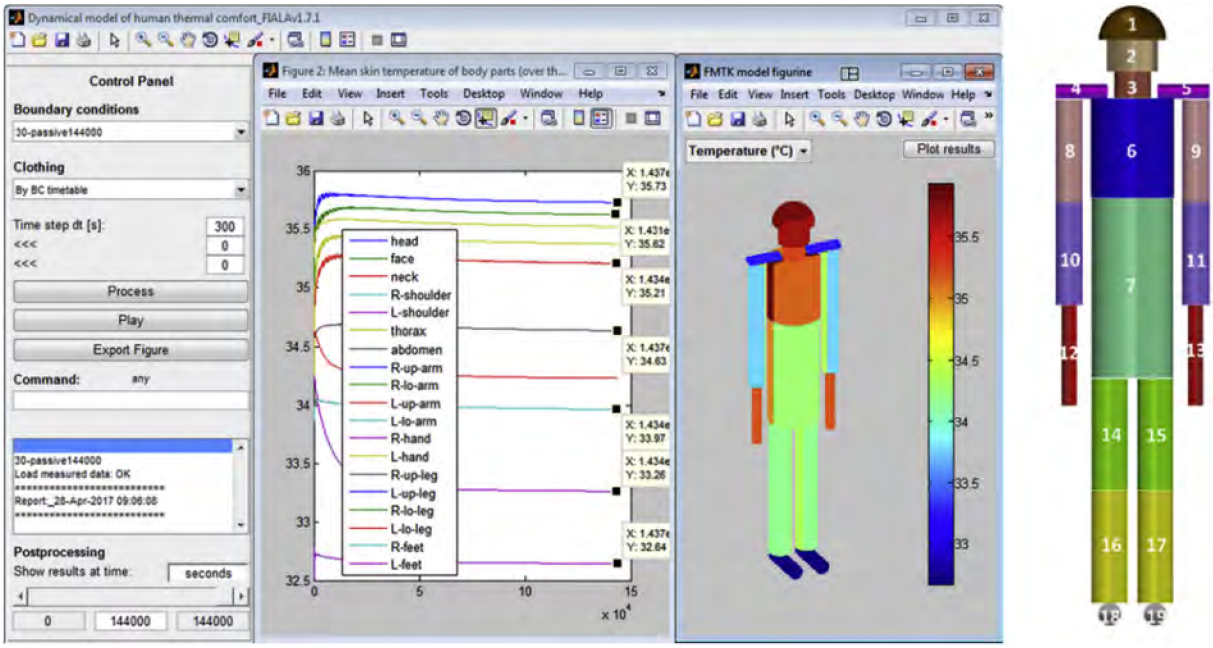

Fig. 1. Left – The graphical user interface of FMTK model, with evaluation of the passive system test case. Right – model proportions and its discretization onto 19 segments and 49 sectors (front view).

Table 1
Overview of considered models to evaluate FMTK model.

Model		Origin	Segments (Sectors)	Tissue nodes	Equations/ Numeric	Remark: Implemented in | by	
Fanger's PMV	[4]	Original	1 (1)	1	Algebraic/BM	Excel	Pokorny
Tanabe-based	[35]	Based on [9]	16 (16)	64	DAEs/DASSL	Dymola	Pokorny
Fiala	[8]	Original	15 (33)	193[a]	PDEs/FDM	Delphi	Fiala
Theseus-FE	[17]	Based on [8]	19 (45)	478[a]	PDEs/FEM	Fortran, C++	P+Z
FMTK model		Based on [8]	19 (49)	1230[a]	PDE/FVM	Matlab	Pokorny

AbbreviationsBM - bisection method; ODEs & PDEs - ordinary & partial differential equations; FDM & FVM & FEM - Finite Difference & & Volume & Element Method; DAEs - differential algebraic equations; DASSL - a differential/algebraic system solver used in Dymola.
[a] The number of tissue nodes representing PDEs depends on the spatial discretization of layers and sectors.

thermoregulation. In the third step, a correlation of thermal comfort with experimental data is derived.

For these three steps, datasets from literature including experimental data were used. A list of test cases was chosen according to the validation manual [39] where also the comparison of the original Fiala model [8] and Theseus-FE model [17] is stated. These models were chosen as the etalon for the verification of the passive and active system. Moreover, the Tanabe-based model [35] was added to this study as a comparison to show the performance of a simpler, but still reliable model. This model extends the Tanabe model [9] by the counter-current heat exchange of blood flow in blood-vessels. Table 1 specifies basic characteristics of all human models considered in this study to evaluate FMTK model.

A simulation of the passive system solves the heat transfer in a human body without any consideration of thermoregulation. The importance of a correctly working passive system lies in utilization of the skin temperatures for the simulation of the active system as set-points. In the passive system simulations, the virtual manikin was nude (0 clo) in standing posture with metabolic rate $M = 0.8$ met. Further boundary conditions are specified in Table 2, i.e. ambient air temperature T_a, mean radiant temperature T_r, relative humidity RH and air velocity v.

All tests of the active system were done for various metabolic rates, ambient temperatures and relative humidities. Other parameters such as air velocity $v = 0.1$ m/s, standing posture, and in intrinsic clothing insulation $I_{cl} = 0.04$ clo ("Shorts only", see Table 5) were common to all cases. Each of them started with a preconditioning phase to stabilize the human subjects, at least for 20 min, typically 60 min. The preconditioning phase is marked with grey background (Table 3). The results of preconditioning were not an object of interest and are not plotted in the resulting graphs in Chapter 3.1.

2.2. Application of FMTK model to protective clothing

This chapter presents an application of the FMTK model for higher metabolic rates and the protective clothing used for chemical protection to extend the validation database presented by Psikuta [33]. The experimental data were collected by Czech National Institute for Nuclear, Chemical and Biological Protection (NINCBP) in a dedicated climate chamber.

A motivation of the NINCBP to perform the presented tests was to create a database of safe exposure time for defined metabolic rate, various warm/hot ambient conditions, and protective clothing types. The range of tested temperatures was from 25 °C to 40 °C because the ventilation and permeability of this clothing is limited, which may lead to hyperthermia in hot environments. Based on this data, NINCBP establishes the recommendations of how and how long to use the protective ensembles to avoid health risk during the mission.

Three types of ensembles (Fig. 2) were investigated as follows: (1) Klimatex underwear; (2) military NBC suit FOP M2000 (shortly FOP, Czech translation of NBC suit). (3) chemical-protective clothing Tychem-F.

In total, the FMTK model was applied in 9 cases (Table 4). The relative humidity (RH) was kept constant (20%) except for the case 5 *FOP 35 °C* (RH = 50%) and the case 8 *Tychem-F 35 °C* (RH = 27%). The air velocity in the test chamber was caused only by the movement of the test person and it was up to 0.2 m/s, apart from the case 8 *Tychem-F 35 °C* ($v = 1.5$ m/s).

The test procedure consisted of the following steps. Firstly, the person was preconditioned for 10 min in the desired conditions at the room temperature of 23 °C. During preconditioning, a volunteer was equipped with the skin and rectal temperature probes, cardio pulse meter, and dressed up in the specific clothing (estimated as a standing activity 1.5 met, in Shorts only). Then the person entered the climatic chamber to start the test procedure by 5-min rest. Finally, the protocol prescribes the following procedure which was repeated until the end of the test: 20 min exercise (walking of 4 m/s on the treadmill with 10% elevation, 3.2–4.3 met) and then 5 min rest (sitting, 1 met). The maximum total time of exposure was 125 min. The objective criterion to stop the test before the appointed time was to exceed the limit of the rectal temperature of 38.5 °C. Next, if the test person started to be fully exhausted, the test was immediately ended to avoid severe strain or even a loss of consciousness.

The rectal (deep body core temperature) and surface temperatures were measured every minute in accordance with ISO 9886 [44]. The local surface temperatures were measured on the Forehead, R scapula, L thorax, R arm, L arm, L hand, R thigh and L calf using ALMEMO 2590-4AS data logger and calibrated thermocouples with precision of 0.01 °C. The rectal temperature and the heart rate were measured with a MEDIPORT-System. Another recorded parameter was the sweat production determined on the basis of weight difference of the test person and the clothing before and after the experiment. A metabolic rate was identified according to ISO 8996 [25] using a spirometric-telemetric device Oxycon Mobile measuring the oxygen consumption.

Clothing properties were identified independently on the test procedure see Table 5. The material properties of "Shorts only"

Table 2
Passive system test case.

Test case/parameter		t (hours)	$T_a = T_r$ (°C)	RH (%)	v (m/s)	M (met)
1	Neutral 30 °C naked (0 clo)	40	30	40	0.05	0.8

Table 3
Active system test cases [7,40-43].

Test case\parameter			t (min)	T_a=T_r (°C)	RH (%)	M (met)
1	Very cold	[40]	25-125	28-5	45-70	0.8-0.8
2	Very cold	[41]	20-130	30-10	67-67	0.8-0.8
3	Very cold	[42]	60-240	17-13	40-40	4.0-1.0
4	Cold	[43]	60-120	20-15	40-40	1.5-0.9
5	Neutral and cold	[42]	60-60-120-60	22-28-18-28	40-40-40-40	2.5-1.15
6	Neutral and hot	[42]	60-60-120-60	29-28-48-28	43-43-27-43	2.0-1.0
7	Hot and cold	[42]	60-60-120-60	25-43-17-43	30-30-30-30	2.5-1
8	Neutral and warm	[42]	60-60-120-60	26-28-33-28	34-34-37-34	2.0-1.0
9	Cold and hot	[42]	60-60-120-60	24-18-42-18	30-30-30-30	2.0-1.0
10	High activity	[7]	60-30-30-30-30-30-30-30	27-30-30-30-30-30-30-30	40-40-40-40-40-40-40-40	1-1-3-1-5-1-8-1

Fig. 2. Tested clothing, from the left to the right: Klimatex underwear, FOP and Tychem-F.

Table 4
Tests cases made in climate chamber of NINCBP.

Test case/parameter		t (min)	$T_a = T_r$ (°C)	RH (%)	M (met)	M (W/m^2)
1–4	Klimatex underwear	125, 95, 95, 65	25, 30, 35, 40	20,20,20,20	3.2	170–200
5–6	FOP	83, 125	35, 40	50, 20	3.7	213
7–9	Tychem-F	75, 60, 55	30, 35, 40	20,27,20	4.3	250

ensemble (0.04 clo) were taken from Theory manual [17], other ensembles were measured by thermal manikin Newton. Because the FMTK model requires intrinsic thermal resistances of clothing, additional measurements were performed with nude manikin to subtract the effect of air layer on the outer surface of clothing. The overall intrinsic thermal resistances of clothing were as follows: Tychem-F (1.06 clo), FOP (1.08 clo), both including the Klimatex underwear (0.37 clo). These values were calculated from local intrinsic resistances by a parallel method using the passive system simulation as was described in Ref. [8].

The clothing surface area factor f_{cl} was estimated according to formula (1) [45], where R_{cl} (m^{2}K/W) and I_{cl} (clo) are intrinsic thermal resistances of clothing.

$$f_{cl} = 1 + I_{cl} \times 0.31 = 1 + (R_{cl}/0.155) \times 0.31\ (-) \quad (1)$$

The resultant thermal resistance was considered different for the resting and walking (4 km/h) period. During walking the thermal insulation was estimated as 71% of stationary value. These values were calculated by using ISO 9920 formulas [46]. An average value of moisture permeability index of clothing i_{cl} (−) was suggested for Klimatex underwear ($i_{cl} = 0.4$) and the FOP ($i_{cl} = 0.34$), roughly according to the findings from McCullough et al. [47]. Using this estimate allows to calculate directly the evaporative resistance according to formula (2), where L_e is Lewis constant 0.0165 K/Pa.

$$R_{ecl} = R_{cl}/(i_{cl} \times L_e)\ (\mathrm{m^2Pa/W}) \quad (2)$$

A calculation of evaporative resistance should be used only if the real measured values of R_{ecl} are not known, because i_{cl} estimate brings an error into the input data. Only in the case of Tychem-F, the moisture permeability index $i_{cl} = 0.03$ was determined from the overall value of evaporative R_{ecl} and thermal R_{cl} resistance obtained from the measurement using the sweating manikin [48]. However,

no information on local evaporative properties of the FOP and Tychem-F ensemble was found. In Tychem-F simulations, it is assumed that the moisture permeability index for all parts equals to 0.03. In the case of FOP for the respirator (face), rubber boots (feet) and rubber gloves (hands), i_{cl} of 0.03 is assumed instead of 0.34. The NINCBP tests were focused on the comparison of various types of clothing ensembles worn by one and the same subject rather than testing of only one ensemble by a larger group of people. It means that the standard deviation of the measurement with test persons could not be identified. However, it was possible to estimate a typical deviation based on the experience with similar experiments, which was considered 0.2 °C in the case of deep body core temperature, mean skin temperature of 0.5 °C, and local skin temperature of 1 °C.

A prediction error was then expressed using the mean absolute deviation (MAD), which is the sum of absolute differences between the actual and the predicted value divided by the number of observations (equation (3)), where y_i is the i-th estimated value, x_i the i-th measured value.

$$\mathrm{MAD} = \sum_{i=1}^{n} |y_i - x_i| / n \tag{3}$$

3. Results

This chapter refers to the results of FMTK model for the cases defined in the methodology. At first, the verification of FMTK model using the dataset from literature is presented and then its application to the chemical protective clothing is shown.

3.1. Verification of FMTK model

This chapter presents the passive system parameters – mean skin and rectal temperatures together with the evaporative heat loss – for the following conditions: ambient temperatures from 5 °C to 48 °C and metabolic production from 0.8 to 9 met.

3.1.1. Passive system

The passive system was evaluated for the case *Neutral 30 °C naked* while all thermoregulation signals were switched off. The surface area of human was considered 1.86 m^2 for Fiala-based models and 1.87 m^2 for Fanger and Tanabe-based models. Table 6 shows a comparison of the main results of typical overall parameters for various types of models including the Fanger's PMV model according to ISO 7730. The basal metabolic rate, mean skin temperatures, and hypothalamus temperatures in all models were approximately the same. It can be seen that the definition of convective HTC (heat transfer coefficients) in the Fiala model and the Fanger models yield different results for the same condition, i.e. 3.45 vs 2.7 W/m^2K. In the FMTK model, the same formula was used for local HTC as in Fiala [8] and Theseus-FE [17].

All the above mentioned parameters of the passive system, presented in Table 6, indicate that the FMTK model can solve uniform steady state conditions. However, even more important than whole body parameters are the results of the local temperatures (mostly skin and muscles), which are used to establish the set points for the active system. A comparison of the local skin temperatures with the Theseus-FE model for all 49 sectors is shown in Fig. 3. MAD of skin temperatures over all sectors is equal to 0.07 °C, the maximal absolute deviation is 0.14 °C for the Face. MAD of blood temperatures of all segments is 0.06 °C.

3.1.2. Active system

The verification of the active system was done for 10 cases based on the experimental data referred to in Table 3. Results of the study are summarized as follow: (1) mean skin temperatures Fig. 4 and Fig. 5; (2) rectal temperatures Fig. 6; (3) evaporative heat losses Fig. 7.

3.1.3. Thermal sensation

The DTS index (Dynamic Thermal Sensation) was introduced by Fiala [8] to predict a thermal sensation using a thermophysiological model. The advantage of DTS is its comparability with the PMV model and experimental data because of the same 7-point scale (from −3 to +3) defined by ASHRAE Standard 55 [49]. The index of overall thermal sensation *So* related to the Berkeley model [50] is also based on the core temperature, mean skin temperatures, and their time derivation. The results of thermal sensation predictions are plotted in the graphs in Fig. 8. The difference between the sensation models lies in the fact that the Berkeley model uses the extended 9-point ASHRAE scale (+4 Very hot, +3 Hot, +2 Warm, +1 Slightly warm, 0 Neutral, −1 Slightly cool, −2 Cool, −3 Cold, −4 Very cold). Moreover, the Berkeley model has the ability to predict thermal comfort locally, which DTS cannot.

Table 5
Clothing parameters used in the simulations.

Clothing	Underwear		FOP		Tychem-F		Shorts only	
Segment	R_{cl}	R_{ecl}	R_{cl}	R_{ecl}	R_{cl}	R_{ecl}	R_{cl}	R_{ecl}
	m^2K/W	m^2Pa/W	m^2K/W	m^2Pa/W	m^2K/W	m^2Pa/W	m^2K/W	m^2Pa/W
Head, Neck	0.000	0.0	0.051	9.1	0.051	103.0	0.000	0.0
Face	0.000	0.0	0.051	103.0	0.051	103.0	0.000	0.0
Shoulders	0.030	4.5	0.126	22.5	0.185	373.7	0.000	0.0
Abdomen Posterior	0.071	15.2	0.217	38.7	0.230	464.6	0.036	4.0
Anterior, Inferior	0.058	12.3	0.231	41.2	0.239	482.8		
Thorax Posterior	0.071	15.2	0.217	38.7	0.230	464.6	0.000	0.0
Anterior, Inferior	0.058	12.3	0.231	41.2	0.239	482.8		
Up. arm	0.050	7.6	0.209	37.3	0.177	357.6	0.000	0.0
Lo. arm	0.051	7.7	0.151	26.9	0.146	294.9	0.000	0.0
Hands	0.000	0.0	0.051	103.0	0.051	103.0	0.000	0.0
Up. leg	0.091	13.8	0.400	71.3	0.287	579.8	0.000	0.0
Lo. leg	0.039	5.9	0.123	21.9	0.129	260.6	0.000	0.0
Feet	0.097	14.7	0.103	208.0	0.109	220.2	0.000	0.0
Overall resistance	**0.058**	**8.8**	**0.168**	**51.9**	**0.165**	**334.7**	**0.006**	**0.9**

Values are valid for resting period (1 met). Values applied for walking simulations are considered as 71% of stated values in the table.

Table 6
Passive system simulation – neutral environment.

Parameter			Fanger (ISO 7730)	Fiala model	Theseus-FE	Tanabe-based model	(FMTK, 2017)
M	W	Basal metabolic rate	87.07	87.10	87.13	87.05	**87.14**
$T_{sk,m}$	°C	Mean skin temperature	34.40	34.40	34.42	34.40	**34.39**
$T_{mu,m}$	°C	Mean muscle temperature	–	36.20	36.02	35.25	**36.29**
T_{hy}	°C	Hypothalamus temperature	–	37.00	36.89	36.97	**36.94**
T_{re}	°C	Rectal temperature	–	36.88	36.79	37.06	**36.84**
$h_{c,m}$	W/m^2·K	Convection HTC	3.45[a]	2.70	2.66	2.79	**2.66**
$h_{r,m}$	W/m^2·K	Radiation HTC	–	5.00	4.50	4.62	**4.50**
Q_c	W	Convection heat loss	28.33[a]	21.50	21.83	23.63	**22.47**
Q_r	W	Radiation heat loss	37.02	38.90	36.94	37.05	**36.28**
Q_e	W	Evaporation heat loss	21.16	18.10	19.43	19.72	**19.43**
Q_{res}	W	Respiration heat loss	6.66	8.50	8.93	6.66	**8.95**
Q_{sum}	**W**	**Total heat loss**	**93.16**[a]	**87.00**	**87.13**	**87.06**	**87.13**

[a] If the value of $h_{c,m}$ in the case of Fanger model will be assumed 2.71 instead of 3.45, then the convention heat loss Q_c would be lower by 6.05 W and total heat loss Q_{sum} in the case of Fanger model will be 87.11 W. This example illustrates the importance of defining HTC as accurate as possible especially for the convection.

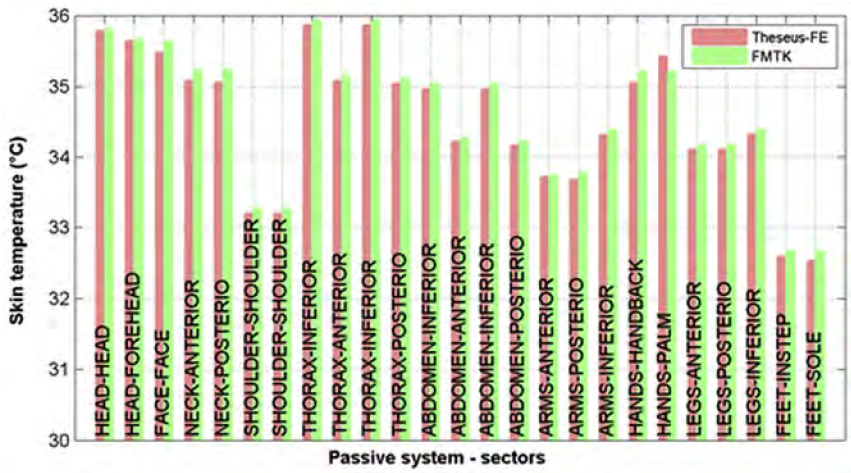

Fig. 3. Passive system simulation – neutral environment. Comparison of local skin temperatures for all 49 sectors. Pair segments yield identical results in the uniform environment, only 25 sectors are plotted.

3.2. Application of FMTK model to protective clothing

The FMTK model was applied for tests defined in Table 4. The aim of simulations was to predict the rectal temperature increase and the time to reach a safety limit (38.5 °C) for various types of protective clothing.

Presented simulations use the intrinsic thermal insulation calculated using the measured local thermal insulations for nude manikin and other prescribed ensembles in Table 5. Moreover, the effect of the walking on the reduction of thermal insulation was considered. A 10-min preconditioning period outside the chamber at 23 °C, 1.5 met, semi-nude ("Shorts only") is not plotted.

3.2.1. Mean skin and rectal temperature

The rectal temperature is the critical parameter to assess the heat stress, whereas the mean skin temperature is suitable to indicate the sweating effectiveness. The results of tests with underwear are plotted in Fig. 9 while those with FOP and Tychem-F are plotted in Fig. 10.

In the latter figure, the first graph on the left shows a time schedule of activity levels prescribed for the experiment. However, some tests had to be interrupted because the safety limit was reached. Further, even if the test person was walking on the treadmill in the same way during all tests, the metabolic rates differed. They were dependent on the selected clothing ensemble mainly due to the weight of clothing and the effect of respiratory mask. In the case of underwear, the metabolic rates correspond to 3.2 met, FOP 3.7 met, and Tychem-F 4.3 met. These values represent an average metabolic rate during walking period.

Table 7 presents the summary of the results; the prediction error is expressed by MAD calculated for all samples of the given case (1 min sampling rate). The prediction error of rectal temperature at the end of the test is up to 1.1 °C in the case of *FOP 40 °C*, with the overall MAD = 0.59 °C. The prediction error of the mean skin temperature at the end of the test is up to 2.3 °C, also in the case *FOP 40 °C*, with the overall MAD = 1.51 °C.

The overall value of MAD is then calculated from all samples of all tests: the prediction of rectal temperature shows MAD = 0.20 °C and the mean skin temperature shows the MAD = 0.78 °C.

3.2.2. Local skin temperatures

The overall MAD of local temperature prediction is 1.25 °C (see Table 8), where also the values of MADs for specific body parts and types of clothing are stated. The most problematic specific parts to predict the local temperatures were Forehead (Tychem-F) and R. arm (FOP); however, in average, the highest difference was in the case of underwear. Predictions on the Forehead were inaccurate mainly because of the respiration mask that covers the whole face. In the case of underwear, the results would be closer to the experiment if a lower insulation was considered.

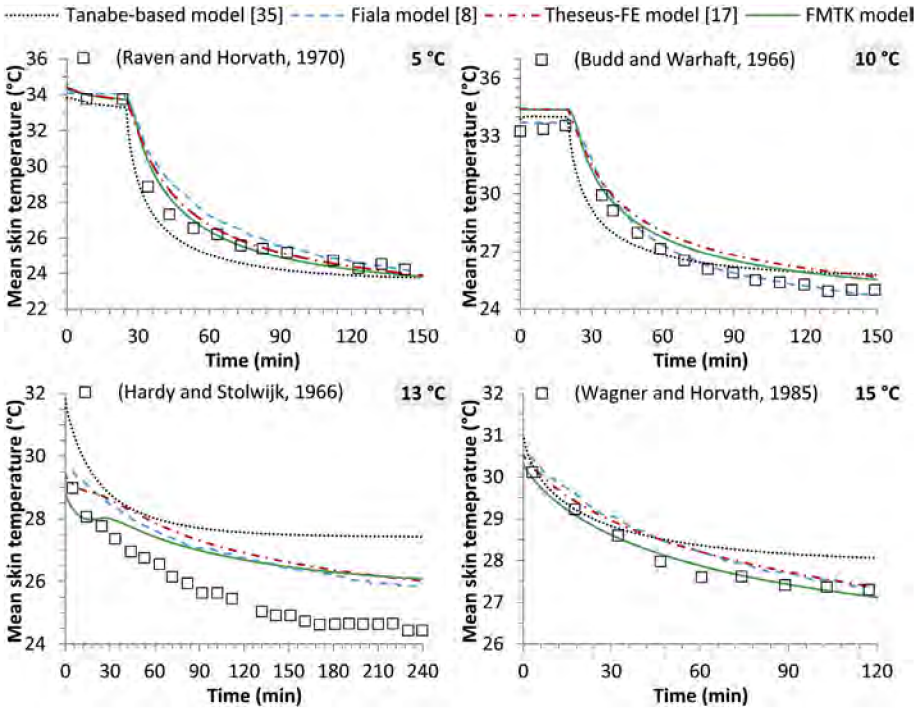

Fig. 4. Active system simulation – mean skin temperature – cold environment with stable conditions.

3.2.3. Metabolic rate

In all protective clothing tests, the values of metabolic rates were measured using an oxygen consumption method. In the field tests, simpler methods, such as measurement of heart rate, are more practical. Therefore, it was of our interest to find out how the measured metabolic rates correlate with the calculated rates using the estimation formulas from ISO 8996 (Fig. 11). It can be seen that when the protective clothing is not used, the correlation between the measured *M (met)* value and that calculated from the heart beat rate (ISO 8996) is good. However, metabolic rates determined according to simple formulas show the results with a significant error (up to 2 met) when applied to less permeable protective clothing (FOP and Tychem-F). Our explanation of this phenomenon is as follows: an overheated human body tends to increase the blood flow rate to be cooled down. Moreover, a restricted evaporation, given by the protective garment, creates unnatural boundary conditions for which the formulas listed in ISO 8996 were not derived.

4. Discussion

4.1. Verification of the model

In the first part of this paper, the Fiala model, commercial Fiala-based model and our Tanabe-based and Fiala-based (FMTK) models were compared in a wide range of environmental conditions. These models can provide similar results only if the predictions of skin temperatures by the passive system are quite the same because the simulated skin temperatures define the set points of active system, which has a substantial impact on the model predictions.

4.1.1. Passive system

A match between the Fanger's PMV, Fiala, Fiala-based, and Tanabe-based models in the case of passive system parameters is very good. PMV model is not able to predict all physiological parameters such as the core and local skin temperatures, but it provides credible results of overall heat exchange with the environment close to neutral and steady state conditions. From the heat loss parameters, it is clear that FMTK's predictions are closer to the Theseus-FE model than the original Fiala model, which is mainly due to the changes in accordance with the Theseus-FE model. Small discrepancies appear in the case of respiratory losses when the Tanabe-based and PMV models predict lower values compared to the Fiala and Fiala-based models.

A very good agreement was achieved in the validation of the passive system where the maximum error of local skin temperature is 0.14 °C (Face sector) and in average only 0.07 °C. Local temperatures of FMTK for all 49 sectors match very well with the Theseus-FE model, see Fig. 3. This initial step of the study proved that the passive system of FMTK works comparably well similarly to the other models. Therefore, the verified passive system can be used as a basis for the active system simulation of the FMTK model.

4.1.2. Active system

The active system validation followed the Theseus-FE virtual manikin validation manual [39]. The agreement was very good in all transient test cases (in the ambient temperature range from 5 to 48 °C), small differences were found in the simulation of higher metabolic rates. The presented results show a very good agreement between the FMTK model and the Theseus-FE model, and the conformity of these models with the original Fiala model is also eminent. The Tanabe-based model is less accurate in the prediction of core temperature in cold environment (5 °C). Nevertheless, this type of model is also convenient for the use in heat stress and thermal comfort applications.

As the first conclusion, it is true to say that the FMTK model has been verified. The results of all models provide a very good estimate of human thermoregulatory response to the ambient environment. The original Fiala and Fiala-based models fit data more precisely than the Tanabe-based model, although there are slight differences between these models (see Table 1). It should be noted that even the two models of the same type may yield slightly different results because they may use different input data (e.g., heat transfer

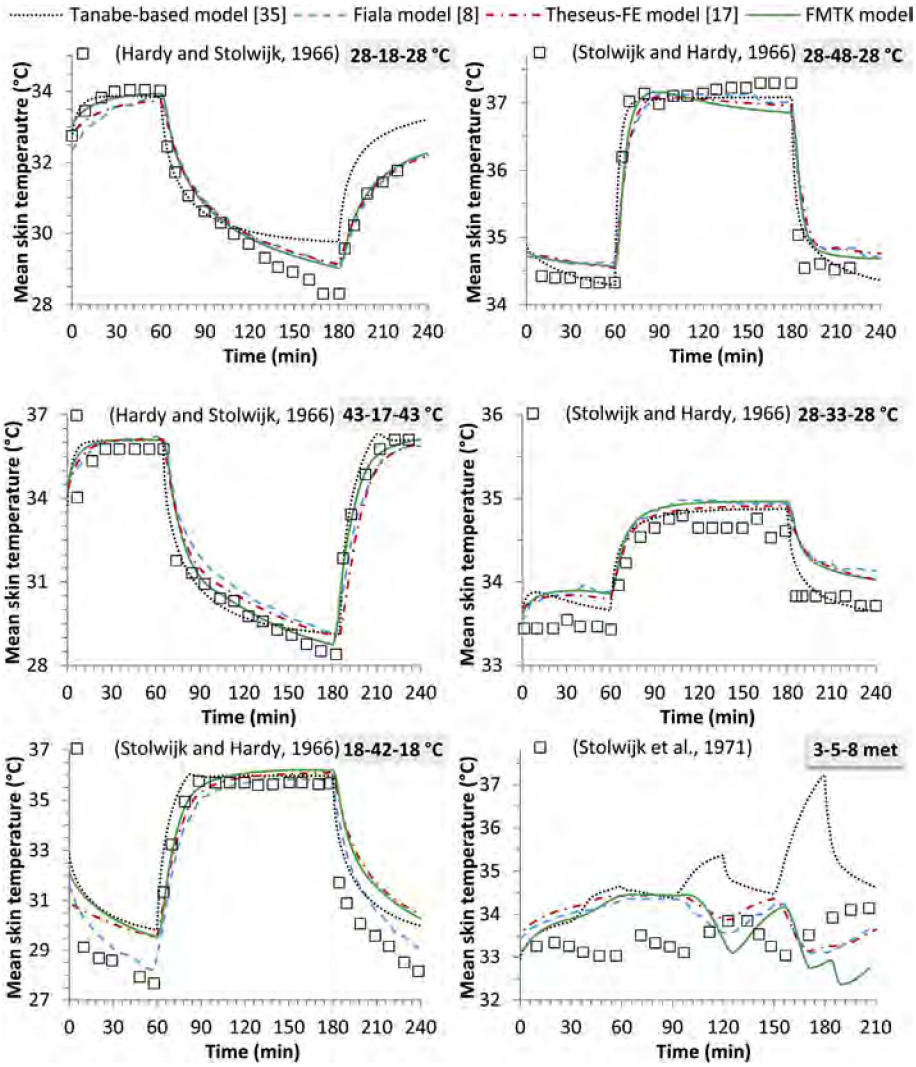

Fig. 5. Active system simulation – mean skin temperature – changing conditions.

coefficients, discretization method – number and shape of the sectors and layers). Generally, the models are less sensitive to the change of number of discretization points in radial axis (six points per layer are sufficient, in the case of a thin layer with low temperature gradient even two points are sufficient).

4.1.3. Thermal sensation

The evaluation of thermal sensation was not the main objective of this study, yet the DTS index was examined. The prediction of this index is very close to the prediction of the Theseus-FE model and the original Fiala model for all 10 test cases from Table 2. This is mainly because of the close predictions of mean skin temperatures and their time derivatives. Together with hypothalamus temperature, these are essential parameters to calculate DTS. The ability of Berkeley model was also evaluated; however, further research into the local thermal sensation/comfort models for transient conditions is necessary. In the field of thermal sensation and comfort, the FMTK model coupled with the Berkeley model (local model) is still not so reliable compared to the DTS index (overall model only).

4.2. Application of the model

The second part of this paper presented the application of the FMTK model to the chemical protective clothing in warm/hot environmental conditions: namely FOP, Tychem-F including underwear, which was also evaluated separately. The main focus was on the prediction of rectal temperature, with error of 0.20 °C and the mean skin temperature error of 0.78 °C. Except for these two main parameters, the local skin temperatures were evaluated with the overall error over all body parts of 1.25 °C.

In 89% of test cases, the FMTK model proves that it is able to reproduce a deep body core (rectal) temperature very well. Only in the case *FOP 40 °C*, the rectal temperature was overestimated. For the underwear, the FMTK model provides good overall results with some issues in prediction of local skin temperatures. In the case of chemical protective clothing FOP, the prediction of mean skin temperature is less accurate, especially in the case *FOP 40 °C*. It is mainly due to the imprecise identification of moisture permeability, but also a small number of evaluated tests plays its role. In the case of chemical protective clothing (Tychem-F), the relevant source about evaporative thermal resistance helped to improve the prediction of both the core and skin temperatures, except for the forehead where the error was too high.

The prediction of recommended exposure time in the case of underwear did not cause problems because in none of these cases the limit rectal temperature 38.5 °C was exceeded. In the case of

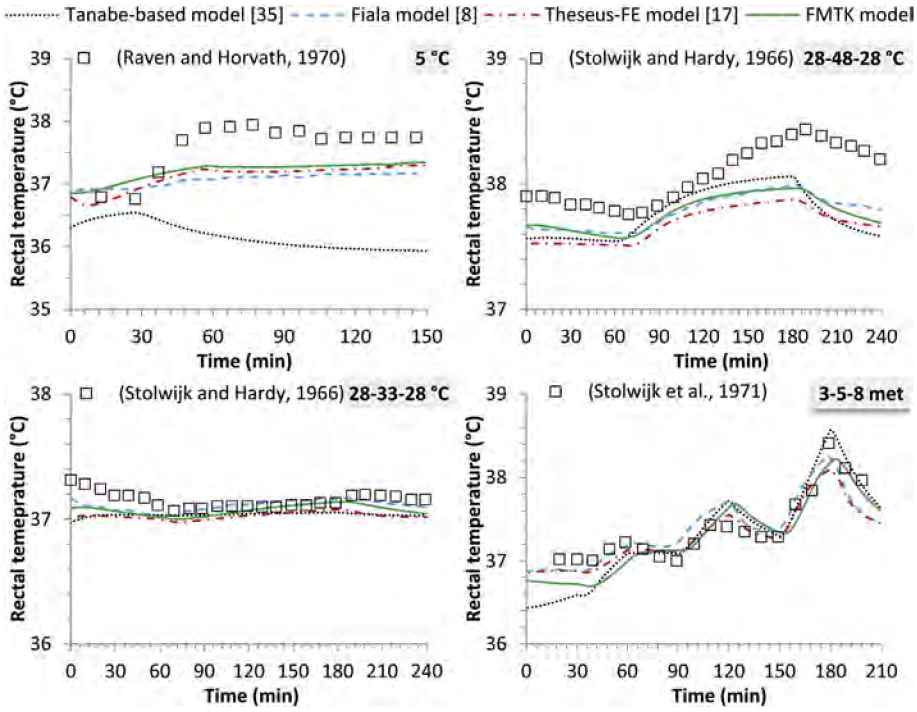

Fig. 6. Active system simulation – rectal temperature.

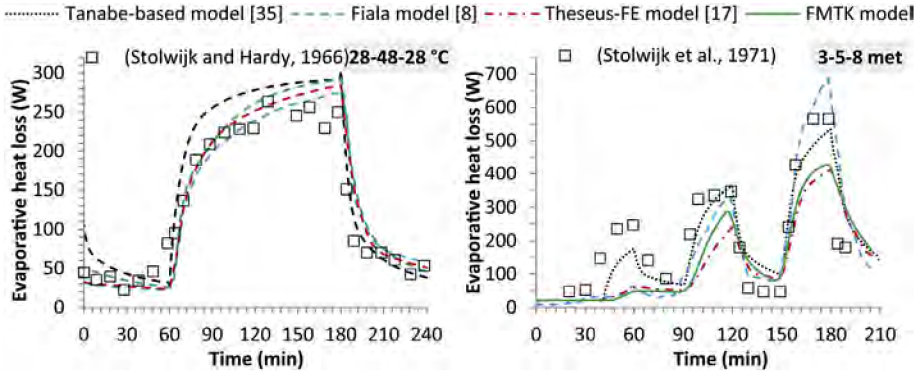

Fig. 7. Active system simulation – evaporative heat loss.

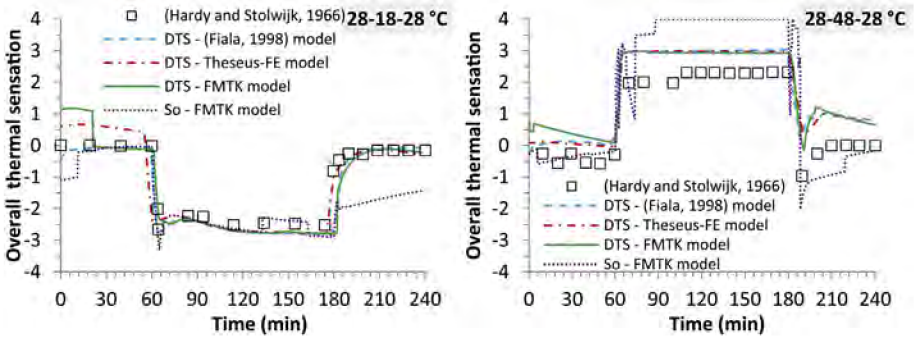

Fig. 8. Prediction of thermal sensation.

experiments with FOP and Tychem-F, the safety limit was achieved in certain time; therefore a question has arisen of how accurate the prediction was.

- *FOP 35 °C* - the model suggests ending up the test approximately 7 min later (after 90 min) compared to the measured data (83 min).

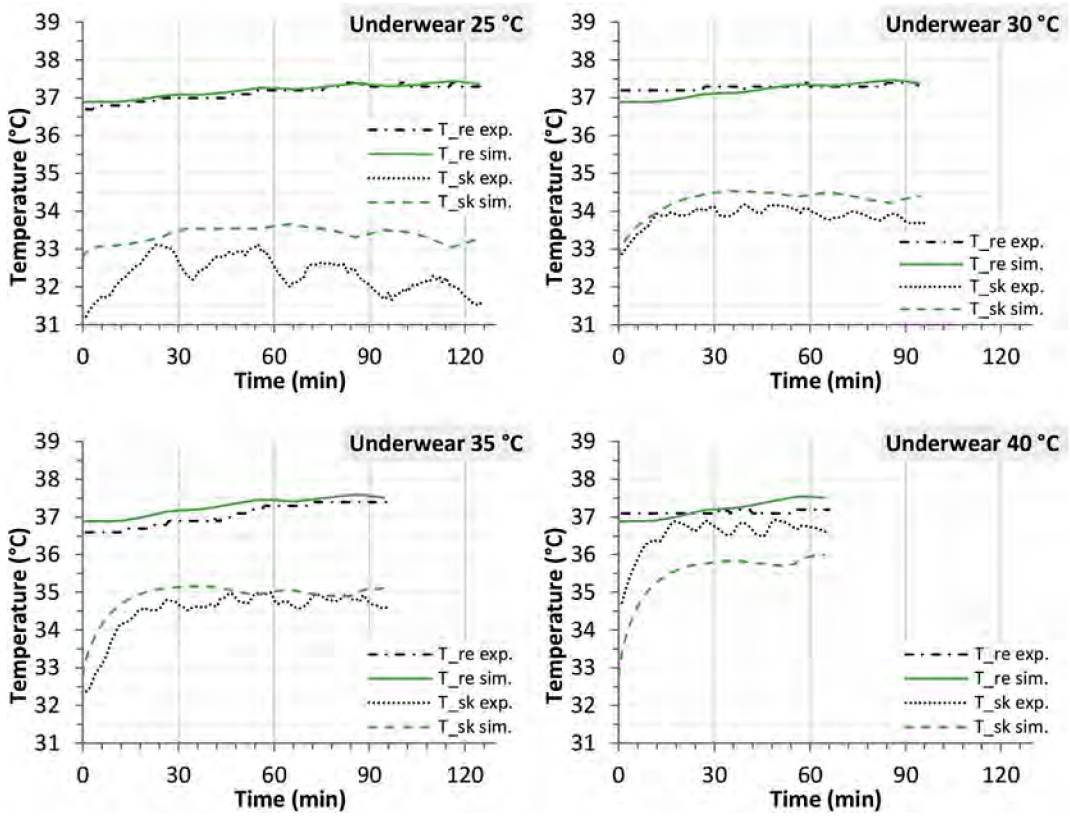

Fig. 9. Mean skin temperature and rectal temperature: simulation vs. experiment (underwear).

- *FOP 40 °C* - the prediction recommends ending up the test 42 min earlier, after 83 min, instead of 125 min, which is on the safe side. Interestingly, even though the temperature was 40 °C and RH = 20% the heat strain was lower than in the case *FOP 35 °C* when RH was 50%. This illustrates the importance of humidity effects in warm environment as a high RH restricts the evaporative heat loss.
- *Tychem 30 °C* - the test was stopped earlier because the tested subject felt exhausted though his rectal temperature was "only" 37.8 °C. In that moment, the model predicted 38.1 °C.
- *Tychem 35 °C* and *Tychem 40 °C* - the model underestimates the heat stress and the predicted recommended time of exposure is about 80 min and 65 min, i.e. longer, compared to the experimental data of 60 min and 55 min.

It was experimentally proved that Tychem-F has generally the shortest time of recommended safe exposure in hot conditions. FMTK predictions confirm this; it was also verified that the model can provide the relevant information on thermophysiological responses of a human dressed in different clothing ensembles even in extreme conditions as protective ensembles may be. Therefore, such models have a potential to become a basis for building the new and more complex heat stress indices or thermal comfort models dealing with unsteady and non-uniform conditions. From the practical point of view, thermophysiological models are designed mostly for engineers to identify a general behaviour of the human body with respect to applications in clothing industry, environmental ergonomics of buildings and passenger vehicles.

On the other hand, these results show the demand for deeper verification of the Fiala-based model for protective clothing applications. Validation of the model should be not only for the mean skin temperatures, but also for local temperatures (there is a need for well documented experimental data). Such complexity of thermophysiological models brings several disadvantages especially, in terms of proper definition of input data and boundary conditions. The most problematic issues to deal with are:

- Clothing properties – relevant and detailed data on worn clothing, as accurate as possible. Measurement of local thermal and evaporative resistances, including the effect of air gaps between the clothing layers.
- Heat transfer coefficient database for various activities.
- Determination of the metabolic rate.

Although we verified that the FMTK model itself is well constructed, a more attention should be paid to a more complex clothing model. The most of the inaccuracies stem from the estimation of local insulation parameters of clothing and from the effect of walking on the treadmill. Finally, it was found that it is a challenge to apply the thermophysiological model for the field tests together with the real-time identification of clothing properties and metabolic rate during the exposure.

5. Conclusion

1) The Fiala-based model FMTK was verified using available experimental data from literature and compared with the state-of-the-art thermophysiological models for a wide range of environmental conditions.
   - Passive and active system: prediction of the skin, deep body temperatures (hypothalamus and rectal), evaporation losses, and thermal sensation (DTS) were evaluated.

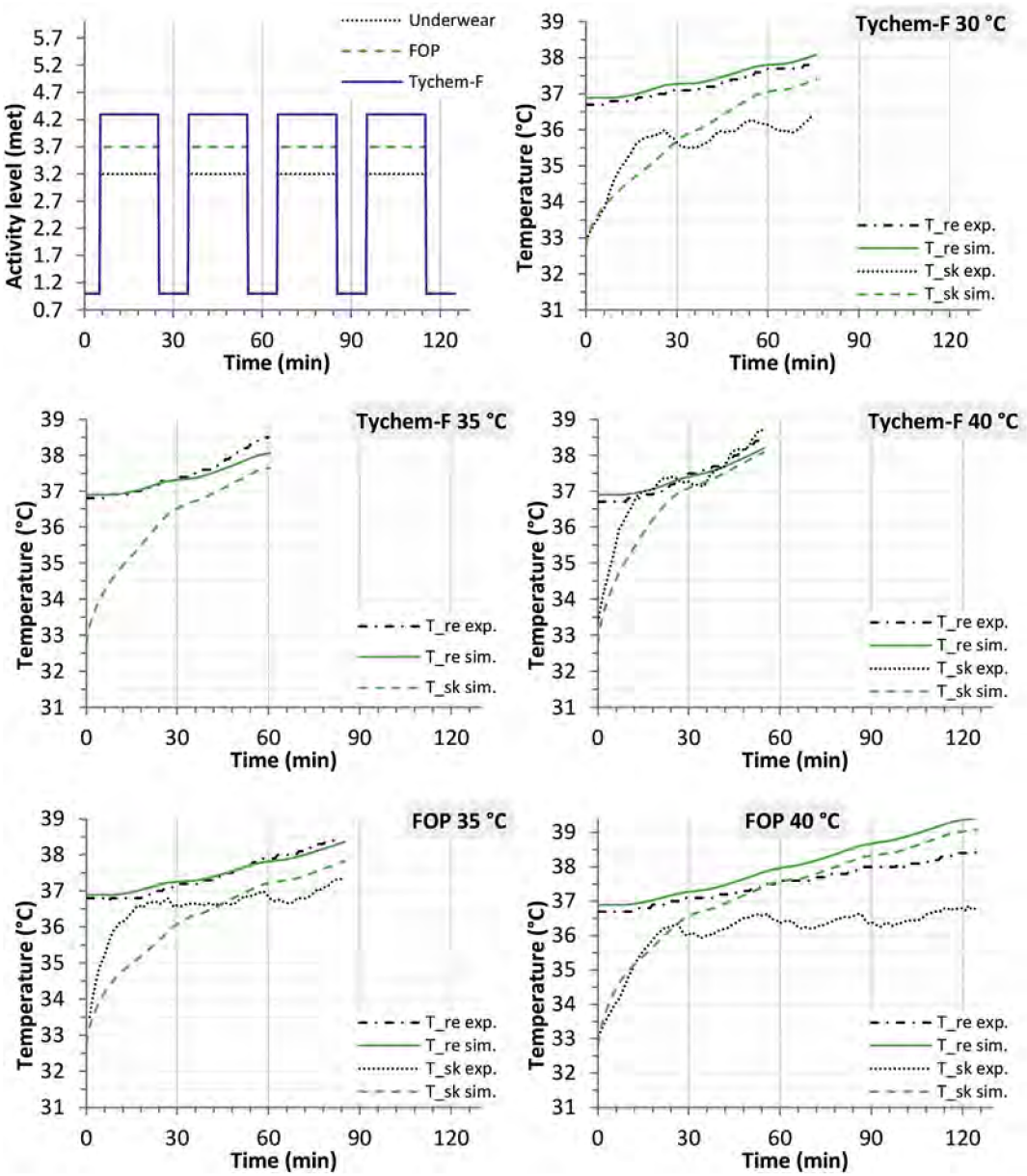

Fig. 10. Mean skin temperature and rectal temperature: simulation vs. experiment (protective clothing).

Table 7
Mean absolute deviation (MAD) of mean skin temperature for all cases and types of clothing.

MAD	Underwear				FOP		Tychem-F			All
	25 °C	30 °C	35 °C	40 °C	35 °C	40 °C	30 °C	35 °C	40 °C	
T_{re} (°C)	0.07	0.13	0.22	0.15	0.13	0.59	0.17	0.14	0.14	**0.20**
T_{skm} (°C)	1.06	0.41	0.36	0.74	0.69	1.51	0.63	x	0.59	**0.78**

Table 8
Mean absolute deviation (MAD) of local skin temperatures for all cases, type of clothing and body parts.

Part	Forehead	R scapula	L thorax	R arm	L arm	L hand	R thigh	L calf	All
Underwear	1.07	0.92	1.87	1.42	1.19	1.57	1.61	1.07	**1.34**
FOP	0.86	1.44	0.81	2.14	1.63	1.11	0.69	1.11	**1.22**
Tychem-F	3.02	0.97	1.01	0.67	0.59	0.88	0.86	0.96	**1.12**
All	**1.32**	**1.06**	**1.36**	**1.55**	**1.23**	**1.28**	**1.19**	**1.05**	**1.25**

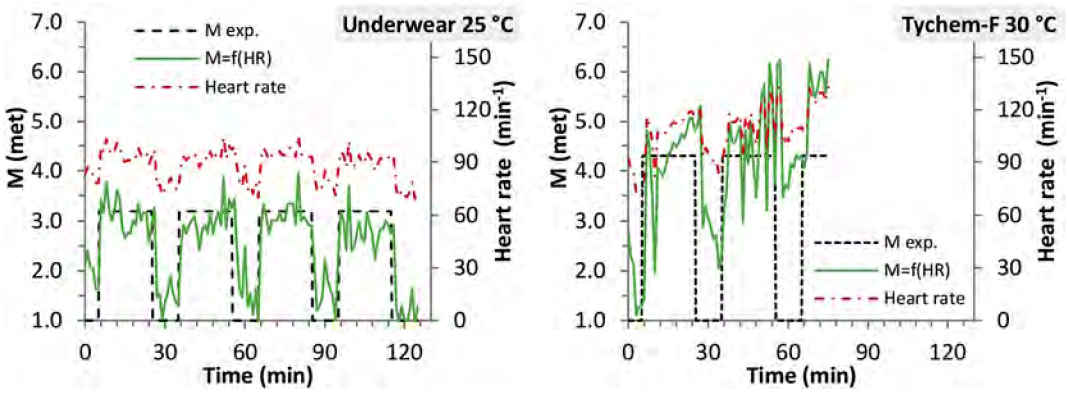

Fig. 11. Metabolic rate (M) calculated from the heart rate (HR) by ISO 8996. Example: 49 years old man: M = 4.9*HR-288. E.g. for HR = 70.6 min^{-1} = 58.2 W/m^2 = 1 met.

- Verification of the model shows that it is comparable with the other Fiala-based models and commercial codes, and it well matches the experimental data from literature.

2) The model was applied to the evaluation of chemical protective clothing in warm/hot conditions at higher metabolic rates up to 4.3 met. The application to the protective clothing demonstrates the ability of the FMTK model to predict the heat strain.
   - The match of measured and predicted rectal temperature is good (MAD = 0.20 °C).
   - Mean skin temperature (MAD = 0.78 °C) and local temperatures (MAD = 1.25 °C) predictions are less accurate mainly due to the difficulty to predict the efficiency of evaporation.
   - Thermal resistances of clothing ensembles were measured with a thermal manikin, the literature data were used for estimation of evaporation resistance.
   - The capability of precise predictions of the model can be improved by detailed identification of clothing moisture permeability.
   - The metabolic rate can be estimated by heart rate, if more precise methods are not available. However, such estimation is very rough for a human body under heat stress.

Acknowledgement

The research was supported by the project LO1202 Netme Centre Plus with the financial support from the Ministry of Education, Youth and Sports of the Czech Republic under the "National Sustainability Programme I", the project Reg. No. FSI-S-17-4444 of the Brno University of Technology and by the Ministry of Interior of the Czech Republic under the project of the Safety research, No. VF20112015013.

References

[1] O.M. Fletcher, R. Guerrina, C.D. Ashley, T.E. Bernard, Heat stress evaluation of two-layer chemical demilitarization ensembles with a full face negative pressure respirator, Ind. Health 52 (4) (2014) 304–312. http://doi.org/10.2486/indhealth.2012-0197.
[2] ISO 7933, Ergonomics of the Thermal Environment — Analytical Determination and Interpretation of Heat Stress Using Calculation of the Predicted Heat Strain, 2004.
[3] G.M. Budd, Wet-bulb globe temperature (WBGT) - its history and its limitations, Sci. Med. Sports 11 (2007) 20–32.
[4] ISO 7730, Ergonomics of the Thermal Environment –Analytical Determination and Interpretation of Thermal Comfort Using Calculation of the PMV and PPD Indices and Local Thermal Comfort Criteria, 2005.
[5] G. Havenith, D. Fiala, Thermal indices and thermophysiological modelling for heat stress, Compr. Physiol. 6 (2015) 255–302. http://dx.doi.org/10.1002/cphy.c140051.
[6] E.H. Wissler, A mathematical model of the human thermal system, Bull. Math. Biol. 26 (2) (1964) 147–166.
[7] J.A.J. Stolwijk, A Mathematical Model of Physiological Temperature Regulation in Man, NASA Report NASA-CR-1855, 1971, http://ntrs.nasa.gov/archive/nasa/casi.ntrs.nasa.gov/19710023925.pdf.
[8] D. Fiala, Dynamic Simulation of Human Heat Transfer and Thermal Comfort, Ph.D. Thesis, De Montfort University, 1998.
[9] S. Tanabe, K. Kobayashi, J. Nakano, Y. Ozeki, Evaluation of thermal comfort using combined multi-node thermoregulation (65MN) and radiation models and computational fluid dynamics (CFD), Energ. Build. 34 (2002) 637–646.
[10] P.O. Fanger, Thermal Comfort Analysis and Applications in Environmental Engineering, Copenhagen Danish Technical Press, Copenhagen, 1970.
[11] A.P. Gagge, J.A.J. Stolwijk, Y. Nishi, An effective temperature scale based on a simple model of human physiological regulatory response, ASHRAE Trans. 77 (1971) 247–262.
[12] B. Koelblen, A. Psikuta, A. Bogdan, S. Annaheim, R.M. Rossi, Thermal sensation models: a systematic comparison, Indoor Air 2016 (2016) 1–10. http://dx.doi.org/10.1111/ina.12329.
[13] D.W. Hensley, A.E. Mark, J.R. Abella, G.M. Netscher, E.H. Wissler, K.R. Diller, 50 years of computer simulation of the human thermoregulatory system, JBiomechEng 135–2 (2013) 021006, http://dx.doi.org/10.1115/1.4023383.
[14] D. Fiala, G. Havenith, Modelling human heat transfer and temperature regulation, in: Studies in Mechanobiology, Tissue Engineering and Biomaterials, Springer-Verlag Berlin Heidelberg, 2015, pp. 1–38. http://dx.doi.org/10.1007/8415.
[15] B. Kingma, Human Thermoregulation - a Synergy between Physiology and Mathematical Modelling, Ph.D thesis, Maastricht University, 2012.
[16] L. Schellen, M.G.L.C. Loomans, B.R.M. Kingma, M.H. de Wit, A.J.H. Frijns, W.D. van Marken Lichtenbelt, The use of a thermophysiologic model in the built environment to predict thermal sensation, Build. Environ. 59 (2013) 10–22. http://dx.doi.org/10.1016/j.buildenv.2012.07.010.
[17] P+Z Engineering GmbH, Theseus-FE 4.0 – Theory Manual, 2011. Münich.
[18] M. Hepokoski, A. Curran, A. Gullman, D. Jacobsson, Coupling a Passive Sensor Manikin with a Human Thermal Comfort Model to Predict Human Perception in Transient and Asymmetric Environments, 2017.
[19] D. Fiala, G. Havenith, P. Brode, B. Kampmann, G. Jendritzky, UTCI-Fiala multinode model of human heat transfer and temperature regulation, Int. J. Biometeorol. 56 (2012) 429–441. http://dx.doi.org/10.1007/s00484-011-0424-7.
[20] P. Brode, K. Błazejczyk, D. Fiala, G. Havenith, I. Holmer, G. Jendritzky, B. Kampmann, The Universal Thermal Climate Index UTCI compared to ergonomics standards for assessing the thermal environment, Ind. Health 51 (1) (2013) 16–24.
[21] C. Van Treeck, J. Frisch, et al., Integrated thermal comfort analysis using a parametric manikin model for interactive real-time simulation, J. Build. Perform. Simulat. 2 (4) (2009) 233–250.
[22] P.C. Cropper, T. Yang, M. Cook, D. Fiala, R. Yousaf, Coupling a model of human thermoregulation with computational fluid dynamics for predicting human-environment interaction, J. Build. Perform. Simulat. 3 (2010) 233–243. http://dx.doi.org/10.1080/19401491003615669.
[23] J. Turnow, S. Knochenhauer, R. Kewitz, N. Kornev, Coupling of human thermoregulation and URANS computation for investigation of local heat transfer and flow structures in a generic car cabin, Flow. Turbul. Combust. 97 (2016) 1281–1296. http://dx.doi.org/10.1007/s10494-016-9780-z.
[24] K. Katić, R. Li, W. Zeiler, Thermophysiological models and their applications: a review, Build. Environ. 106 (2016) 286–300. http://dx.doi.org/10.1016/j.buildenv.2016.06.031.
[25] ISO 8996, Ergonomics - Determination of Metabolic Rate, International Standards Organization, Geneva, 2004.
[26] L. Giedraityte, Identification and Validation of Risk Factors in Cold Work, Ph.D. thesis, Luleå University of Technology, 2005.
[27] ISO 9920, Ergonomics of the Thermal Environment - Estimation of the Thermal Resistance and Evaporative Resistance of a Clothing Ensemble, International Standards Organization, Geneva, 2005.
[28] ISO 11092, Textiles–physiological Effects–measurement of Thermal and

Water-vapour Resistance under SteadyState Conditions (Sweating Guarded-hotplate Test), 2015.
[29] ISO 15831, Clothing - Physiological Effects - Measurement of Thermal Insulation by Means of a Thermal Manikin, 2004.
[30] R. de Dear, E. Arens, Z. Hui, et al., Convective and radiative heat transfer coefficients for individual human body segments, Int. J. Biometeorol. 40 (3) (1997) 141–156. http://dx.doi.org/10.1007/s004840050035.
[31] M. Fojtlín, J. Fišer, M. Jícha, Determination of convective and radiative heat transfer coefficients using 34-zones thermal manikin: uncertainty and reproducibility evaluation, Elsevier Inc, Exp. Therm. Fluid Sci. 77 (2016) 257–264. ISSN 0894–1777.
[32] N. Martínez, A. Psikuta, K. Kuklane, J.I. Quesada, R.M. de Anda, P.P. Soriano, R.S. Palmer, J.M. Corberán, R.M. Rossi, S. Annaheim, Validation of the thermophysiological model by Fiala for prediction of local skin temperatures, Int. J. Biometeorol. 60 (12) (2016) 1969–1982.
[33] A. Psikuta, D. Fiala, G. Laschewski, et al., Validation of the Fiala multi-node thermophysiological model for UTCI application, Int. J. Biometeorol. 56 (2012) 443–460. http://dx.doi.org/10.1007/s00484-011-0450-5.
[34] R.R. Gonzalez, T.M. McLellan, W.R. Withey, S.K. Chang, K.B. Pandolf, Heat strain models applicable for protective clothing systems: comparison of core temperature response, J. Appl. Physiol. 83 (3) (1997) 1017–1032.
[35] J. Pokorný, Coupling of the Models of Human Physiology and Thermal Comfort, PhD Thesis, Brno University of Technology, Faculty of Mechanical Engineering, 2012 (in Czech).
[36] J. Pokorny, M. Jicha, Coupling of the models of human physiology and thermal comfort, EPJ Web Conf. 45 (2013) 01077. http://doi.org/10.1051/epjconf/20134501077.
[37] J. Pokorný, M. Jícha, Implementation of Fiala thermophysiological thermal comfort model in Matlab (in Czech), Vytápění větrání Instal. 4 (2015) 99–102. ISSN: 1210-1389.
[38] T. Miller, D. Nelson, G. Bue, L. Kuznetz, Dynamic simulation of human thermoregulation and heat transfer for spaceflight applications, in: 41st International Conference on Environmental Systems, 2011. Portland, Oregon, USA.
[39] P+Z Engineering GmbH, Theseus-FE 4.0 – Validations Manual, 2011. Münich.
[40] P.R. Raven, S.M. Horvath, Variability of physiological parameters of unacclimatized males during a two-hour cold stress of 5 °C, Int. J. Biometeorol. 14 (3) (1970) 309–320.
[41] G.M. Budd, N. Warhaft, Body temperature, shivering, blood pressure and heart rate during a standard cold stress in Australia and Antarctica, J. Physiol. Lond. 186 (1966) 216–232.
[42] J.A.J. Stolwijk, J.D. Hardy, Partitioned calorimetric studies of responses of man to thermal transients, J. Appl. Physiol. 21 (1966) 967–977.
[43] J.A. Wagner, S.M. Horvath, Influences of age and gender on human thermoregulatory responses to cold exposures, J. Appl. Physiol. 58 (1985) 180–186.
[44] ISO 9886, Ergonomics - Evaluation of Thermal Strain by Physiological Measurements, 2004.
[45] E.A. McCullough, B.W. Jones, J. Huck, A comprehensive data base for estimating clothing insulation, ASHRAE Trans. 91 (2A) (1985) 29–47.
[46] F.R. d'Ambrosio Alfano, B.I. Palella, G. Riccio, J. Malchaire, On the effect of thermophysical properties of clothing on the heat strain predicted by PHS model, Ann. Occup. Hyg. 60 (2) (2016) 231–251, http://dx.doi.org/10.1093/annhyg/mev070.
[47] E.A. McCullough, B.W. Jones, T. Tamura, A data base for determining the evaporative resistance of clothing, ASHRAE Trans. 95 (2) (1989) 316–328.
[48] S. Wen, Physiological Strain and Physical Burden in Chemical Protective Coveralls, PhD Thesis, University of Alberta, Department of Human Ecology, 2014.
[49] ANSI/ASHRAE Standard 55-2013, Thermal Environmental Conditions for Human Occupancy, American Society of Heating, Refrigerating and Air Conditioning Engineers, Atlanta, 2013.
[50] H. Zhang, E. Arens, C. Huizenga, T. Han, Thermal sensation and comfort models for non-uniform and transient environments, Part I: local sensation of individual body parts. Part II: local comfort of individual body parts. Part III: whole-body sensation and comfort, Build. Environ. 45 (2010) 380–410.

Building and Environment 155 (2019) 376–388

Contents lists available at ScienceDirect

Building and Environment

journal homepage: www.elsevier.com/locate/buildenv

Local clothing properties for thermo-physiological modelling: Comparison of methods and body positions

Miloš Fojtlín[a,b], Agnes Psikuta[a,*], Jan Fišer[b], Róbert Toma[b], Simon Annaheim[a], Miroslav Jícha[b]

[a] Empa Swiss Federal Laboratories for Material Science and Technology, Laboratory for Biomimetic Membranes and Textiles, St. Gallen, Switzerland
[b] Brno University of Technology, Faculty of Mechanical Engineering, Energy Institute, Department of Thermodynamics and Environmental Engineering, Czech Republic

ARTICLE INFO

Keywords:
Clothing
Thermal insulation
Evaporative resistance
Sitting
Clothing area factor
Thermal sensation

ABSTRACT

Thermo-physiological modelling has become a frequently used and valuable tool for simulations of thermoregulatory responses in a variety of applications, such as building and vehicular comfort studies. To achieve reliable results, it is necessary to provide precise inputs, such as clothing thermal parameters. These values are usually presented in a standing body position and scarcely reported locally for individual body parts. Moreover, as an air gap distribution is both highly affected by a given body position and critical for clothing insulation, this needs to be taken into account. Therefore, the aim of this study was to examine eight probable approaches to assess the clothing parameters using state-of-the-art measurements, analytical and empirical models, and estimation. Next, we studied the effects of the eight clothing inputs on predicted thermo-physiological response under the same environmental conditions conducted with the Fiala model. Secondly, the study focuses on differences between seated and standing positions, both using two clothing sets representing typical European, indoor, summer and winter ensembles. The results show clear differences in clothing thermal properties between sitting and standing positions on both lower limbs and torso. The outputs of the eight examined methods showed discrepancies between them, in the range of up to 200%. The discrepancies from the eight clothing inputs were also propagated in the results of thermo-physiological responses. These varied significantly in terms of their impact on predicted thermal sensation, highlighting the importance of using adequate inputs for modelling.

1. Introduction

Efforts to minimize energy expenditure for heating ventilation and air-conditioning (HVAC) in a variety of indoor environments – such as transportation and occupational settings – with help of local conditioning technologies are a subject to substantial research attention [1–4]. Effects of localised heating and cooling on a human thermo-physiological response are usually investigated in human or thermal manikin studies [5,6]. Alternatively, one can utilise validated thermo-physiological models that allow prompt simulations of human thermo-physiological responses and reduce the need for costly physical studies [7–9]. In addition, these responses can be further translated into the prediction of thermal sensation or thermal comfort using dedicated models [10].

At the same time, to accurately simulate thermal interactions between the human body and the surrounding environment, using thermo-physiological models, there is a need for precise inputs defining: the environmental conditions, metabolic activity, and clothing [11]. Clothing governs heat and mass transfer between the human body and the ambient environment. Local clothing thermal properties may vary considerably over the body, thus, having a major impact on the development of skin temperatures, sweating, and perception of thermal sensation and comfort [12]. Yet, these properties, namely intrinsic clothing insulation (I_{cl}), evaporative clothing resistance ($R_{e,cl}$), and clothing area factor (f_{cl}), are rarely reported in literature [11]. Moreover, previous research has shown that body posture change has a significant impact on the resulting global clothing properties [13–15], however, only globally as an average for the whole body. The findings by Mert et al. [16,17] show differences in air gap thicknesses between sitting and standing positions that change relative to localised body parts and directly influence the local thermal and evaporative resistance of a garment. Nonetheless, the impact of variations between body postures on the human thermo-physiology has not been investigated and the majority of authors provide the local clothing properties applicable only for the standing body position [18–25].

The most realistic method to determine local clothing thermal properties is the use of a thermal manikin with detailed body segmentation [5]. Nevertheless, the accessibility of this apparatus is

* Corresponding author. Empa Swiss Federal Laboratories for Material Science and Technology, Lerchenfeldstrasse 5, 9014, St. Gallen, Switzerland.
E-mail address: agnes.psikuta@empa.ch (A. Psikuta).

https://doi.org/10.1016/j.buildenv.2019.03.026
Received 6 December 2018; Received in revised form 14 March 2019; Accepted 16 March 2019
Available online 25 March 2019
0360-1323/

restrictive on the account of the high costs of both the device and the necessity of additional equipment, including a climatic chamber. Therefore, other ways to obtain clothing properties can be found in the literature, which do not require specialised equipment. The most common approach is to choose a desired ensemble from an exhaustive database of clothing from standard ISO 9920 [18]. According to the definition of the *clo* unit, measured using a standing thermal manikin, all three clothing parameters are presented as global values for the whole-body (in essence virtual insulation covering the whole body) [18]. As a matter of fact, the uniform distribution yields unrealistic physiological responses, since the local extremes are averaged and the mean value is prescribed even for body parts without clothing in reality, typically face and hands [17,26]. To address this problem, Curlee [19] and Nelson et al. [23] developed a method to calculate local clothing parameters based on global parameters from McCullough et al. [24] and ISO 9920 [18] valid for 106 garments. This approach was presented only for single-layer clothing and the resolution of the model is limited to a single value for parts covered by the garment. Yet, there are obvious differences within air gaps, between some of the body parts considered by the model [16,17].

Another option is to estimate local clothing properties based on empirical formulae relating outdoor temperature and clothing insulation, such as the UTCI clothing model [20]. The data for the model was gathered from several independent studies on clothing habits of Europeans. The model has a resolution of 7 body segments, applicable for a standing person, and temperatures from approximately −30 °C to 32 °C [20]. The paper also presents compensation of thermal insulation for an increased air-speed.

Local air gap thickness mainly affects local clothing parameters and because of this, one of the emerging methods to precisely examine these parameters is three-dimensional (3D) body scanning. This allows detailed assessment of the mean local air gap thicknesses, percentage of clothing contact area, and calculation of clothing area factors [27,28]. With the use of this information, prediction of thermal clothing insulation is possible based on basic laws of physics, using dedicated models for major body parts [29,30].

The optimal number of body segments for thermo-physiological modelling is conditioned by the specific application. The standard ISO 14505–2 [31] addresses cabin environments with seated positions and proposes segmentation of at least 16 body parts (11 parts if right-left symmetry is assumed for limbs) where distinct thermal conditions are expected, such as shade or a seat. Another standard ISO 15831 [32] recommends at least 15 segments (9 parts if right-left symmetry is assumed for limbs), and the most cited thermo-physiological models have similar resolutions to the ISO 15831 of up to 19 segments, with an additional spatial subdivision [33]. Similarly, the prevailing local thermal sensation models, such as models by Zhang [34,35], Jin [36], and Nilsson [37], have resolution covering major body parts of up to 13 segments assuming right-left symmetry. It is therefore reasonable to use a number of clothing segments equal to the number of segments of thermo-physiological and thermal sensation models to achieve the most realistic simulation of heat and mass transfer between the body and the environment.

Other parameters that are bound to the seated position are the thermal properties of the seat. Their determination requires specific instrumentation that can mimic contact pressure of a seated person, such as a seat tester STAN (Thermetrics, USA) [38] or a stamp tester as presented by Bartels [39]. The additional pressure is important because of the compression of seat layers, as well as the consequent changes in their thermal properties [39] and contact area with the body. Therefore, a measurement using a thermal manikin without realistic weight distribution and seat contact yields unrealistic results [40]. Values of additional thermal insulation provided by chairs were presented by McCullough et al. [41] and Wu et al. [42], both used thermal manikins, however, without explaining whether and how the realistic contact was achieved.

The next parameter that is often neglected is the clothing fit and the associated air gap distribution, which influences resulting thermal and evaporative resistance [17]. Standard ISO 9920 recommends using clothing with normal fit, whereas ISO 14505 recommends tightly fitting clothing to get repeatable results. Thus, there is a need for an objective parameter that would describe fit of the clothing, for example, clothing ease allowance (*EA*) that is defined as a difference between girths of the body and clothing at given body landmarks. This parameter was found to be strongly correlated with air gap thickness, and hence, clothing thermal and evaporative resistance [21,27,43].

The aim of this study is to examine typical approaches of obtaining the local clothing thermal properties for simulations of physiological and perceptual responses with respect to their use in spatially heterogeneous conditions. Next, the focus is on differences between seated and standing body positions that to the best of our knowledge have not been addressed locally. The impact of the differences is shown by means of simulated thermo-physiological responses that are directly linked to thermal sensation. The application of the findings is in passenger transportation and a range of occupational settings, including but not limited to professional driving, machinery operation, and the office environment.

2. Methods

2.1. Study design

The study included the determination of clothing thermal properties for two clothing sets based on distinct approaches comprising measurement, modelling, and estimation of clothing properties. Thus, this study provides relevant information for laboratories following different approaches and with potential access to equipment listed in Table 1. *Cases 1* and *2* are assumed as references for sitting and standing positions, respectively, because of the state-of-the-art methods used. Moreover, the consistency of the methodology was achieved using the same clothing throughout the study.

The second part of the work is focused on the investigation of the sensitivity of the thermo-physiological model by Fiala [46] (FPCm5.3, Ergonsim, Germany) to changes in boundary clothing conditions. The model was chosen on a basis of its broad validation documentation [47–49]. The study focuses on the seated position in a neutral steady

Table 1
Overview of the examined cases and methods to determine clothing area factor (f_{cl}), intrinsic clothing insulation (I_{cl}), evaporative clothing resistance ($R_{e,cl}$). Right-left symmetry is assumed.

Case	f_{cl} (−)	I_{cl} ($m^2K.W^{-1}$)	$R_{e,cl}$ ($m^2Pa.W^{-1}$)	Position	No. of segments
1	3D scanning	Manikin heat loss method [32]	Manikin heat loss method [44]	sitting	13
2	Photography [18]	Manikin heat loss method [32]	Manikin heat loss method [44]	standing	13
3	Physical model [30,45]	Physical model [30,45]	Physical model [30,45]	sitting	8
4	Physical model [30,45]	Physical model [30,45]	Physical model [30,45]	standing	10
5	Regression model [21]	Regression model [21]	Physical model [30,45]	standing	11
6	ISO based model [23]; Table 1	ISO based model [23]; Table 1	ISO based model [19]; Appendix A	standing	3
7	ISO Database [18]; Table. A2	UTCI model [20]	ISO Database [18]; Formula 31	standing	7
8	ISO Database [18]; Table. A2	ISO Database [18]; Table. A2	ISO Database [18]; Formula 31	standing	1

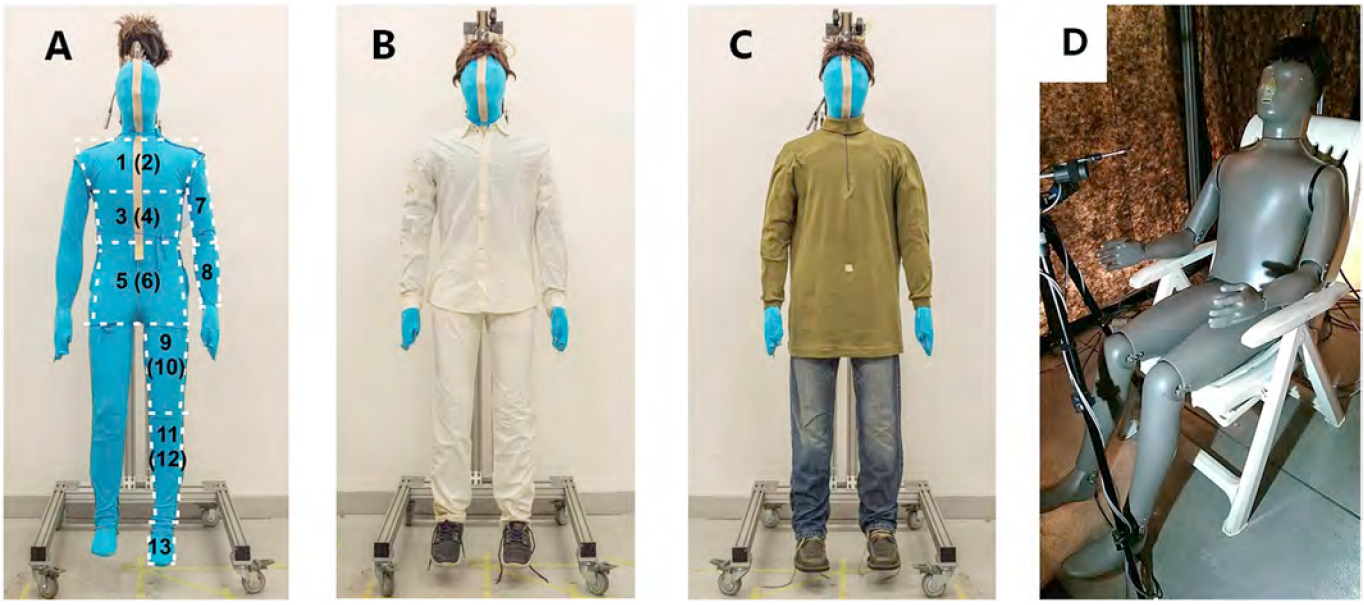

Fig. 1. Illustration of the manikin used and the clothing sets applied. A – segmentation of a nude manikin with an artificial skin, posterior parts in brackets; B – summer indoor clothing; C – winter indoor clothing; D – seated position. *Note: segmentation from* Fig. 1A *– 1 Chest, 2 Back, 3 Abdomen, 4 Lumbus, 5 Anterior pelvis, 6 Buttocks, 7 Upper arm, 8 Lower arm, 9 Anterior thigh, 10 Posterior thigh, 11 Shin, 12 Calf, 13 Foot.*

environment that is typical for a broad variety of indoor environments, and should serve as a benchmark for comparison of the eight individual approaches.

2.2. Definition of clothing sets and body positions for the study

The clothing sets included in this study represent typical indoor summer and winter clothing and were selected from the database of clothing presented by Psikuta et al. [27]. Most importantly, the focus was on the consistency of the clothing ease allowances (defined as the difference between the girth of clothing and a nude manikin at relevant body landmarks) throughout the study, as they affect resulting clothing area factor, thermal resistances, and evaporative resistances. The summer set consists of a collar shirt, light cotton jeans, briefs, short socks, and leather sneakers (Fig. 1 B). The winter set was comprised a turtle-neck shirt with a T-shirt worn underneath, heavier cotton jeans, leather shoes, as well as the same underwear as in the summer case (Fig. 1C). Detailed descriptions and the ease allowances of the clothing are given in Table 2.

A seating position typical of postures adopted for driving, operating of machinery, or office work, was adopted from the work of Mert et al. [28] in which an elbow angle of 120°, hip angle of 110°, and knee angle of 120° are specified (Fig. 1D). The thermal manikin was seated on a plastic chair with openings accounting for approximately 40% of its surface. The standing upright position with hands down (Fig. 1) is typically reported in literature and was used to quantify the differences in comparison to the sitting position.

2.3. Case 1 – 3D scanning and heat loss method in seated position

The first studied case was considered as a reference case providing highest precision for determination of clothing thermal parameters in the seated position. The clothing area factor was measured by a 3D body scanning technique combined with post-processing software, which allows for the quantification of nude and dressed surface areas of individual body regions in a given position [17,27,50]. Details of the methodology and equipment were adopted from the study by Mert et al. [28]. The surface area was quantified four times for each clothing set,

Table 2
Overview of clothing and *ease allowance (EA)* related to the size of a western type Newton thermal manikin.

	Indoor summer set			Indoor winter set				Both sets
Type	Smart shirt	Jeans light	Sneakers	Shirt	T-shirt	Jeans	Shoes	Briefs
Item in Psikuta et al. [27]	21	45	–	3	24	33	–	31
Fit	Regular	Regular	Regular	Regular	Regular	Loose	Regular	Regular
Fibre content (%)	100 CO	100 CO	Leather	100 CO	95 CO/5 EL	100 CO	Leather	100 CO
Specific weight (g/m^2)	137	179	Size	227	176	366	Size	145
Fabric structure	Plain weave	3/1 twill	EUR 42.5	Interlock	Single jersey	3/1 twill	EUR 42.5	1 × 1 rib
EA chest (cm)	14.5	–	–	10.5	11.5	–	–	–
EA waist (cm)	24.0	–	–	30.0	22.0	–	–	–
EA hips (cm)	13.0	8.0	–	12.0	10.0	14.0	–	−4.0
EA biceps (cm)	9.0	–	–	4.0	–	–	–	–
EA lower arm (cm)	8.0	–	–	2.5	–	–	–	–
EA thigh (cm)	–	6.0	–		–	3.0	–	–
EA lower leg (cm)	–	6.0	–	–	–	7.0	–	–

Notes: CO – cotton, EL – elastane.

as well as for an undressed flexible manikin [28]. This manikin has, however, a different body geometry than the western Newton type thermal manikin (Thermetrics, USA) used to measure thermal and evaporative resistances. The differences in griths at given body land marks were typically of 2 cm, having the maximum of 6 cm at *Upper arm*. Linear interpolation was therefore used to compensate for the discrepancies between the manikins girths and consequently clothing ease allowances based on the clothing presented in Mert et al. [28]. This was done according to the findings by Vesela et al. [21], where the linear relationship between the garment ease allowance and f_{cl} was demonstrated.

The local intrinsic clothing thermal (I_{cl}) and evaporative resistances ($R_{e,cl}$) were determined using the 34 zones Newton type manikin in a climatic chamber (detailed description of the chamber and the manikin in Fojtlín et al. [51]). The manikin was seated onto an adjustable plastic chair with perforation wearing the garments listed in Table 2. The 34 zones were merged into 13 segments (Fig. 1A) to represent body segmentation of the Fiala model with resolution of upper and lower limbs, anterior and posterior torso. The measurement of both clothing sets and clothing resistances was executed three times independently, including dressing and undressing of the manikin.

The test conditions for the local intrinsic thermal resistances were adopted from ISO 15831 [32], which establishes requirements of a 34 °C manikin skin temperature, as well as air, mean ambient, and radiant temperatures of 24 °C, and relative humidity of 50%. The air speed in the test was 0.1 ± 0.05 m/s that suits the target application in indoor environments with low air velocities. The calculation of the thermal resistances was done using the heat loss method according to Equation (A.3a) from ISO 15831 [32].

The evaporative clothing resistance was determined using a tightly fitting, long sleeve overall (Fig. 1A) that was pre-wetted and worn only during evaporative resistance measurements [52,53]. The fabric for the overall was selected according to the recommendations from the study by Koelblen et al. [54] with thickness of 0.92 ± 0.03 mm, specific weight of 208 g/m, and fibre composition of 95% cotton and 5% elastane. The measurement was carried out at isothermal conditions of 34 °C (skin temperature equal to ambient temperature), relative humidity of 18% (partial water vapour pressure of 957 Pa), and air speed of 0.1 ± 0.05 m/s. This setup allowed measurements in steady state conditions for at least 20 min to ensure reliable calculation of evaporative resistance. The calculation of evaporative resistance was done using the heat loss method described in ASTM F2370 [44].

2.4. Case 2 – photographic and heat loss method in standing position

Case 2 represents an example of experimental approach when an upright standing, non-articulated manikin (Fig. 1A) and a camera are available. The methodology to determine *Icl* and *Re, cl* is identical with *Case 1*, whilst the calculation of f_{cl} is based on superposition of photographs of nude and dressed manikin using graphical software (CorelDRAW X8, Corel Corporation, USA) according to the standard ISO 15831, Equation (A7) [32]. In this case, the western Newton type thermal manikin was photographed using a full frame camera with a 35 mm lens placed 4.33 m in front of the manikin from four azimuth angles (front 0°, two side views 45°, 90°, and 180°) and a horizontal view of 0°. The standard [32] suggests using one additional horizontal angle of 60°, however, this was not feasible due to the ceiling clearance limitation of the laboratory. Although the original method was proposed to calculate the whole body f_{cl}, we divided the manikin's body into *Upper arm, Lower arm, Chest, Abdomen, Anterior hip, Back, Lumbus, Posterior hip, Upper leg, Lower leg, and Foot*, before determining their local values.

2.5. Cases 3 and 4 – analytical heat transfer model

Cases 3 and 4 represent one of the emerging methods to realistically and rapidly simulate f_{cl}, I_{cl}, *and* $R_{e,cl}$, taking the air gap thickness and contact area into account for a corresponding body part both in seated and standing positions. All three local clothing parameters were calculated using the in-house analytical clothing model developed at Empa [30,43]. The model exploits basic thermodynamic phenomena (conduction, radiation, and natural convection) and allows the calculation of local clothing parameters of multiple, layered garments. The physical model resolution is equal to the number of input parameters that were calculated according to the linear regression model proposed by Psikuta et al. [27] in *Case 4*. The model yields corresponding air gap thickness and contact area, in standing positions, based on the ease allowances of clothing (Table 2) for 14 body parts excluding feet. However, the upper and lower chest as well as upper and lower back were averaged (area weighed) into two respective body parts to match the segmentation in Fig. 1A and the body resolution of the thermal manikin.

In *Case 3*, the resolution of the model was reduced to eight parts, since the four body parts in contact with the seat were not considered. The air gap thickness and contact area were taken from the database of garments in the seated position by Mert et al. [16] (positions U5, L4). The air gap thickness and contact area were obtained by linear interpolation based on the ease allowances.

2.6. Case 5 – regression and analytical heat transfer models

Case 5 represents an approach based on predictions of local f_{cl} and I_{cl} on clothing ease allowances proposed by Vesela et al. [21]. This allows simple calculation of the clothing properties based on readily available parameters. The regression models were derived from single layer garments in standing position. Yet, the behaviour of the multilayer clothing was described in the study by Mark et al. [55] using the 3D scanning technique. The main findings indicate that the inner layer is negligibly influenced by the outer layer as long as the ease allowance of the outer layer is bigger than that of the inner one. Further, for the majority of casual clothing, it can be assumed that the representative f_{cl} and I_{cl} can be calculated according to the ease allowances of the outer garment, and was also performed in this study. The overview of the ease allowances is given in Table 2. The methodology to calculate $R_{e,cl}$ was not presented in the study by Vesela et al. [21] and was adopted from *Case 4* [30].

2.7. Case 6 – ISO 9920 based model

Curlee [19] and Nelson et al. [23] developed a method to calculate all three local clothing parameters valid for 106 garments from McCullough et al. [24] and ISO 9920 [18]. However, the resolution of the algorithm is limited to individual clothing items covering given body parts, such as a shirt covering the whole torso and arms. As the method does not clarify an approach to calculating the resistances of multiple, layered garments lying atop one-another, the clothing resistances were instead totalled to match the procedure of Vesela et al. [11]. The clothing area factors of the outer layers were calculated as described in section 2.6.

Following clothing was selected for this study from Appendix A [19]:

- Summer clothing: Long sleeve collar shirt (broadcloth); Straight long fitted trousers (denim); Soft soled athletic shoes; Calf length dress socks.
- Winter clothing: Long-sleeve turtleneck (thin knit); Short sleeve collar shirt (broadcloth); Straight long lose trousers (denim); Hard soled athletic shoes; Calf length dress socks.

2.8. Case 7 – empirical model

The UTCI clothing model predicts local thermal insulation for 7 body parts (head, torso with upper arms, lower arms, hands, upper legs,

lower legs, feet) [20]. Despite the model's focus on outdoor applications, we assumed similar clothing preferences for indoor and outdoor environments based on two mild ambient temperatures of 24 °C (summer indoor clothing) and 21 °C (winter indoor clothing). These two temperatures were defined according to the PMV-PPD thermal sensation model described in the ISO 7730:2005 [56] as a thermo-neutral environment for activity level representing office work or driving at 1.3 met, clothing insulation according to ISO 9920 of 0.62 (summer) and 1.01 clo (winter), and air speed of 0.1 m/s.

2.9. Case 8 – estimation based on ISO 9920

Standard ISO 9920 [18] provides an exhaustive list of civil, working, and non-western clothing properties determined by a standing thermal manikin. Therefore, this approach is of main interest for a variety of engineering applications where there is no dedicated equipment available. The I_{cl} and f_{cl} are presented as a resultant insulation prescribed to all body parts, even to those parts, which are not covered by the clothing in reality. Similarly, the $R_{e,cl}$ was calculated as a whole body value according to Equation (31) from the standard [18] as intrinsic thermal insulation multiplied by a constant of 0.18.

Two clothing sets were selected from the standard (Table A.2) [18] based on the closest match of the description of the garments as follows:

- Summer clothing: *Ensemble 108* – briefs, long-sleeve shirt, fitted, trousers, calf-length socks, shoes.
- Winter clothing: *Ensemble 114* – briefs, T-shirt, shirt, loose trousers, round-neck sweater, calf-length socks, shoes.

2.10. Determination of seat thermal properties

As a consequence of the seat, the body segments in contact with it experience increased thermal and water vapour resistances. Direct measurement of these parameters with the Newton type manikin is not accurate because of the manikin's rigid body construction and low body weight, which inhibit the resulting contact area from imitating the interaction of a representative body and seat [40]. As a result, lower compression of seat layers and smaller contact area with differences in shape are expected for manikins when comparing to humans. For this reason, the corresponding data was adopted from the study on aeroplane seats with similar construction to automotive seats, with moulded foam cushioning and leather cover. Using a stamp tester, a thermal resistance of 0.55 m^2K/W (Fig. 7 in Ref. [39]) was measured for the seat, whilst an evaporative resistance of 100 m^2Pa/W [39] was determined using the same seat in human trials. Finally, we estimated the seat clothing area factor to be 2.0 units based on the dimensions of the seat.

2.11. Thermo-physiological simulations

Benchmark tests of clothing thermal properties are helpful in the development and evaluation of clothing systems, but thermo-physiological responses do not show a similar sensitivity to clothing properties as can be detected by benchmark tests [48]. Therefore, the eight studied cases were used as separate inputs for thermo-physiological modelling under the same environmental conditions to quantify the resulting differences in physiological responses among the methods.

To do so, two setups corresponding to summer ($t_{air} = t_{rad} = 24°$) and winter ($t_{air} = t_{rad} = 21°$) indoor environments with an ambient air speed of 0.1 m/s, and relative humidity of 50% were carried out using the broadly validated Fiala model FPCm 5.3 [46]. The metabolic production of 1.3 met was selected from a database presented by Ainsworth et al. [57] as an average from reading, typing, and driving. The simulations were run for 4 h with a 5 min simulation interval to reveal the development of thermo-physiological response in a long steady exposure.

In the simulations, the clothing thermal properties of shoes were obtained from *Case 2 and* considered in f_{cl} for *Cases 1,3,4,5*, I_{cl} for *Cases 3,4,5*, and $R_{e,cl}$ for *Cases 3,4,5,6*. Additionally, the simulations account for the thermal effects of the seat (Section 2.10). The seats were applied as the clothing boundary conditions to posterior thighs, posterior hip, posterior abdomen, and posterior thorax of the virtual humanoid according to the findings from Fojtlín et al. [40]. This was done for *Cases 1* to *7*, whereas the eighth case was executed according to the directions from ISO 9920 [18], such that an additional thermal insulation of 0.039 $m^2K.W^{-1}$ was added to the whole-body resistance. As the standard does not clarify how to treat f_{cl} and $R_{e,cl}$, the values were unchanged for *Case 8* in the standing position.

Firstly, to assess the effects of clothing boundary conditions, we examined mean skin and rectal temperatures to provide a global overview of the body thermal state. Secondly, the cumulative sweating was investigated to quantify the amount of liquid sweat excreted from the whole body. Next, to measure the development of local parameters, skin temperatures were examined at Chest and Anterior thighs, which were selected because of their dominant surface area that is not in the contact with the seat and their distinct susceptibility to change air gap thickness with the change of position. Furthermore, dynamic thermal sensation (*DTS*) was calculated to predict whole body thermal sensation on the 7-point scale ranging from - *3 Cold*, through *0 Neutral*, to *3 Hot* [56]. Finally, skin wettedness was examined at *Chest* and can be considered as a perception of wet discomfort being physically defined as the ratio of the actual sweat rate to the potentially evaporating amount of sweat.

3. Results

3.1. Comparison of the methods

Local clothing properties f_{cl}, I_{cl}, and $R_{e,cl}$ were divided into four groups of body parts, namely anterior and posterior torso, and upper and lower limbs (Figs. 2 and 3). Furthermore, Figs. 2 and 3 show the local clothing properties obtained from all examined methods for a given body part in one plot. A result from one body part is connected with a dashed line for easier tracking of its development depending on the method. The results from methods having body parts resolutions lower than reference (13) were either left blank, if missing, or presented as one value for related body parts, for instance lower leg from UTCI model [20] covers *Shin* and *Calf*. Where applicable in Figs. 2 and 3, error bars represent standard deviation of the repeated measurements. The differences between repeated manikin measurements in I_{cl} fell within the recommended 4% [32], thus, the standard deviation was too small to be visualised and was not plotted. Despite the anatomically unrealistic contact of the manikin with the seat [40], the I_{cl} and $R_{e,cl}$ from the contact area in *Case 1* (Figs. 2 and 3 – *Back, Lumbus, Buttocks, and Anterior thighs*) are shown for full overview. Because of the limitations of the 3D scanning method in the contact area, in *Case 3*, the f_{cl} was calculated based on an increase of the skin surface area by the thickness of the fabrics. As reference body geometry we used a virtual humanoid from the Fiala thermo-physiological model [46]. Further, the I_{cl} and $R_{e,cl}$ was estimated as thermal and evaporative resistances of the fabrics only.

Assuming that *Case 1* (manikin measurement in seated position) is the most accurate method, the variation between all the methods for both clothing ensembles was as follows:

- 13–43% of the reference value for clothing area factor (f_{cl}) depending on body part;
- 35–198% of the reference value for intrinsic thermal insulation (I_{cl}) depending on body part;
- 53–233% of the reference value for intrinsic evaporative resistance ($R_{e,cl}$) depending on body part.

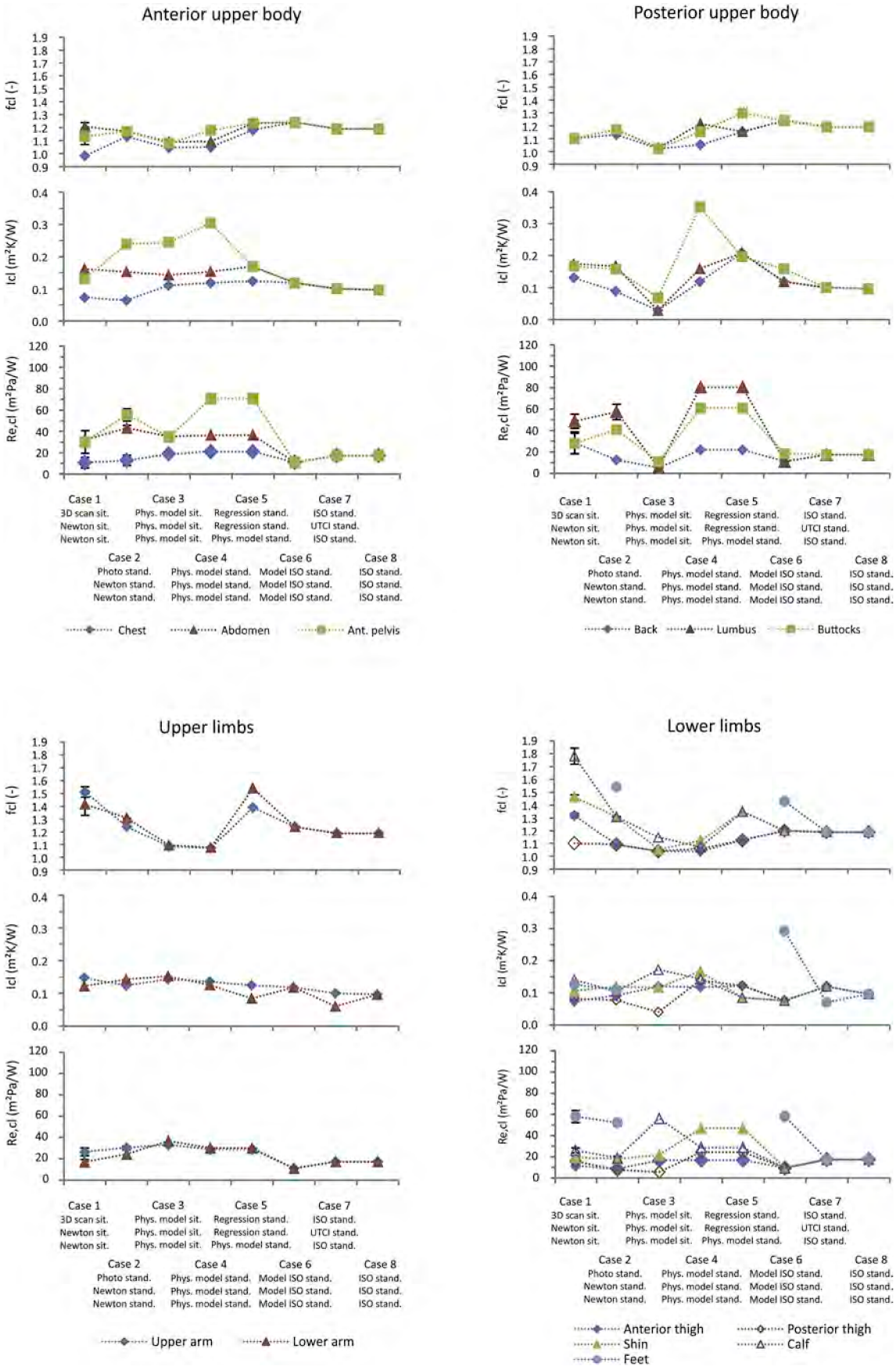

Fig. 2. The clothing thermal properties of the summer indoor clothing set shown for 13 body parts excluding the seat thermal properties. Error bars depict standard deviation.

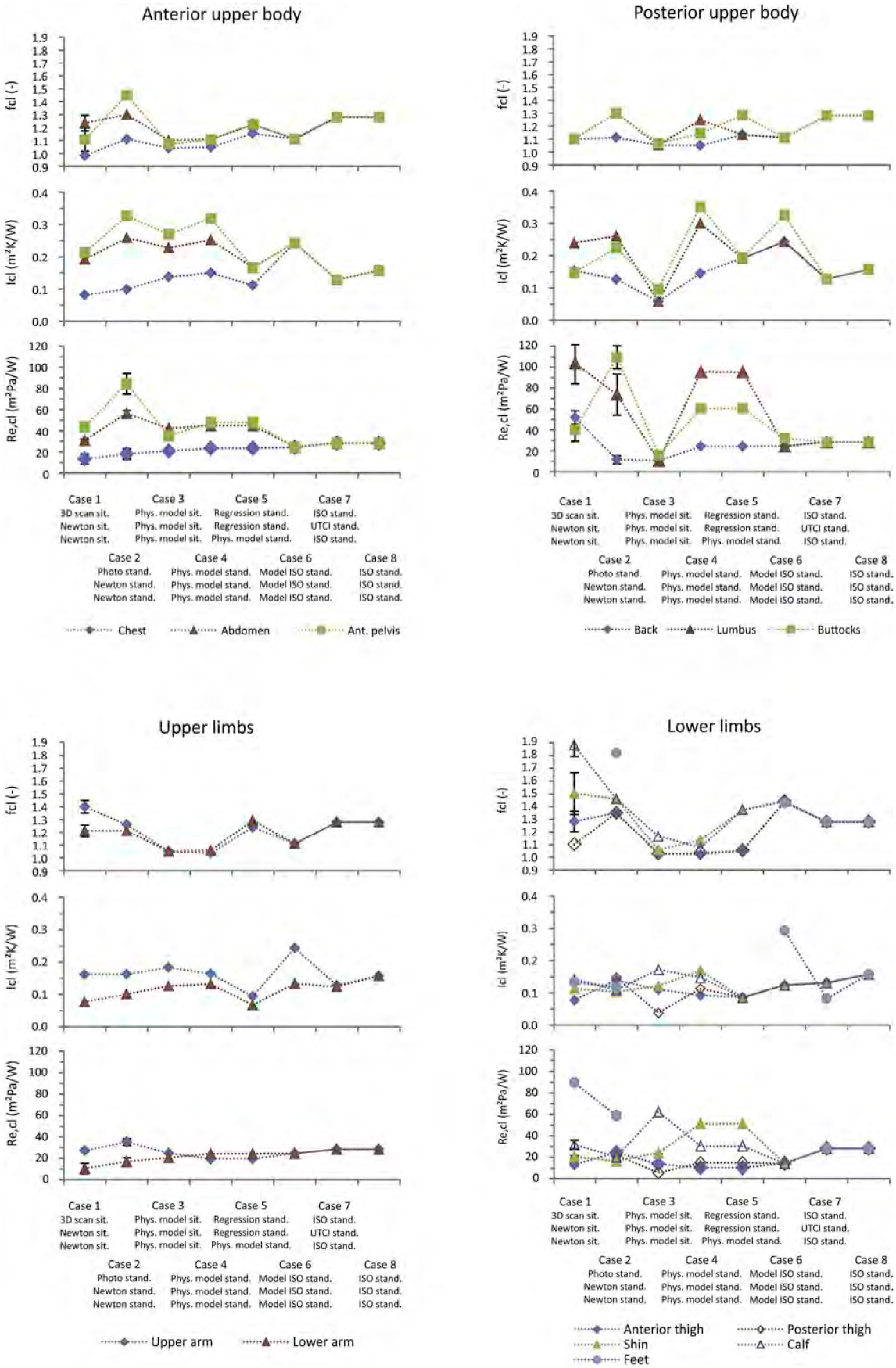

Fig. 3. The clothing thermal properties of the winter indoor clothing set shown for 13 body parts excluding the seat thermal properties. Error bars depict standard deviation.

These variations were found to be very similar for both clothing ensembles with somewhat higher values for the looser, multilayer winter ensemble (Figs. 2 and 3). When comparing 6 cases based on standing body position only (*Cases 2, 4, 5, 6, 7,* and *8*, Table 1), their variation was as follows:

- 6–36% of the reference value for clothing area factor (f_{cl}) depending on body part;
- 32–204% of the reference value for intrinsic thermal insulation (I_{cl}) depending on body part;
- 45–232% of the reference value for intrinsic evaporative resistance ($R_{e,cl}$) depending on body part.

3.2. Differences in manikin measurements between sitting and standing body positions

The differences between parameters for both sitting and standing positions are depicted in Fig. 4 for selected representative body parts with and without a major change in their orientation. The body parts in contact with the seat were considered without the seat thermal insulation. The following difference margins between sitting and standing positions were found, namely:

- up to 31% of the reference value (*Case 1*) for f_{cl} depending on body part;
- up to 80% of the reference value (*Case 1*) for I_{cl} depending on body part;
- and up to 92% of the reference value (*Case 1*) for $R_{e,cl}$ depending on body part.

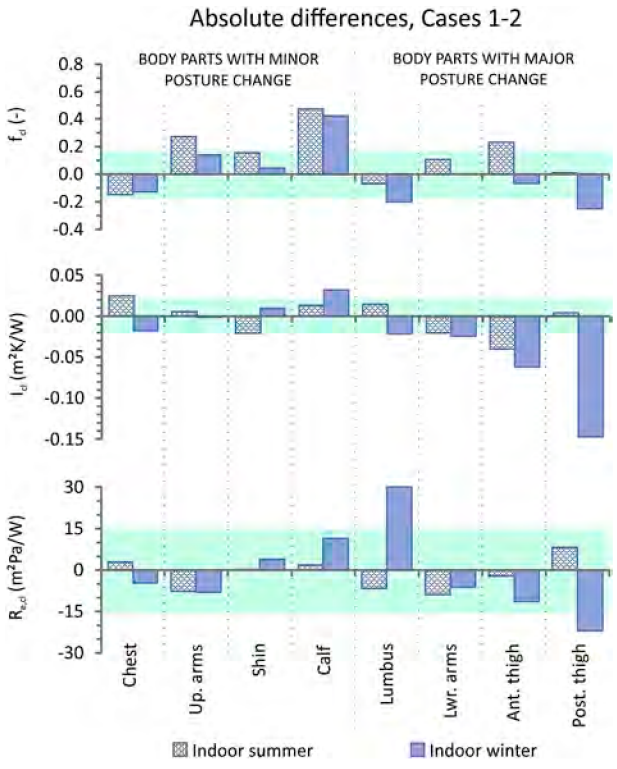

Fig. 4. Absolute differences between clothing thermal properties between the positions (Cases 1–2) for summer and winter indoor clothing, respectively. The transparent field depicts a range of three standard deviations of the methods used in Case 1 covering 99.7% of observations being ± 0.17 units for f_{cl}, ± 0.02 m^2K/W for I_{cl}, and ± 15 m^2Pa/W for $R_{e,cl}$.

3.3. Effects of the clothing and body position on thermo-physiology

The results for the whole-body and local thermal responses from thermo-physiological simulations are depicted in Fig. 5, separately for summer and winter scenarios. In total, eight responses were plotted such as mean skin temperature, rectal temperature, skin temperature at chest, skin temperature anterior thigh, cumulative sweating, dynamic thermal sensation (DTS), and skin wettedness at *Chest*. Each line represents a development of a given simulated response corresponding to one of the examined methods to determine the clothing properties. To differentiate between sitting and standing body positions, the sitting positions are represented within the plots by continuous lines, whilst standing positions are denoted by dashed lines.

4. Discussion

4.1. Comparison of the methods

In this study, we compared six various methods to obtain clothing area factor, seven methods for intrinsic thermal insulation, and five methods for intrinsic evaporative resistance determination. These methods were combined into eight distinct cases corresponding to different availabilities of advanced equipment to determine the clothing properties in an exemplary laboratory. In theory, all the examined methods should yield the same results. Contrary to this, large differences of more than 200% were found for all three clothing parameters and body parts covered by the clothing (Figs. 2 and 3) assuming that *Case 1* (manikin measurement in seated position) is the most accurate reference method (13–43%, 35–198%, and 53–233% of the reference value for clothing area factor (f_{cl}), intrinsic thermal insulation (I_{cl}) and intrinsic evaporative resistance ($R_{e,cl}$), respectively, depending on body part).

It is worth to mention that this variation cannot be predominantly attributed to the body position. When comparing 6 cases based on standing body position only (*Cases 2, 4, 5, 6, 7,* and *8*, Table 1), their variation was slightly lower, such as 6–36%, 32–204%, and 45–232% of the reference value for clothing area factor, intrinsic thermal insulation, and evaporative resistance, respectively, depending on body part.

The error in f_{cl} was greater at the limbs (0.16–0.81 units of difference among the methods) than at the torso (0.15–0.38 units of difference among the methods). The median of error among all cases was 0.36 units, whereas the most outstanding difference was observed at calves of up to 0.81 units (Fig. 3, *Case 3*). Here, the method assumes a cylinder as a base shape wrapped by clothing which includes the average air gap thickness. This does not fully represent the real situation of the hanging trouser leg in the sitting position. Regarding I_{cl} and $R_{e,cl}$, amongst the methods tested the upper limbs presented the best matching predictions, resulting in differences of 0.05–0.15 m^2K/W and 15.8–25.7 m^2Pa/W, respectively. The rest of the body parts did not show any clear trends in prediction accuracy, having average differences among the methods in I_{cl} and $R_{e,cl}$ of 0.14 m^2K/W and 38.8 m^2Pa/W respectively, with the greatest span of predictions of 0.2 m^2K/W in I_{cl} and of 60.1 m^2Pa/W in $R_{e,cl}$ at *Anterior pelvis*.

The predictions of all clothing parameters were the most realistic in *Cases 3, 4,* and *5* compared to the reference values from *Case 1*. Presumably, the rest of the methods poorly capture changes in the clothing parameters because of their limited body resolution. *Cases 1* and *2* were carried out with resolutions of 13 segments as well as *Cases 3, 4,* and *5,* whereas the methods used in *Cases 6, 7,* and *8* work with body segmentation of three, seven, and one components, respectively. Thus, distinct body parts (such as *Chest, Abdomen, Ant. Pelvis, Back, Lumbus, and Arms* in *Case 6*) are lumped into one segment that yields an averaged value in *Case 6* of 0.12 m^2K/W for summer clothing and of 0.24 m^2K/W for winter clothing when neglecting local extremes. Area weighted average from the same segments from the more detailed *Case 2* shows comparable results of 0.15 m^2K/W and 0.20 m^2K/W in summer

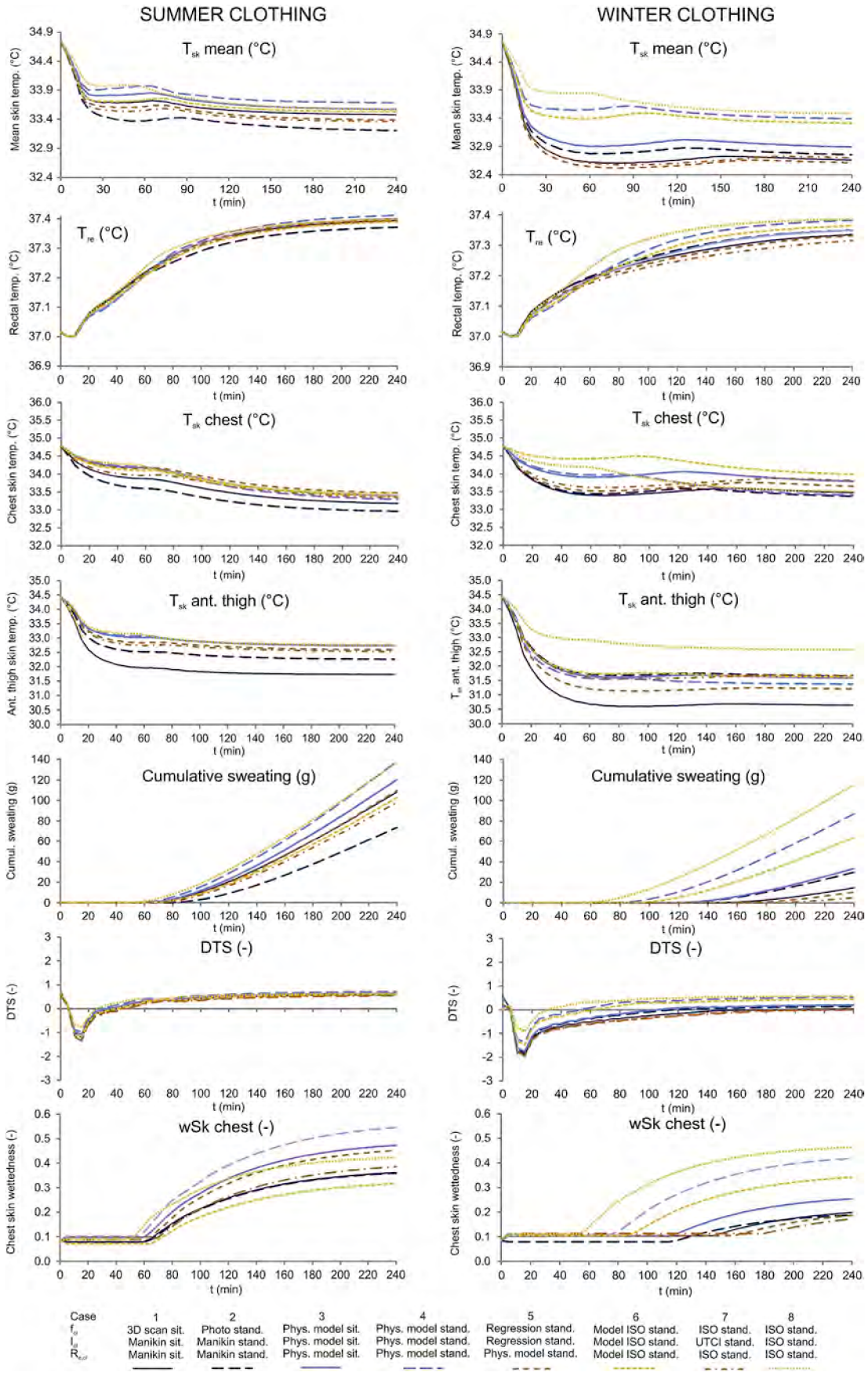

Fig. 5. Results of the thermo-physiological simulations separately for summer and winter clothing.

and winter clothing, respectively. At the same time, the local values in *Case 2* differ substantially from their average, with extremes at *Chest* and *Anterior Pelvis* of 0.06 m^2K/W and 0.24 m^2K/W for summer clothing and of 0.10 m^2K/W and 0.33 m^2K/W for winter clothing, respectively. Therefore, it is essential to account for local extremes.

4.2. Differences in manikin measurements between sitting and standing positions (cases 1 and 2)

The change of body position implies a change in orientation for several regions of the body to varying extents. This is particularly evident when one considers the significant degree of thigh reorientation, when contrasted to the minor reorientation of the chest when moving between standing and sitting positions. The differences in all three clothing thermal properties for both positions were found and are depicted in Fig. 4 for selected representative body parts with and without a major change in their orientation. The least pronounced deviations (of up to 31%) were discovered in f_{cl}. Despite slight postural changes at *Calf* and *Upper arm*, here, an error in f_{cl} was three standard deviations higher than of other typical measurements (Fig. 4).

Although minor variations would be expected due to slight postural changes, it was found that the an error in f_{cl} at the *Calf* and *Upper arm* was three standard deviations higher than of other typical measurements. Despite minor changes were expected only because of the minor posture change, we found the opposite in f_{cl} at the *Calf* and *Upper arm*, being higher than three standard deviations of typical measurement (Fig. 5). The error at *Calf* can be explained by the hanging trouser leg in the seated position yielding a difference of approximately 0.5 f_{cl} units. The discrepancy at *Upper arm* is plausibly related to methodological differences between *Cases 1* and *2*.

The photographic method is based on the projection of a three-dimensional object to a two-dimensional plane. Whilst there is an expected loss of detail in the clothing topography through this approach in C*ase 2*, the 3D scanning method of *Case 1* accounts for clothing folds which affect total clothing surface area. Thus, the error between the scanning and the photography is of 0.28 f_{cl} units for summer and 0.12 f_{cl} units for winter clothing. However, it is difficult to generalise the methodological error because the number and the size of the folds vary over the body surface. Next, in the sitting position, the 3D scanning method yields f_{cl} at *Chest* lower than 1 as opposed to the photographic method. The probable reason for this is the anatomic curvature of the flexible manikin's chest [16] that has a greater surface area than the stretched flat garment that covers the chest, whereas the Newton thermal manikin (*Case 2*) has simplified concave chest curvature. Thus, its skin surface is smaller than the surface of the outer garment yielding f_{cl} greater than 1.

The results in I_{cl} and $R_{e,cl}$ from *Cases 1* and *2* exhibit greater variation (of up to 80% and 92%, respectively) and correspond to a redistribution of the mean air gap thicknesses between the positions reported by Mert at al. [28], and its consequent impact on thermal and evaporative resistances as reported by Psikuta et al. [45]. In compliance with these two studies, we found decrease in I_{cl} and $R_{e,cl}$ greater than three standard deviations of measurement at *Anterior pelvis*, *Anterior thighs*, *Abdomen,* and *Lower arm* (Fig. 4). At these parts, air gaps collapse and the I_{cl} of two-layer winter clothing might be equalled to standing summer clothing. This underlines the importance of distinguishing between the body orientations and using local values.

4.3. Effects of the clothing and position on thermo-physiology

Differences in local clothing properties may be integrated by human thermoregulation and, thus, result in minimal discrepancy of global parameters such as mean skin or core temperatures. The variation of mean skin temperatures among the eight methods was within 0.6 and 1.3 °C in summer and winter clothing, respectively. This rather remarkable error can be related to a considerable change in local thermal sensation from approximately 0.5 to 1.5 units, depending on the thermal sensation model, and its scale as demonstrated by Koelblen and Veselá et al. [11,58]. However, the differences between the body positions were marginal within 0.3 °C. Finally, we found minor impact of the eight clothing inputs on the predicted rectal temperature of less than 0.1 °C.

The local thermo-physiological parameters show substantial variation that corresponds to variation in the clothing inputs even if applied in a neutral, steady, and uniform environment (Fig. 5). In reference to *Case 1*, the approaches whose results which most closely matched were found to be the same as in the investigation on the clothing thermal properties, namely *Case 3* (modelling based on air gap thicknesses in sitting) and *Case 5* (regression model based on air gap thickness). The worst performing approach was *Case 8* based on the whole-body estimation of clothing parameters and the ISO based model from *Case 6* (Fig. 5). It seems to be not possible to recover any local data based on whole body values with reasonable accuracy when local data is necessary, as shown by performance of *Case 6*.

Next, the development of the local skin temperatures is clearly affected by the variation of local clothing thermal properties. For instance, relatively low differences in the clothing properties at *Chest* (Figs. 2, 3 and 5) result in the absolute differences in skin temperatures of 0.5 °C among all methods and of 0.2 °C between the body positions (Fig. 5). On the contrary, higher variability of input parameters, such as at *Anterior thighs*, leads to a spread of the predicted local skin temperature of 1 and 2 °C in summer and winter clothing, respectively. Next, cumulative sweating indicates low to mild sweat excretion that amounts between 5 g (*Case 7* winter clothing) and 138 g (*Case 4* summer clothing). The onset of sweating varied substantially in the winter clothing between 60th (*Case 8*) and 190th minute (*Case 7*).

The precise predictions of the sweat amount and onset of sweating can enhance a proper prediction of skin wettedness linked to so-called wet discomfort from sweating. At the end of the exposure, this parameter ranged from 0.03 to 0.61 and from 0.06 to 0.71 in summer and winter clothing, respectively. The highest values were always found in the contact parts with the seat and the lowest for bare body parts, such as hands. The variability of predictions can be demonstrated on *Chest*, where the threshold for discomfort of 0.42 units [59] was exceeded in the winter clothing tests of *Cases 4* and *8* (value reached in 210 min and 145 min, respectively), and in the summer clothing *Cases 3* (125 min)*, 4, 5,* and *8* (185 min). The threshold was not reached in the *Cases 1* and *2* (Fig. 5).

Although, the examined deviations in thermo-physiological parameters are not critical in regards to medical relevance, such as uncompensated heat storage or dehydration, they negatively influence accuracy of thermal sensation prediction. The benchmark value for the assessment of thermal sensation was adopted from ISO 7730 [56] as ± 0.5 units (thermal environment category B corresponding to less than 10% of dissatisfied occupants with the thermal environment). The whole-body thermal sensation index *DTS* showed minor variations between the methods which was within 0.2 units for summer clothing and significant discrepancies were found in the winter scenario of up to 0.6 units (*Cases 4, 7, 8* compared to *Case 1,* Fig. 5). Yet, the contribution of the position change, demonstrated in *Cases 1* and *2*, did not reveal any significant differences in *DTS* (below 0.1 units). However, it can be expected to see major differences in the local thermal sensation predictions.

The whole body values are not sufficient for local modelling and the seated posture induces a drop in thermal and evaporative resistance due to collapse of air layers underneath the clothing. Furthermore, the previously discussed variability of the thermo-physiological responses induced by the clothing inputs urges the use of precise local clothing parameters. Only then with these parameters can reliable simulations of thermo-physiological responses be conducted. In addition, the discrepancies between the predictions may inflate for conditions further away from thermo-neutrality and cause even larger errors in

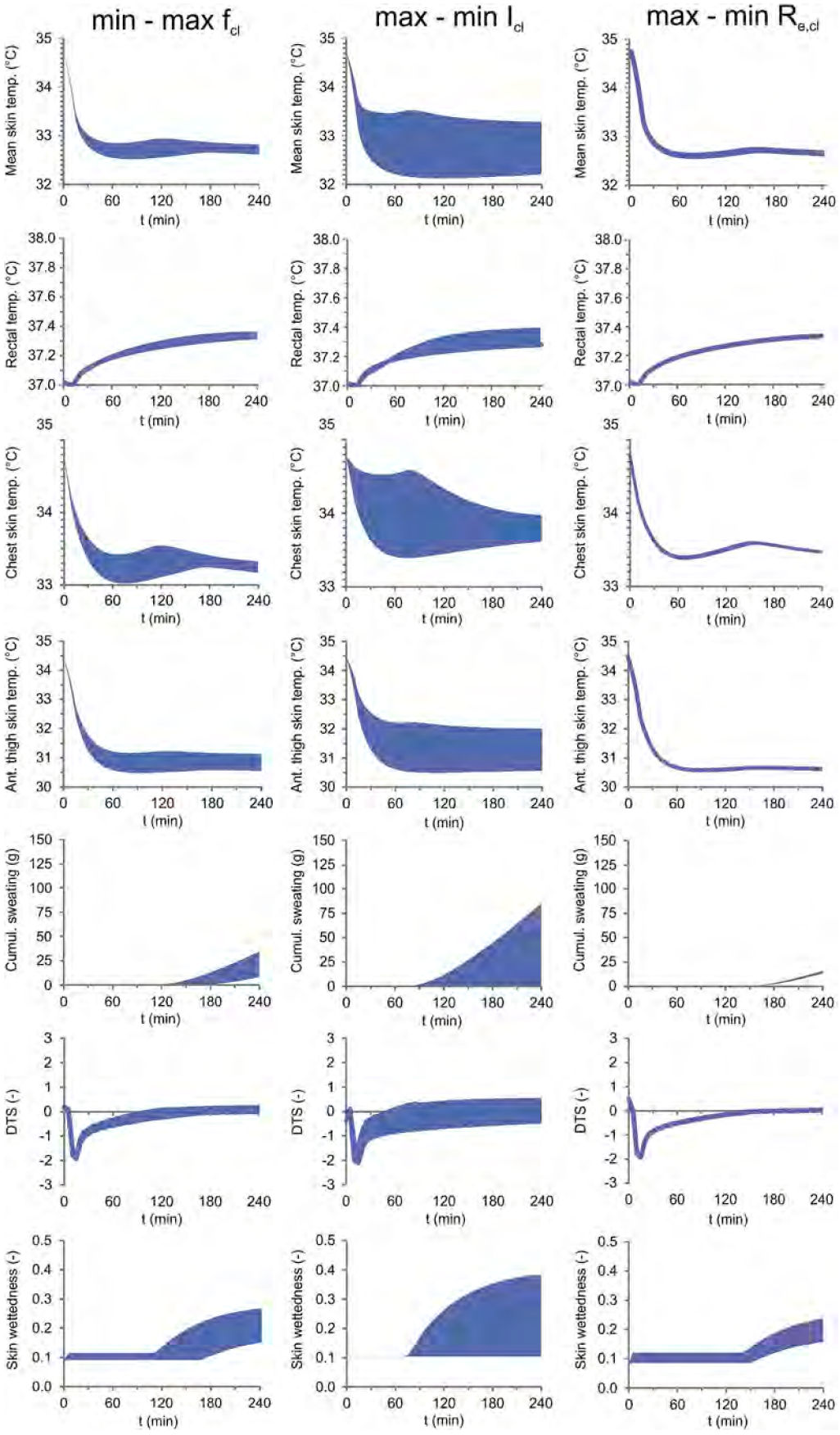

Fig. 6. Sensitivity of thermo-physiological responses to changes in individual clothing parameters.

predictions of thermal sensation, comfort or performance of the occupants [58,60]. This applies for instance in free running buildings with a larger temperature range, vehicles, and industrial spaces with special conditioning due to technological processes.

4.4. Sensitivity analysis

In order to examine the sensitivity of the physiological response to variations in clothing parameter inputs, we reproduced the winter case using upper and lower extremes of the clothing parameters out of the 8 cases. Only one clothing parameter was changed at a time (for instance f_{cl}) while keeping the rest (in this case I_{cl} and $R_{e,cl}$) as the reference – *Case 1* sitting.

The results are displayed in Fig. 6 and clearly show the variability of I_{cl} inducing the greatest effect on all monitored thermo-physiological parameters in thermo-neutral environmental conditions (Details in Section 2.11). Differences in skin temperatures and DTS exceeded 1 °C and 1 unit, respectively. As previously discussed, such discrepancies have measurable impact on the perceived thermal sensation and/or comfort. Despite high deviations in f_{cl} (up to 43%) and $R_{e,cl}$ (up to 233%), the effect of these two parameters on thermo-physiology is practically negligible. However, it can be expected that the importance of $R_{e,cl}$ in warm conditions will play a more significant role, as a larger amount of sweat is excreted and needs to be transported through the clothing system. Secondly, the variation of $R_{e,cl}$ between methods might be larger when protective clothing with higher evaporative resistance is considered, since this clothing is less represented and more difficult to unambiguously identify in databases used in regression and reference table methods.

4.5. Reliability of the reference methods

Despite using the state-of-the-art methods as a reference, several remarks should be noted on their reliability. Firstly, the precision of 3D scanning method – used in this study to determine clothing area factor – is typically better than 1.7 mm [28,61]. Based on the dimensions of the passive body geometry in the Fiala model [46], an addition of 1.7 mm to the body part radius causes a change in f_{cl} as low as 0.01 units. This increment is, thus, negligible compared to observed f_{cl} variation between examined methods and we conclude high reliability of this method. Secondly, the measurement of I_{cl} has the typical error among the repeated measurements of less than 4% that is recommended by the standard ISO 15831 [32]. The only two local extremes of 10% were found at the *Abdomen* and *Back*. Finally, the precision of the methodology to determine $R_{e,cl}$ has several methodological limitations that are bound to complexity of the heat and mass transfer through the garment, such as heat pipe effect, wicking, partial drying, wet conduction [62], evaporative heat energy taken from the environment [53], and inability to control the temperature of the wetted manikin's skin [63,64]. Thus, the skin temperature might be lower than assumed and introduce an error in $R_{e,cl}$ of up to 14% [63]. Nevertheless, according to our sensitivity analysis in mild thermal environments, the errors in $R_{e,cl}$ have only a minor impact on the physiological response.

5. Conclusions

Eight typical approaches to determine clothing properties for thermo-physiological and thermal sensation predictions were examined, both in sitting and standing body positions, using two sets of indoor clothing. Considerable differences among the eight examined methods in clothing area factor, intrinsic clothing thermal insulation, and evaporative resistance were found. Next, the findings from the study also confirm a need to differentiate between the local clothing inputs in seated and standing positions and urge to avoid using the whole body values that are not sufficient for local thermo-physiological modelling. The impact of the variation of the clothing parameters was shown in the simulations of physiological responses in thermo-neutral, homogeneous, and steady conditions. Consequently, due to differences in the clothing inputs, we found major deviations of skin temperatures, skin wettedness, and global thermal sensation votes. Furthermore, sensitivity analysis revealed a dominant influence of intrinsic clothing thermal insulation on the simulated responses, while clothing area factor and evaporative resistance had minor influences. Therefore, we recommend using the highest precision method available to determine I_{cl}, such as a manikin measurement, physical modelling or regression modelling. Nonetheless, it can be expected that discrepancies among the methods will be stressed out in heterogeneous and extreme ambient conditions, for instance in vehicular cabins exposed to hot or cold weather conditions, free running buildings or specific working environments.

The findings from this study are beneficial for a broad variety of research and engineering applications, where a design of a thermal environment is essential to ensure comfort and performance of the occupants, such as multiple sitting occupations (office work, assembly or sewing work, driving) and passenger transportation. Here, the acceleration of innovation cycles and reduction of costs for physical studies is advanced by the selection and use of reliable thermo-physiological models, which incorporate realistic clothing boundary conditions whilst also accounting for body position.

Acknowledgements

The part of work conducted at Empa was supported by the [HEATSHIELD project within EU Horizon 2020 program] under Grand [RIA 668786–1]. The experimental part of the work conducted at Brno University of Technology was supported by the [Ministry of Education project Youth and Sports of the Czech Republic] under the “National Sustainability Programme I” [LO1202 Netme Centre Plus]; and the [Brno University of Technology] under the project Reg. No. [FSIeS-17-4444]. The authors would like to thank Ankit Joshi from Empa, St. Gallen for help with calculating clothing thermal properties in *Cases 3 and 4*.

References

[1] M. Veselý, W. Zeiler, Personalized conditioning and its impact on thermal comfort and energy performance - a review, Renew. Sustain. Energy Rev. 34 (2014) 401–408, https://doi.org/10.1016/j.rser.2014.03.024.
[2] M. Veselý, P. Molenaar, M. Vos, R. Li, W. Zeiler, Personalized heating – comparison of heaters and control modes, Build. Environ. 112 (2017) 223–232, https://doi.org/10.1016/j.buildenv.2016.11.036.
[3] W. Pasut, H. Zhang, E. Arens, Y. Zhai, Energy-efficient comfort with a heated/cooled chair: results from human subject tests, Build. Environ. 84 (2015) 10–21, https://doi.org/10.1016/j.buildenv.2014.10.026.
[4] M. Luo, E. Arens, H. Zhang, A. Ghahramani, Z. Wang, Thermal comfort evaluated for combinations of energy-efficient personal heating and cooling devices, Build. Environ. 143 (2018) 206–216, https://doi.org/10.1016/j.buildenv.2018.07.008.
[5] A. Psikuta, J. Allegrini, B. Koelblen, A. Bogdan, S. Annaheim, N. Martínez, D. Derome, J. Carmeliet, R.M. Rossi, Thermal manikins controlled by human thermoregulation models for energy efficiency and thermal comfort research – a review, Renew. Sustain. Energy Rev. 78 (2017) 1315–1330, https://doi.org/10.1016/J.RSER.2017.04.115.
[6] E. Foda, K. Sirén, Design strategy for maximizing the energy-efficiency of a localized floor-heating system using a thermal manikin with human thermoregulatory control, Energy Build. 51 (2012) 111–121, https://doi.org/10.1016/j.enbuild.2012.04.019.
[7] D. Fiala, A. Psikuta, G. Jendritzky, S. Paulke, D.A. Nelson, W.D. van Marken Lichtenbelt, A.J.H. Frijns, Physiological modeling for technical, clinical and research applications, Front. Biosci. S2 (2010) 939–968.
[8] C. Huizenga, Z. Hui, E. Arens, A model of human physiology and comfort for assessing complex thermal environments, Build. Environ. 36 (2001) 691–699, https://doi.org/10.1016/S0360-1323(00)00061-5.
[9] M. Hepokoski, A. Curran, D. Dubiel, Improving the accuracy of physiological response in segmental models of human thermoregulation, in: S. Kounalakis, M. Koskolou (Eds.), XIV Int. Conf. Environemntal Ergon. Nafplio, Nafplio, 2011, pp. 102–103.
[10] B. Koelblen, A. Psikuta, A. Bogdan, S. Annaheim, R.M. Rossi, Thermal sensation models: a systematic comparison, Indoor Air 27 (2016) 1–10, https://doi.org/10.1111/ina.12329.
[11] S. Veselá, B.R., A.J. Frijns Kingma, Local thermal sensation modeling: a review on the necessity and availability of local clothing properties and local metabolic heat

production, Indoor Air 27 (2017) 261–272, https://doi.org/10.1111/ina.12324.
[12] G. Havenith, D. Fiala, Thermal indices and thermophysiological modeling for heat stress, Comp. Physiol. 6 (2015) 255–302, https://doi.org/10.1002/cphy.c140051.
[13] G. Havenith, R. Heus, W.A. Lotens, Resultant clothing insulation: a function of body movement, posture, wind, clothing fit and ensemble thickness, Ergonomics 33 (1990) 67–84, https://doi.org/10.1080/00140139008927094.
[14] G. Havenith, R. Heus, W.A. Lotens, Clothing ventilation, vapour resistance and permeability index: changes due to posture, movement and wind, Ergonomics 33 (1990) 989–1005, https://doi.org/10.1080/00140139008925308.
[15] Y.S. Wu, J.T. Fan, W. Yu, Effect of posture positions on the evaporative resistance and thermal insulation of clothing, Ergonomics 54 (2011) 301–313, https://doi.org/10.1080/00140139.2010.547604.
[16] E. Mert, A. Psikuta, M.A. Bueno, R.M. Rossi, The effect of body postures on the distribution of air gap thickness and contact area, Int. J. Biometeorol. (2016) 1–13, https://doi.org/10.1007/s00484-016-1217-9.
[17] E. Mert, A. Psikuta, M.A. Bueno, R.M. Rossi, Effect of heterogenous and homogenous air gaps on dry heat loss through the garment, Int. J. Biometeorol. 59 (2015) 1701–1710, https://doi.org/10.1007/s00484-015-0978-x.
[18] International Organization for Standardization, ISO 9920 Ergonomics of the Thermal Environment - Estimation of Thermal Insulation and Water Vapour Resistance of a Clothing Ensemble, (2007), p. 104.
[19] J.S. Curlee, An Approach for Determining Localized Thermal Clothing Insulation for Use in an Element Based Thermoregulation and Human Comfort Code, Master Thesis Michigan Technological University, 2004.
[20] G. Havenith, D. Fiala, K. Blazejczyk, M. Richards, P. Bröde, I. Holmér, H. Rintamaki, Y. Benshabat, G. Jendritzky, The UTCI-clothing model, Int. J. Biometeorol. 56 (2012) 461–470, https://doi.org/10.1007/s00484-011-0451-4.
[21] S. Veselá, A. Psikuta, A.J.H. Frijns, Local clothing thermal properties of typical office ensembles under realistic static and dynamic conditions, Int. J. Biometeorol. (2018) 15, https://doi.org/10.1007/s00484-018-1625-0.
[22] Y. Lu, F. Wang, X. Wan, G. Song, C. Zhang, W. Shi, Clothing resultant thermal insulation determined on a movable thermal manikin, Part II: Eff. Wind Body Mov. Local Insul. 59 (2015) 1487–1498, https://doi.org/10.1007/s00484-015-0959-0.
[23] D.A. Nelson, J.S. Curlee, A.R. Curran, J.M. Ziriax, P.A. Mason, Determining localized garment insulation values from manikin studies : computational method and results, Eur. J. Appl. Physiol. 95 (2005) 464–473 https://doi.org/10.1007/s00421-005-0033-4.
[24] E. McCullough, B. Jones, A comprehensive data base for estimating clothing insulation, ASHRAE Res. Proj. Rep. RP 411 (1985) 162.
[25] J. Pokorný, J. Fišer, M. Fojtlín, B. Kopečková, R. Toma, J. Slabotínský, M. Jícha, Verification of Fiala-based human thermophysiological model and its application to protective clothing under high metabolic rates, Build. Environ. (2017), https://doi.org/10.1016/j.buildenv.2017.08.017.
[26] E. Mert, S. Böhnisch, A. Psikuta, M.-A. Bueno, R.M. Rossi, Contribution of garment fit and style to thermal comfort at the lower body, Int. J. Biometeorol. 60 (2016) 1995–2004, https://doi.org/10.1007/s00484-016-1258-0.
[27] A. Psikuta, E. Mert, S. Annaheim, R.M. Rossi, Local air gap thickness and contact area models for realistic simulation of human thermo-physiological response, Int. J. Biometeorol. (2018) 1–14 https://doi.org/10.1007/s00484-018-1515-5.
[28] E. Mert, A. Psikuta, M. Bueno, R.M. Rossi, The effect of body postures on the distribution of air gap thickness and contact area, Int. J. Biometeorol. 61 (2017) 363–375, https://doi.org/10.1007/s00484-016-1217-9.
[29] E. Mert, S. Böhnisch, A. Psikuta, M.-A. Bueno, R.M. Rossi, Contribution of garment fit and style to thermal comfort at the lower body, Int. J. Biometeorol. 60 (2016) 1995–2004, https://doi.org/10.1007/s00484-016-1258-0.
[30] A. Joshi, A. Psikuta, M.A. Bueno, S. Annaheim, R.M. Rossi, Mathematical formulation of sensible heat transfer in the spatially heterogeneous skin-clothing-environment system, in: A. Psikuta (Ed.), 12th International Manikin and Modelling Meeting (12i3m), St. Gallen, Switzerland, 2018 https://doi.org/10.5281/zenodo.1404475.
[31] International Organization for Standardization, EN ISO 14505-2 Ergonomics of the Thermal Environment - Evaluation of Thermal Environments in Vehicles - Part 2: Determination of Equivalent Temperature, (2006), p. 25.
[32] International Organization for Standardization, ISO 15831 Clothing - Physiological Effects - Measurement of Thermal Insulation by Means of a Thermal Manikin, (2004), p. 11.
[33] K. Katic, R. Li, W. Zeiler, Thermophysiological models and their applications: a review, Build. Environ. 106 (2016) 286–300, https://doi.org/10.1016/j.buildenv.2016.06.031.
[34] H. Zhang, E. Arens, C. Huizenga, T. Han, Thermal sensation and comfort models for non-uniform and transient environments: Part I: local sensation of individual body parts, Build. Environ. 45 (2010) 380–388, https://doi.org/10.1016/j.buildenv.2009.06.018.
[35] H. Zhang, E. Arens, C. Huizenga, T. Han, Thermal sensation and comfort models for non-uniform and transient environments, part II: local comfort of individual body parts, Build. Environ. 45 (2010) 389–398, https://doi.org/10.1016/j.buildenv.2009.06.015.
[36] Q. Jin, X. Li, L. Duanmu, H. Shu, Y. Sun, Q. Ding, Predictive model of local and overall thermal sensations for non-uniform environments, Build. Environ. 51 (2012) 330–344, https://doi.org/10.1016/j.buildenv.2011.12.005.
[37] H.O. Nilsson, I. Holmér, Comfort climate evaluation with thermal manikin methods and computer simulation models, Indoor Air 13 (2003) 28–37, https://doi.org/10.1034/j.1600-0668.2003.01113.x.
[38] Thermetrics, Seat Test Automotive Manikin, Prod. Broch. (2015) 2. http://www.thermetrics.com/sites/default/files/product_brochures/STAN Manikin Thermetrics 2015.pdf (accessed March 2, 2018).
[39] V.T. Bartels, Thermal comfort of aeroplane seats: influence of different seat materials and the use of laboratory test methods, Appl. Ergon. 34 (2003) 393–399, https://doi.org/10.1016/S0003-6870(03)00058-9.
[40] M. Fojtlín, A. Psikuta, R. Toma, J. Fiser, M. Jícha, Determination of car seat contact area for personalised thermal sensation modelling, PLoS One 13 (2018), https://10.1371/journal.pone.0208599.
[41] E.A. McCullough, B.W. Olsen, S. Hong, Thermal insulation provided by chairs, ASHRAE Trans. Soc. Heat. Refrig. Aircond. Engin. 100 (1994) 795–804 http://www.cbe.berkeley.edu/research/other-papers/McCullough et al 1994 Thermal insulation provided by chairs.pdf.
[42] T. Wu, W. Cui, B. Cao, Y. Zhu, Q. Ouyang, Measurements of the additional thermal insulation of aircraft seat with clothing ensembles of different seasons, Build. Environ. 108 (2016) 23–29, https://doi.org/10.1016/j.buildenv.2016.08.008.
[43] E. Mert, A. Psikuta, M.-A. Bueno, R.M. Rossi, Effect of heterogenous and homogenous air gaps on dry heat loss through the garment, Int. J. Biometeorol. 59 (2015) 1701–1710, https://doi.org/10.1007/s00484-015-0978-x.
[44] ASTM, F2370-16 Standard Test Method for Measuring the Thermal Insulation of Clothing Using a Heated Manikin, (2015), pp. 1–7, https://doi.org/10.1520/F1291-15.1.
[45] A. Psikuta, Local air gap thickness and contact area models for realistic simulation of thermal effects in clothing, Int. J. Biometeorol. (2018) 1–14 https://doi.org/10.1007/s00484-018-1515-5.
[46] D. Fiala, G. Havenith, Modelling human heat transfer and temperature regulation, Mechanobiol. Mechanophysiology Mil. Inj, Springer, Berlin, 2015, pp. 265–302, , https://doi.org/10.1007/978-3-319-33012-9.
[47] D. Fiala, K.J. Lomas, M. Stohrer, Computer prediction of human thermoregulatory and temperature responses to a wide range of environmental conditions, Int. J. Biometeorol. 45 (2001) 143–159, https://doi.org/10.1007/s004840100099.
[48] A. Psikuta, D. Fiala, G. Laschewski, G. Jendritzky, M. Richards, K. Blazejczyk, I. Mekjavič, H. Rintamäki, R. de Dear, G. Havenith, Validation of the Fiala multi-node thermophysiological model for UTCI application, Int. J. Biometeorol. 56 (2011) 443–460, https://doi.org/10.1007/s00484-011-0450-5.
[49] N. Martínez, A. Psikuta, K. Kuklane, J.I.P. Quesada, R.M.C.O. de Anda, P.P. Soriano, R.S. Palmer, J.M. Corberán, R.M. Rossi, S. Annaheim, Validation of the thermophysiological model by Fiala for prediction of local skin temperatures, Int. J. Biometeorol. 60 (2016) 1969–1982, https://doi.org/10.1007/s00484-016-1184-1.
[50] H.A.M. Daanen, A. Psikuta, 3D body scanning, Autom. Garment Manuf, first ed., Woodhead Publishing, 2017, pp. 237–252, , https://doi.org/10.1016/B978-0-08-101211-6.00010-0.
[51] M. Fojtlín, J. Fišer, M. Jícha, Determination of convective and radiative heat transfer coefficients using 34-zones thermal manikin: uncertainty and reproducibility evaluation, Exp. Therm. Fluid Sci. 77 (2016) 257–264, https://doi.org/10.1016/j.expthermflusci.2016.04.015.
[52] M.G.M. Richards, R. Rossi, H. Meinander, P. Broede, V. Candas, E. den Hartog, I. Holmér, W. Nocker, G. Havenith, Dry and wet heat transfer through clothing dependent on the clothing properties under cold conditions, Int. J. Occup. Saf. Ergon. 14 (2015) 69–76, https://doi.org/10.1080/10803548.2008.11076750.
[53] F. Wang, C. Gao, K. Kuklane, I. Holmer, Determination of clothing evaporative resistance on a sweating thermal manikin in an isothermal Condition : heat loss method or mass loss method? Ann. Occup. Hyg. 55 (2011) 775–783, https://doi.org/10.1093/annhyg/mer034.
[54] B. Koelblen, A. Psikuta, A. Bogdan, S. Annaheim, R.M. Rossi, Comparison of fabric skins for the simulation of sweating on thermal manikins, Int. J. Biometeorol. 61 (2017) 1519–1529, https://doi.org/10.1007/s00484-017-1331-3.
[55] A. Mark, The Impact of the Individual Layers in Multi-Layer Clothing Systems on the Distribution of the Air Gap Thickness and Contact Area, Master Thesis Albstadt-Sigmaringen University of Applied Science, 2013.
[56] International Organization for Standardization, ISO 7730 Ergonomics of the Thermal Environment — Analytical Determination and Interpretation of Thermal Comfort Using Calculation of the PMV and PPD Indices and Local Thermal Comfort Criteria vol 3, (2005), p. 52.
[57] B.E. Ainsworth, W.L. Haskell, M.C. Whitt, M.L. Irwin, A.M. Swart, S.J. Strath, O.W. L, Compendium of Physical Activities: an update of activity codes and MET intensities, Med. Sci. Sports Exerc. 32 (2000) 498–516.
[58] B. Koelblen, A. Psikuta, A. Bogdan, S. Annaheim, R.M. Rossi, Thermal sensation models: validation and sensitivity towards thermo-physiological parameters, Build. Environ. 130 (2018) 200–211, https://doi.org/10.1016/j.buildenv.2017.12.020.
[59] T. Fukazawa, G. Havenith, Differences in comfort perception in relation to local and whole body skin wettedness, Eur. J. Appl. Physiol. 106 (2009) 15–24, https://doi.org/10.1007/s00421-009-0983-z.
[60] H.A.M. Daanen, E. Van De Vliert, X. Huang, Driving performance in cold, warm, and thermoneutral environments, Appl. Ergon. 34 (2003) 597–602, https://doi.org/10.1016/S0003-6870(03)00055-3.
[61] A. Psikuta, J. Frackiewicz-Kaczmarek, E. Mert, M.A. Bueno, R.M. Rossi, Validation of a novel 3D scanning method for determination of the air gap in clothing, Meas. J. Int. Meas. Confed. 67 (2015) 61–70, https://doi.org/10.1016/j.measurement.2015.02.024.
[62] G. Havenith, M.G. Richards, X. Wang, P. Brode, V. Candas, E. den Hartog, I. Holmer, K. Kuklane, H. Meinander, W. Nocker, Apparent latent heat of evaporation from clothing: attenuation and “heat pipe” effects, J. Appl. Physiol. 104 (2007) 142–149, https://doi.org/10.1152/japplphysiol.00612.2007.
[63] S. Ueno, S.I. Sawada, Correction of the evaporative resistance of clothing by the temperature of skin fabric on a sweating and walking thermal manikin, Textil. Res. J. 82 (2012) 1143–1156, https://doi.org/10.1177/0040517511427966.
[64] F. Wang, K. Kuklane, C. Gao, I. Holmér, Development and validity of a universal empirical equation to predict skin surface temperature on thermal manikins, J. Therm. Biol. 35 (2010) 197–203, https://doi.org/10.1016/j.jtherbio.2010.03.004.

Article

Journal of Industrial Textiles

2021, Vol. 50(9) 1493–1515

DOI: 10.1177/1528083719900672
journals.sagepub.com/home/jit
SAGE

Using a thermal manikin to determine evaporative resistance and thermal insulation – A comparison of methods

Róbert Toma[1], Kalev Kuklane[2], Miloš Fojtlín[3], Jan Fišer[1] and Miroslav Jícha[1]

Abstract

Heat transfer from the human body, especially through the evaporation of sweat from the skin, is often restricted when protective clothing is used, which may result in overheating. For this reason, it is important to consider the parameters of protective clothing as input data in physiological models, such as predicted heat strain. The two most important parameters are thermal insulation and evaporative resistance with clothing area factor strongly influencing both. These parameters were determined for two clothing ensembles using a (dry) non-sweating thermal manikin. First, the clothing area factor was determined using the photographic method. Second, thermal insulation was measured in both static and dynamic conditions, and multiple equations for predicting dynamic thermal insulation from static ones were evaluated. Third, methodology for measuring evaporative resistance based on pre-wetted skin was adopted and multiple corrections were assessed. Finally, sensitivity analyses were completed using PHS to determine the impact of different equations on the duration limited exposure. For the thermal insulation measurements, we found that predictive equation (32) from ISO 9920 was the most accurate, but choosing the correct equation for protective clothing proved challenging. Although a manikin's surface temperature is

[1]Faculty of Mechanical Engineering, Brno University of Technology, Brno, Czech Republic
[2]Lund University, Sölvegatan, Lund, Sweden
[3]Energy Institute, Brno University of Technology, Technická 2, Brno, Czech Republic

Corresponding author:
Róbert Toma, Faculty of Mechanical Engineering, Brno University of Technology, Brno, Jihomoravský Kraj 616 69, Czech Republic.
Email: 145743@vutbr.cz

widely used for calculating evaporative resistance, the skin temperature should be used instead, since it is correct from a physical point of view and there is a difference of up to 15% in the results. Because these measures are used in thermal risk analyses conditions, a high degree of accuracy and a knowledge of the inputs must be guaranteed.

Keywords
Evaporative resistance, thermal manikin, resultant thermal insulation, protective clothing

Introduction

Heat stress is the net heat load to which a person is exposed and is caused by various factors, such as high ambient temperature, the duration of exposure, worn protective clothing and equipment and heavy labor. The physiological response to a heat stress is called a heat strain and it has an impact on a human body via heat transfer processes [1–3]. In hot conditions, evaporation is the main pathway for heat dissipation from the human body into the environment [4,5]. Multiple physically demanding jobs, e.g. firefighting or agricultural work, are often carried out in hot working environments. In many cases, less permeable, well insulating protective clothing is used. However, these types of clothing often result in reduced sweat evaporation, leading to an elevation in skin temperature, core temperature and/or sweat rate [4]. Combined with insufficient water replacement and resting periods, this can lead to work-related disorders and various serious diseases (cardiac issues or chronic kidney disease (CKD) [6–8], for example) in the long term.

To prevent occupational disorders, various heat stress prediction models (e.g. PHS) [9] and thermo-physiological prediction models, such as the Fiala model [10] or the FMTK model (an abbreviation in Czech for the Fiala-based thermal comfort model) [11], also contain clothing properties as some of their most important input parameters. This is why clothing parameters should be measured with the highest possible degree of precision to mitigate prediction errors [12–14]. As it is important to protect workers' health, the main purpose of these models is to calculate the maximum exposure to a given environment with a given activity level without endangering the subject. Today, more emphasis is being placed on this area of research as weather conditions continue to change and extreme climatic events (e.g. hurricanes, heat waves) become more commonplace [15,16]. Multiple methods for measuring or estimating of clothing properties are currently in use, but the most realistic option involves using a thermal manikin with detailed body segmentation [12,17–19], since a thermal manikin accurately represents the shape of the human body and its movements in real-life situations. Non-sweating thermal manikins (i.e. manikins that lack a built-in sweating system) are often used as they are simpler, more affordable and more commonplace around the world.

In both thermal insulation and evaporative resistance measurements, the manikin's surface temperature is heated to a constant temperature, and the heat flux in each zone is recorded continuously. For the evaporative resistance measurements, a pre-wetted skin method is incorporated to simulate the evaporation of sweat from the body's surface [20].

The measurement of resultant total thermal insulation (I_{tr}) is well established as it is part of the ISO 9920 standard [21] and can be repeated with an accuracy of 4% between repetitions. Although it can be used as input data for the physiological modelling to simulate reality as closely as possible, it is an expensive method with regard to time and the extra equipment necessary to enable the manikin to walk, equipment that is not accessible for many laboratories. Obviously, a reliable alternative is needed. One option is to calculate the resultant total thermal insulation values (I_{tr}) from the static total thermal insulation values (I_t).

There are multiple equations (32) to (36) available in the standard ISO 9920 [21] that can be used to predict the resultant total thermal insulation (I_{tr}) from non-moving manikin values. Equation (33) from the standard can only be applied to a nude manikin or very low insulated clothing. The rest of the equations differ depending on the properties, such as thermal insulation and air permeability, of the clothing ensembles being tested, or on properties of the environments in which the clothing sets are being measured or used, e.g. low wind speed (Table 1). Standard EN 342 from 2004 [22] includes a similar equation with a similar purpose: predicting resultant thermal insulation (I_{tr}) for cold protective clothing.

Another important clothing parameter that has an impact on heat stress and physiological modelling is evaporative resistance [5, 20]. At present, there is no dedicated EU standard for measuring this quantity, highlighting the fact that more research is needed in this field. Two calculation methods for the evaporative resistance of clothing are provided in the ASTM standard from 2010 [23] – the mass loss method and the heat loss method. The mass loss method was removed from the newest version of the ASTM standard [24]. Its omission was probably related to the challenges associated with using the mass loss method to calculate the localized values for separate body parts, which were added to this new ASTM standard [24], as well as to reduce the number of discrepancies between laboratories caused

Table 1. Overview of multiple investigated equations from standards for predicting resultant thermal insulation from total thermal insulation values.

Equation label		Area of application	
Standard ISO 9920	(32)	Light or normal clothing	$0.6 < I_{cl} < 1.4$ clo
	(33)	No clothing	$I_{cl} = 0$ clo
	(34)	LOW insulated clothing	$0 < I_{cl} < 0.6$ clo
	(35)	Specialized or high insulated clothing	$I_{cl} > 1.4$ clo
	(36)	Very low wind activity	
Standard EN 342	(EN342)	Cold protective clothing	

by different measuring and calculation methodology [25]. According to Wang et al. [26], the exclusion of the mass loss method was not an ideal solution as this method is inherently correct from a physical point of view.

It was previously reported that measuring evaporative resistance in non-isothermal conditions ($T_{manikin} \neq T_{ambient} \neq T_{sk}$) may cause significant error as clothing insulation changes dramatically with absorbed moisture; therefore, isothermal conditions should be used [27–29]. However, we were unable to set up isothermal conditions ($T_{manikin} = T_{ambient} = T_{sk}$) for our thermal manikin since most of the available manikins are only able to control manikin's surface temperature and not the wetted skin temperature. For this reason, a so-called isothermal condition ($T_{manikin} = T_{ambient} \neq T_{sk}$) had to be used instead. Issues connected to the manikin's surface temperature reach beyond the measurement setup where this temperature is also used incorrectly in the calculations of evaporative resistance via both of the methods that were mentioned. Because the water (simulating sweat) evaporates from the pre-wetted skin of the manikin, the skin temperature should be used in the calculations. Multiple corrections from different researchers and for different sweating simulation systems were presented to mitigate this and other possible errors [26,29–35].

Material characteristics of individual garments also play significant role on a heat stress of the workers. For example, it was previously reported that increase in an air permeability (porosity) of an over-garment causes an increase in a ventilation, and thus increases in the heat dissipation from a human body [36, 37]. Porosity and capillary drift have strong effects if we look on a material in detail, however when we consider clothing system, then due to many layers and airgaps present in the ensemble, the influence of a specific material and its porosity is partially reduced. That is probably the reason why porosity is included in the moisture performance evaluation of textile materials, but if we look in any standards and methods for measuring parameters of clothing ensembles, then porosity is not considered specifically in any of these. When measuring evaporative resistance of an ensemble on a thermal manikin, in as stable state as possible, we obtain total evaporative resistance values of the whole ensemble, including the effects of layers, pores etc. As the aim of this paper was related to a standardized and repeatable manikin testing and related calculations to define a technical parameter of an ensemble, we will not focus on the material parameters and layering of the garments in the ensembles in this paper.

The aim of this study was to identify, and possibly enhance, reliable and applicable methods to obtain protective clothing parameters by means of a non-sweating thermal manikin using pre-wetted skin. Both the mass loss and the heat loss methods were used to calculate whole-body total evaporative resistance in this study. Verification of multiple equations used for predicting resultant total thermal insulation (I_{tr}) from total thermal insulation (I_t) on protective clothing from ISO 9920 [21] was also conducted. Our findings can be used to achieve more precise and reliable physiological predictions for people working in hot environments and possibly enhance the prevention of health problems in both the short

and the long term. Published data concerning clothing parameters could be used to estimate values for similar protective clothing ensembles for use in physiological modelling where clothing properties are not available.

Methods

Study design

- Measurement of the total (I_t) and resultant (I_{tr}) thermal insulation and evaporative resistance (R_{et}) by means of a non-sweating thermal manikin.
- Measurement of the clothing area factor (f_{cl}) by the photographic method and calculation of intrinsic values.
- Measured values are considered as reference values.
- Investigation of multiple equations from different standards to predict resultant thermal insulation (I_{tr}) from total thermal insulation (I_t).
- Assessment of multiple published corrections for the evaporative resistance calculation in both the mass loss and the heat loss methods.
- Sensitivity analyses to demonstrate the impact of clothing parameters on the duration limited exposure using the PHS model.

Equipment

This study provides relevant information concerning methodology and measurement procedures for three important clothing parameters. The thermal manikin TORE [38] at Lund University, Sweden (Figure 1), which was used in this study, is made of plastic covering a metal frame inside that supports the body parts and joints. It is the size of an average Swedish male from the first half of the 1980s. The manikin is 1.71 m tall and weighs around 32 kg. The body surface area of 1.772 m^2 is divided into 17 zones. The climatic chamber at Lund University, with dimensions height × width × length: 2400 × 2360 × 3200 mm, was used for the measurements. The chamber can be adjusted from +5 to +60°C and the temperature standard deviation (SD) from the set value is less than ±0.2°C. The relative humidity in this chamber can be adjusted from 10 to 95%, depending on the temperature and the humidity SD from the set value is less than ±5%. Air velocity can be adjusted between 0.1 and 0.7 m/s.

First, the manikin was placed inside the climate chamber in an upright posture with the arms hanging freely (Figure 1(a)). This posture is typically reported in the literature and standards for investigating the thermal properties of clothing in static conditions. The manikin's arms and legs were connected to an articulated stand to enable measurement of the resultant total thermal insulation under walking conditions (I_{tr}). Next, for the evaporative resistance investigation, the articulated stand was not used in order to make room for a scale, which was installed under the manikin to provide mass loss data acquisition. For this reason, the resultant evaporative resistance values were neither measured nor estimated by the ISO 9920 standard [21],

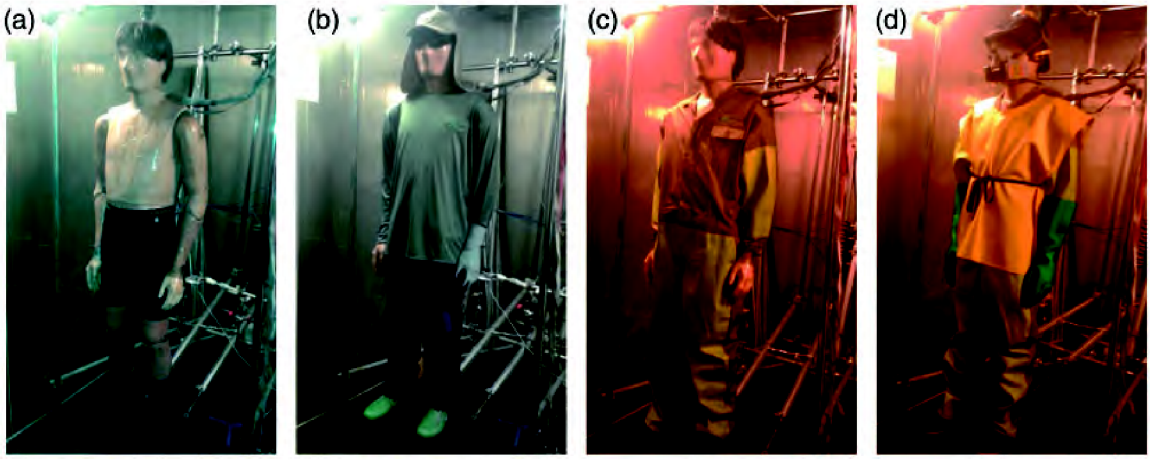

Figure 1. Tested clothing: (a) underwear for both systems (provided by the laboratory); (b) sugarcane harvester's outfit (glove on only one hand and leg protector on only one leg – sugarcane is held by the hand with the glove and cut by machete in the other hand, the leg protector covers the leg in the direction of the machetés swing); (c) pesticide sprayer's protective cover all on top of underwear; (d) pesticide sprayer's complete outfit, complete with outer protective layers.

as it was not possible to verify the accuracy of the estimations. For these measurements, the manikin's pre-wetted skin was used since the thermal manikin TORE has no sweating system. Finally, the manikin was taken out of the chamber to measure the clothing area factor (f_{cl}) as described in the following chapter.

Two different clothing ensembles used by agricultural workers – sugarcane cutters (SC) and pesticide sprayers (PS) were measured, those being the most common types of work in the cultivation of sugarcane fields (Figure 1(a) to (d)). Tested ensembles were obtained from a company that provides protective clothing for workers in the sugarcane fields of Latin America, where very warm (more than 34°C) conditions prevail. The size "large" was chosen as the best fit for the manikin.

Determining the clothing area factor (f_{cl})

The clothing area factor (f_{cl}) is defined as the ratio of the area of a dressed manikin to a nude manikin. This parameter is one of the factors influencing the heat and mass transfer between the skin and the ambient environment. Obtained clothing area factor values allowed us to calculate the intrinsic thermal insulation (I_{cl}) and the resulting intrinsic thermal insulation (I_{clr}) according to equation (7) in ISO 9920 standard [21] for each set

$$I_t = I_{cl} + \frac{I_a}{f_{cl}}$$

Equation (7) from ISO 9920

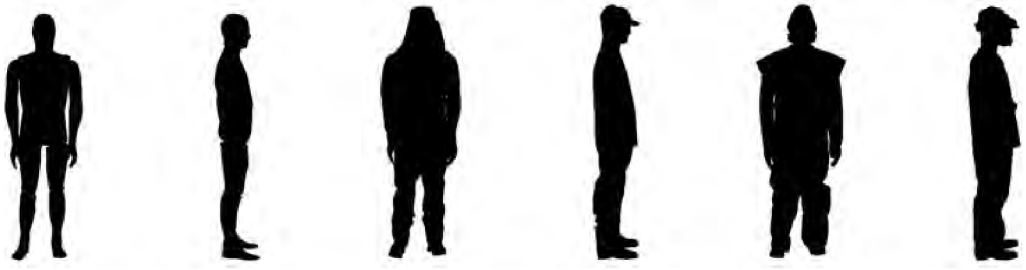

Figure 2. Edited photos of the nude manikin, SC – the sugarcane cutter's outfit, and PS – the pesticide sprayer's outfit, which were used to count black pixels for the clothing area factor (f_{cl}) calculation.

where I_t is the total thermal insulation of the clothing [m^2K/W], I_{cl} is the intrinsic thermal insulation [m^2K/W], I_a is the thermal insulation of the air layer [m^2K/W] obtained by measurements made of the nude manikin and f_{cl} is the clothing area factor.

Several methods for determining the clothing area factor (f_{cl}) exist, such as the 3D scanning method, the photographic method, or its estimation by calculation [12,39]. With respect to the unusual shape of the sugarcane workers' clothing, we decided to use the photographic method. This method provides high degree of accuracy without the need for specialized equipment. While in the early use of this method up to six photographs were taken from different sides and angles, an acceptable accuracy could also be achieved using photographs from only two positions: 0° – front side of the standing manikin and 90° – right/left side of the standing manikin (Figure 2) [40]. All photographs were taken with the same camera (Nikon D-3700, Nikon, Japan) from the same position. The distance of the camera stand from the manikin was 4 m and the camera itself was placed at the height of the center of the manikin. The pictures were then processed in a photo editing program (Photoshop CC 2018, Adobe Systems, USA) and the clothing area factor (f_{cl}) was calculated by comparing the number of black pixels on the nude versus the dressed manikins.

Thermal insulation measurement and evaluation methodology

The heat loss method (using the global calculation method) was used to determine both the total thermal insulation (I_t) and the resultant total thermal insulation (I_{tr}). The procedure is described in ISO 9920 [21] and all parameters were set within the required ranges. The manikin's surface temperature was set and maintained at 34 ± 0.1°C. The ambient temperature was set and maintained at 20.0 ± 0.1°C (checked against the average of three temperature measurements taken at 0.1, 1.1 and 1.7 m above the level of the sole of the manikin's foot) with 0.21 ± 0.08 m/s air velocity aimed at the manikin's back (measured at 1.2 m above floor level). The relative humidity inside the chamber was maintained at

$40 \pm 5\%$. A walking speed of approximately 3.5 km/h (step rate set at 90 steps/min) was used for the resultant total thermal insulation (I_{tr}) measurement.

Two applicable options (Table 1) to predict the resultant total thermal insulation (I_{tr}) for clothing ensembles SC and PS were examined in this study. First, with regard to the total thermal insulation range given in the standard (from 1.2 to 2.0 clo), equation (32) was selected for both ensembles. The second option examined was equation (35), which is recommended for protective clothing and clothing with low air permeability. This applies to our clothing ensembles, especially PS. For the nude manikin, equation (33) from the standard was always used. Equations (34) and (36) were not suitable for our clothing sets and environmental parameters. A comparison of the resultant total thermal insulation (I_{tr}) was drawn between the values from the two predictive equations (32) and (35), from the standard ISO 9920 [21], and the values obtained from our measurements. A similar comparison was done for the resultant intrinsic thermal insulation (I_{clr}) using measured clothing area factor (f_{cl}) values. Despite the fact that the clothing ensembles did not fit the description of standard EN 342 [22] for cold protective clothing, we decided to apply this standard as well to evaluate the error compared to ISO 9920 [21]. The equations used in this article are presented below and are labeled in the same way as in the relevant standards

$$I_{tr\_p(32)} = e^{[-0.281*(v_{ar}-0.15)+0.044*(v_{ar}-0.15)^2-0.492*v_w+0.176*v_w^2]}*I_t \quad (32)$$

$$I_{tr\_p(33)} = e^{[-0.533*(v_{ar}-0.15)+0.069*(v_{ar}-0.15)^2-0.462*v_w+0.201*v_w^2]}*I_t \quad (33)$$

$$I_{tr\_p(35)} = e^{\{[-0.0512*(v_{ar}-0.4)+0.794*10^{-3}*(v_{ar}-0.4)^2-0.0639*v_w]*p^{0.144}\}}*I_t \quad (35)$$

$$I_{tr\_p(EN342)} = (0.54*e^{(-0.15*v_a-0.22*v_w)}*p^{0.075} - 0.06*\ln(p) + 0.5)*I_t \quad (\text{EN342})$$

where I_{tr} are the resultant thermal insulation values from each of the equations [m^2K/W], v_{ar} is the air velocity relative to the person [m/s], v_a is the air velocity [m/s], v_w is the walking speed [m/s], I_t is the total thermal insulation measured on the manikin in static conditions [m^2K/W] and p is the air permeability of the outer layer of the clothing [l/m^2s] [low (e.g. coating) = 1; medium = 50; high (open weave) = 1000]. Air permeability was estimated for our clothing sets (100 for SC and 25 for PS) based on previous experience.

Evaporative resistance measurement methodology

Non-sweating manikins (manikins that lack a dedicated sweating system) can be effectively used to determine evaporative resistance using pre-wetted skin. Despite this method not being standardized, it has been presented in a variety of publications and was used for sweat simulation [41] in our study. The tight-fitting skin

(thickness d= 0.9 mm, 95% cotton, 5% elastane) covered the manikin's entire body except for the hands and feet. To simulate sweat on these body parts, gloves (100% cotton) and socks (67% cotton, 30% polyester, 3% elastane) were used. Before each test, the skin was wetted with 925 ± 15 g of water with no drippage.

The thermal manikin was placed inside the chamber in the same upright position and in the same place as for the previous measurement (thermal insulation). However, this time the whole manikin system was placed on a scale to monitor mass loss throughout the measurement (the mass loss method was used only for one of the three measured repetitions as the extra equipment needed was not available for the rest). Both the thermal manikin's surface temperature and the ambient temperature were set to 34 ± 0.2°C to ensure so-called isothermal conditions [26,33]. Relative humidity was maintained at below 50% to provide good evaporation from the manikin's wetted skin. The air velocity was raised compared to the thermal insulation tests, to 0.54 ± 0.16 m/s to ensure even humidity distribution inside the climatic chamber. Evaporative resistance was only measured in static conditions as the measurement setup (with the scale) did not allow for the use of a walking stand.

Evaporative resistance calculation

There are two calculation methods for clothing evaporative resistance provided in the ASTM standard from 2010 [23] – the mass loss method and the heat loss method [42].

Heat loss method. Two corrections, for the skin temperature of the manikin [29,31] and for the heat gains from the environment [33], (both of which are present when using pre-wetted skin), are examined in this study and explained in detail below.

Evaporative resistance was calculated by the heat loss method from the area-weighted heat loss observed from the thermal manikin software. According to ASTM standard [24], the total evaporative resistance should be calculated from equation (1) from the manikin's surface temperature as it assumes that isothermal conditions are used ($T_{manikin} = T_{sk}$).

$$R_{et,h} = \frac{(p_{sk} - p_a)}{H_{e,heat}} \tag{1a}$$

$$R_{et,h} = \frac{\left[exp\left(18.956 - \frac{4030.18}{T_{manikin}+235}\right) * RH_{sk} - exp\left(18.956 - \frac{4030.18}{T_a+235}\right) * RH_a\right]}{H_{e,heat}} \tag{1b}$$

where $R_{et,h}$ is the total evaporative resistance calculated from the heat loss method [m^2Pa/W], p_{sk} and p_a are the vapor pressures of saturated skin and air, respectively [Pa], $T_{manikin}$ and T_a are the temperatures of the manikin's surface and ambient air,

respectively [°C], RH_{sk} (96% based on previous measurements) and RH_a are relative humidity near the manikin's surface and in the air, respectively [%], and $H_{e,heat}$ is the total heating power supplied to the wetted parts of the manikin [W/m^2]. $R_{et,h\_manikin}$ values were calculated from this equation. To correct for lower skin temperature caused by water evaporation, equation (2) was used to mitigate the error in calculation [31]

$$T_{sk} = T_{manikin} - 0.0132 * H_{e,heat} * A \tag{2}$$

where T_{sk} is the predicted textile skin temperature [°C] and A is the manikin's sweating surface area [m^2]. R_{et,h_skin} values were obtained by accommodating equation (2) for skin temperature into the previous equation (1b).

As there is a temperature gradient between the wetted skin and the environment, part of the heat needed to evaporate the water from the skin is also taken from the environment through conduction, convection, and radiation mechanisms as presented in Figure 3. In some cases (e.g. impermeable clothing, high insulation clothing), evaporation is negligible. This may cause the manikin's power regulation to be episodic, which may, in turn, cause the manikin's surface to overheat and exceed the set temperature. Thus, the effect presented above (Figure 3) can be reversed, and the manikin may exhibit extra dry heat loss instead. That is why another correction for the evaporative resistance calculation was proposed and is presented as equation (3). We get the final equation (4), for calculating the corrected evaporative resistance by incorporating both equations (2) and (3) into equation (1)

$$Q_{evap} = H_{e,heat} + \frac{(T_a - T_{sk})}{I_t} \tag{3}$$

$$R_{et,h\_skin+envi} = \frac{\left[exp\left(18.956 - \frac{4030.18}{T_{sk}+235}\right) * RH_{sk} - exp\left(18.956 - \frac{4030.18}{T_a+235}\right) * RH_a\right]}{H_{e,heat} + \frac{T_a - T_{manikin} + 0.0132 * H_{e,heat} * A}{I_t}} \tag{4}$$

where Q_{evap} is the part of the heat needed for the evaporation taken from the environment [W/m^2], I_t is the total thermal insulation measured on a non-sweating manikin according to 'Determining the clothing area factor (f_{cl})' section [m^2·K/W]. $R_{et,h\_skin+envi}$ were determined according to equation (4).

A comprehensive overview of the corrections and the comparison of heat loss vs. mass loss are presented in the review article by Wang [43]. Other proposed corrections (e.g. for moisture in the clothing, for skin fabric) by Wang et al. [26,3233,43] are more complicated to incorporate into practical measurements (importance of measuring skin fabric parameters, wet thermal insulation of clothing etc.) and were not considered in this study. With the use of the clothing area

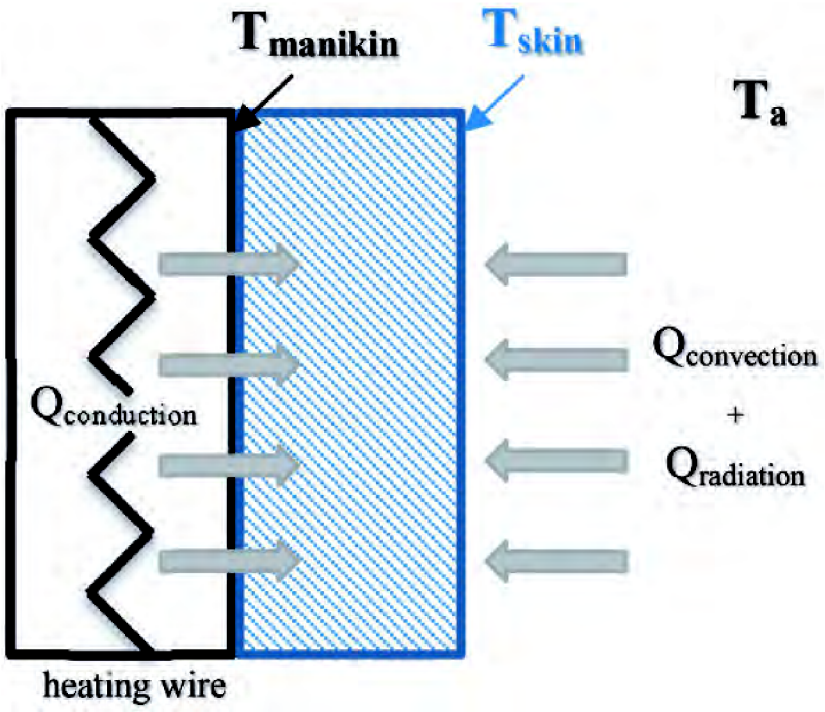

Figure 3. The heat transfer mechanism between the manikin surface, the wetted skin, and the environment in a so-called isothermal conditions ($T_a = T_r = T_{manikin} \neq T_{skin}$) without clothing, adapted from Wang et al.[33].

factor (f_{cl}), the whole body intrinsic evaporative resistance could be calculated for both clothing sets.

Mass loss method. This method is based on the measurement of mass loss rate and its subsequent conversion to evaporative heat loss by multiplying the latent heat of the vaporization of water. The ASTM standard [23] uses the manikin's surface temperature for the calculation of the saturated vapor pressure p_{sk}. The evaporative resistance calculated from the mass loss method is calculated based on equation (5)

$$R_{et,\ m} = \frac{\left[\exp\left(18.956 - \frac{4030}{T_{manikin}+235}\right) * RH_{sk} - \exp\left(18.956 - \frac{4030}{T_a+235}\right) * RH_a\right] * A}{\lambda * \frac{dm}{dt}} \tag{5}$$

where λ is the vaporization heat of water at the measured skin temperature [W·h/g] and dm/dt is the evaporation rate of moisture from the wetted skin [g/h].

To be correct from a physical point of view, this calculation should be corrected in the same way as in the heat loss method, using the predicted skin temperature based on equation (2). R_{et,m_skin} is the evaporative resistance, which is calculated

based on equation (5) with the manikin's surface temperature ($T_{manikin}$) being substituted for the predicted temperature of the wetted skin (T_{sk}).

Data analysis

All thermal insulation values presented in this study are the averaged values of two independent measurements with a difference lower than 4% between them as required by the ISO 9920 standard [21]. For the evaporative resistance measurements, the values presented, including standard deviation from the heat loss method, were calculated as an average of three independent measurements. However, the mass loss method was measured only once for each clothing ensemble as a control measurement; therefore, no standard deviation could be presented.

Sensitivity study

PHS simulations were conducted as sensitivity analyses to observe the impact of the clothing properties, obtained by the different equations and corrections, on the workers' maximum exposure time. The maximum exposure time was evaluated using two different criteria: (a) D_Tre is the time it took an average worker to reach a core temperature limit of 38°C (occupational exposure limit), (b) Dwl_50 is the time it took an average worker to reach the limit for water (sweat) loss. All parameters for PHS simulations except for measured clothing parameters [resultant intrinsic thermal insulation (I_{clr}) and moisture permeability index (i_m), calculated from the measured thermal insulation and evaporative resistance] were constant and corresponded to the environmental parameters during lunch time in the sugarcane fields of Latin America (Table 2). Parameters defining the human body were chosen based on an average male with a posture, walking speed and metabolic production corresponding to work in a sugarcane field. To analyze the difference between multiple predictive equations for the resultant intrinsic thermal insulation (I_{clr}), the intrinsic evaporative resistance (R_{ecl}) values were set to a constant for each clothing ensemble. To investigate the impact of the corrections on the evaporative resistance, the opposite approach was used: the resultant intrinsic thermal insulation (I_{clr}) was set to a constant value and the intrinsic evaporative resistance (R_{ecl}) was changed according to the corrections.

Results

Thermal insulation

In Table 3, the total (I_t) and intrinsic (I_{cl}) thermal insulation and the total (I_{tr}) and intrinsic (I_{clr}) resultant thermal insulation results, both predicted (I_{tr_p}, I_{clr_p}) and measured (I_{tr_m}, I_{clr_m}) are presented. The table gives the complete database of all obtained values. A comparison of the measured and calculated values, both by the standard equation (32) of ISO 9920 [21] (applied based on the clothing insulation range) and by equation (35) of the same standard (used based on the low

Table 2. Constant input parameters for the PHS model for sensitivity analyses of the impact of measured clothing properties on predicted exposure time.

Height	1.85 m
Weight	80 kg
Posture	Standing
Air temperature	34.6°C
Air velocity	0.2 m/s
Relative humidity	23%
Radiant temperature	63.5°C
Metabolic energy production	200 W/m^2
Walking speed	1 m/s

Table 3. Database of total thermal insulation (I_t), resultant total thermal insulation (I_{tr}), and resultant intrinsic thermal insulation (I_{clr}) values obtained by measurements and by multiple predictive equations from different standards.

	I_t	I_{tr_m}	$I_{tr\_p(32)}$	$I_{tr\_p(35)}$	$I_{tr\_p(EN342)}$	I_{clr_m}	$I_{clr\_p(32)}$	$I_{clr\_p(35)}$	$I_{clr\_p(EN342)}$
	[m^{2}K/W]								
SC	0.191	0.143	0.138	0.173	0.157	0.083	0.080	0.115	0.099
PS	0.257	0.188	0.185	0.236	0.217	0.134	0.133	0.184	0.165
SC (SD)	0.002	0.001							
PS (SD)	0.001	0.001							

permeability of the clothing sets being measured) was conducted. The percentage difference (Figure 4) was evaluated based on the resultant intrinsic thermal insulation values, calculated using a clothing area factor of 1.26 for SC and 1.41 for PS, the values having been obtained by the photographic method because these values are used as input data for the PHS model. The difference between the predicted and measured values was −3.6 and −0.6% for SC and PS, respectively, when equation (32) was used and 27.9% and 27.3% for SC and PS, respectively, when using equation (35). Similarly, equation (33) was used for the nude manikin to predict total resultant thermal resistance (I_t), and this value was again compared to the measured value. In this case, the difference was 3.5%. When using the equation from the EN 342 standard [22] (used for cold protective clothing), the difference between predicted and measured values for resultant intrinsic thermal insulation was 16.3% and 18.8% for SC and PS, respectively.

The total thermal insulation of the manikin's skin, which was used for the evaporative resistance calculation was measured only in static conditions and reached 0.131 m^{2}K/W.

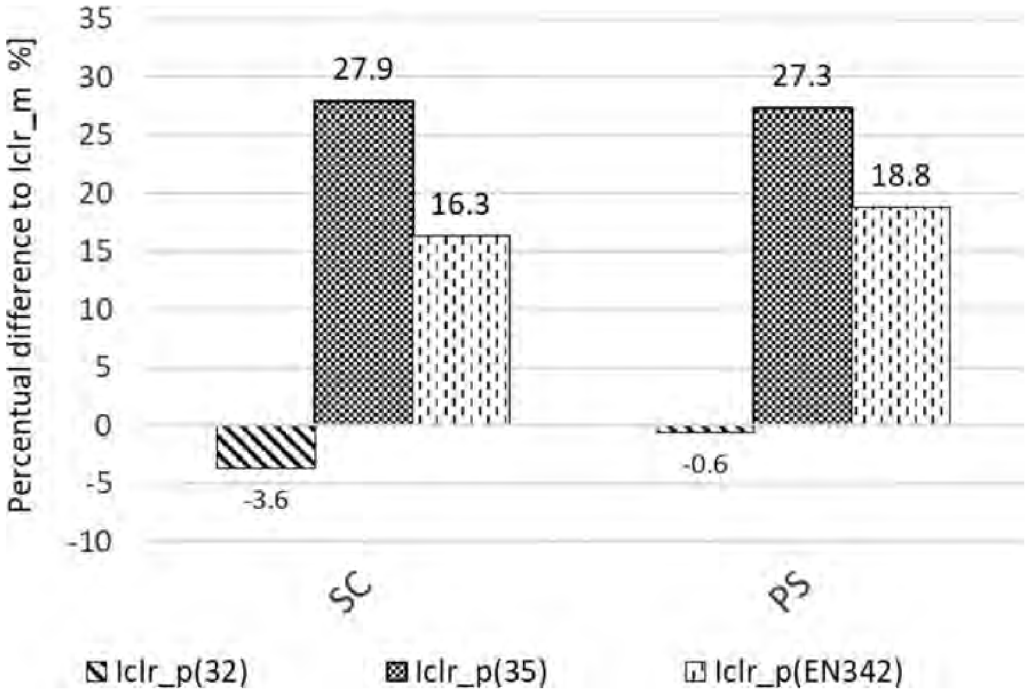

Figure 4. Percentage differences between measured resultant intrinsic thermal insulation (I_{clr_m}) and predicted values from equation (32) from ISO 9920 ($I_{clr\_p(32)}$), from equation (35) from ISO 9920 ($I_{clr\_p(35)}$) and from the equation in the EN342 standard ($I_{clr\_p(EN342)}$).

Table 4. Results from PHS simulations using constant intrinsic evaporative resistance (R_{ecl_m}) as measured by the mass loss method with multiple values of resultant intrinsic thermal insulation (I_{clr}) based on different predictive equations.

	I_{clr}	$R_{ecl,m}$	i_m	*D_Tre* (min)	*Dwl50* (min)
SC					
I_{clr_m}	0.083	20.0	0.248	480	340
$I_{clr\_p(32)}$	0.080	20.0	0.239	480	335
$I_{clr\_p(35)}$	0.115	20.0	0.344	480	382
$I_{clr\_p(EN342))}$	0.099	20.0	0.296	480	362
PS					
I_{clr_m}	0.134	81.4	0.098	25	280
$I_{clr\_p(32)}$	0.133	81.4	0.098	25	280
$I_{clr\_p(35)}$	0.184	81.4	0.135	30	280
$I_{clr\_p(EN342))}$	0.165	81.4	0.121	28	280

The sensitivity analysis was done based on the PHS simulations (Table 4), with all parameters set as constants, except for resultant intrinsic thermal resistance, which was changed according to the equations. The core temperature limit (D_Tre) was not reached during any of the simulations in the selected environmental parameters when clothing set SC was used. However, when clothing set PS was used, the core temperature limit was reached in all cases within 25 to 30 min.

Evaporative resistance

All data for both ensembles are presented in Table 5. Three different values for total evaporative resistance, calculated by the heat loss method and using different corrections, are shown. First, $R_{et,h\_manikin}$ values were calculated from equation (1b). Second, R_{et,h_skin} values were obtained by incorporating the correction for skin temperature [equation (2)] into the previous equation (1b). Third, $R_{et,h\_skin+envi}$ values were determined according to equation (4). Finally, two values were obtained from the mass loss method. R_{et_m} and $R_{et\_m\_skin}$ were calculated according to equation (5), using the manikin's surface temperature and the predicted skin temperature, respectively. The total evaporative resistance of the manikin, wearing only pre-wetted skin, was also measured and calculated from equation (1b) using the heat loss method – 8.2 m^2Pa/W. Because this value was only measured once (when testing the entire measurement setup), no statistical analyses could be applied to it. All intrinsic evaporative values (R_{ecl}) were calculated using the clothing area factor (f_{cl}) and are also presented in Table 5.

Percentage differences between evaporative resistance calculated by the mass loss method using the manikin's surface temperature, a common method at present, and other types of calculations using different corrections are shown in Figure 5. The average deviation and percent deviation were also calculated for five presented calculation methods for both sets, reaching 2.05 and 8.49 for the SC ensemble and 2.42 and 2.92 for the PS ensemble, respectively.

The sensitivity analysis was done based on the PHS simulations (Table 6) with all parameters set as constants except for the intrinsic evaporative resistance, which was changed according to the corrections mentioned in the 'Evaporative resistance calculation' section. Both the core temperature limit (D_Tre) and the water loss limit (Dwl50) could be used for the evaluation as both were reached for both sets in most cases.

The PHS model is simple compared to other physiological models [10, 44, 45] and it would seem that its simplicity demands further consideration. Simplicity might be the reason why a small change in the input data, e.g. pre-set metabolic energy production, causes a considerable change in the final maximal exposure time.

Discussion

Differences between calculated and measured resultant thermal insulation values

We found that the difference between measured values of the resultant intrinsic thermal insulation and those calculated according to equation (32) in ISO 9920 ranged from −0.6 to −3.6%. The difference decreased with the rising total insulation of the clothing being evaluated. The accuracy of the prediction from equation (32) is sufficient; however, it is not clear which of the equations from ISO 9920

Table 5. Database of total (R_{et}) and intrinsic (R_{ecl}) evaporative resistance, obtained by both the mass loss and the heat loss methods, using various possible calculations and corrections.

	$R_{et,m}$	R_{et,m_skin}	$R_{et,h\_manikin}$	R_{et,h_skin}	$R_{et,h\_skin+envi}$	$R_{ecl,m}$	R_{ecl,m_skin}	$R_{ecl,h\_manikin}$	R_{ecl,h_skin}	$R_{ecl,h\_skin+envi}$
	[m^2Pa/W]									
SC	26.7	23.2	26.7	23.0	21.0	20.0	16.5	20.0	16.3	14.3
PS	87.4	83.5	83.7	79.9	79.8	81.4	77.5	77.7	73.9	73.8
SC (SD)			0.9	0.9	0.7					
PS (SD)			2.8	2.8	2.8					

Note: $R_{et,m}$ and $R_{et,h\_manikin}$ are the evaporative resistances calculated by the mass loss and the heat loss method using the manikin's surface temperature, R_{et,m_skin} and R_{et,h_skin} are the evaporative resistances calculated by the mass loss and the heat loss methods using the predicted skin temperature of the manikin and $R_{et,h\_skin+envi}$ is the evaporative resistance calculated by the heat loss method based on the correction for gains from the environment. Additionally, all of these values were recalculated using the clothing area factor (f_{cl}), and their intrinsic values are given as well.

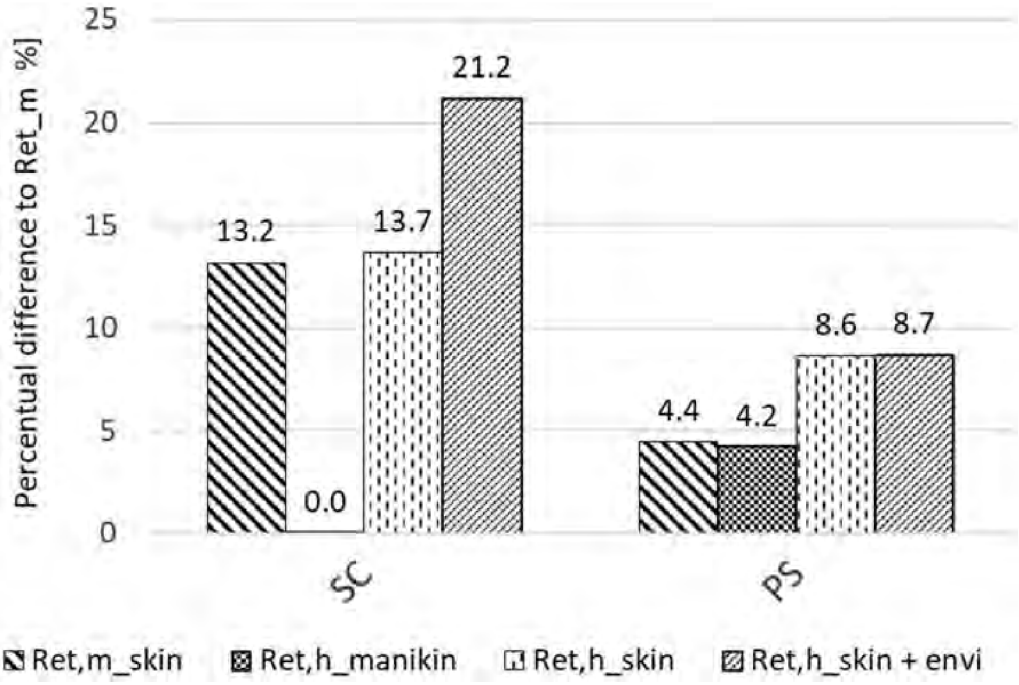

Figure 5. Percentage differences between evaporative resistance calculated by the mass loss method using the manikin's surface temperature (a common method that is currently favoured), evaporative resistance calculated by the mass loss method using skin temperature (R_{et,m_skin}), evaporative resistance calculated by the heat loss method using the manikin's surface temperature ($R_{et,h\_manikin}$), skin temperature (R_{et,h_skin}), and skin temperature with a correction for environmental gains ($R_{et,h\_skin+envi}$).

should have been used for our ensembles. From the perspective of thermal insulation, equation (32) from ISO 9920 is the best fit. On the other hand, equation (35) is meant to be applied to specialized clothing with impermeable layers. When we used equation (35), however, the difference between the predicted and the measured values was significantly higher: −27.9% for SC and −27.3% for PS. Moreover, a similar predictive equation also exists in the standard for cold protective clothing, EN 342 [22]. The difference between the predicted and the measured values of the resultant total thermal insulation for both sets was lower when using this equation (Figure 4) than equation (35) of the ISO 9920 standard. Obviously, the equation from the standard for cold protective clothing yields results that are closer to the measured ones than equation (35), which is meant to be used for impermeable clothing. Our findings underscore the difficulties associated with choosing the correct equation for a given application. To avoid confusion in the future, a versatile and robust predictive equation for protective clothing needs to be developed. Such an equation could then be applied to the predictive models to enhance their accuracy.

In the next step, a sensitivity analysis was carried out to measure the impact of the inputs on the resulting PHS. Based on water loss criteria, the sensitivity analyses showed that there was very little difference in the exposure time in the SC

Table 6. Results from PHS simulations using constant measured resultant intrinsic thermal insulation (I_{clr}) and multiple values of intrinsic evaporative resistance (R_{ecl}) based on different corrections used for its calculation.

	$R_{et,m}$	I_{clr}	i_m	D_Tre (min)	Dwl50 (min)
SC					
$R_{ecl,m}$	20.0	0.083	0.248	480	340
R_{ecl,m_skin}	16.5	0.083	0.301	56	368
$R_{ecl,h\_manikin}$	20.0	0.083	0.248	480	340
R_{ecl,h_skin}	16.3	0.083	0.303	55	369
$R_{ecl,h\_skin+envi}$	14.3	0.083	0.346	45	382
PS					
$R_{ecl,m}$	81.4	0.134	0.098	25	280
R_{ecl,m_skin}	77.5	0.134	0.103	26	280
$R_{ecl,h\_manikin}$	77.7	0.134	0.103	26	280
R_{ecl,h_skin}	73.9	0.134	0.109	27	280
$R_{ecl,h\_skin+envi}$	73.8	0.134	0.109	27	280

ensemble. The most significant time difference between predictions based on the measured value and any of the predictive equations was 42 min [measured vs. the equation (35)], which is relatively small but not negligible, especially in relation to an 8-h workday. The core temperature limit was not reached for the whole working day when the SC clothing set was used. For the PS set, even though there were relatively high differences in absolute values between the results from the measurements and the calculations, no significant differences were found in PHS predictions while using these values. The exposure time based on water loss did not change at all and the core temperature maximum exposure time varied by only 5 min (Table 4). However, we cannot conclude that these error margins have a negligible impact on the PHS predictions. As seen in Figure 5, a small change in metabolic production can cause, in some cases, a significant change in the resulting exposure time. This stems from the simplicity of the PHS model, and it would be of a great interest to carry out a similar analysis on a more sophisticated physiological model. However, the more complicated models are not affordable for many researchers.

Differences between evaporative resistance values obtained using multiple corrections

First, two methods for measuring evaporative resistance were compared (Table 5). For the SC ensemble, the same results were obtained (with a difference of 0.002%) by both methods when the corrections were not used ($R_{et,h\_manikin} = R_{et,m} = 26.7$ m^2Pa/W). For the PS set, the difference between the heat loss method ($R_{et,h\_manikin} = 83.7\,m^2Pa/W$) and the mass loss method ($R_{et,m} = 87.4\,m^2Pa/W$) was slightly higher, amounting to 4.4% (Figure 5).

Second, we investigated the discrepancies caused by the use of multiple corrections (Figure 5). In the mass loss method, the differences between values calculated from the manikin's surface temperature and from the manikin's skin temperature were 13.2% for the SC ensemble and 4.4% for the PS ensemble. Similarly, the heat loss method involved differences of 13.7% and 8.6% for SC and PS respectively. Moreover, when the correction for gains from the environment was used in the heat loss method, the differences compared to the raw values (calculated from the manikin's surface temperature) were even higher 21.2% for SC and 8.7% for PS. We could see that the percentage differences between both the mass loss and the heat loss method are not significant when the same temperature (either the surface temperature or the skin temperature of the manikin) is used for their calculation. However, calculations based on the manikin's surface temperature should not be used as this is not correct from a physical point of view. Water evaporates from the manikin's skin and not its surface, thus the vapor pressure of saturated skin needs to be used in the calculations. As we were neither able to control nor measure the manikin's skin temperature with the manikin available to us, it was necessary to use the predicted skin temperature instead.

The results from the sensitivity analyses (Table 6) support our conclusions about using the manikin's surface temperature. For the SC ensemble, the core temperature criteria were not reached when the manikin's surface temperature was used in either the mass loss or the heat loss method, whereas when the predicted skin temperature was used in both methods, the maximum exposure time was only around 55 min. This represents a huge difference and could result in very inaccurate PHS predictions, which would have the potential to adversely affect the health of the sugarcane workers. As seen in Figure 5, a small change in the input metabolic production in the PHS model can, in some cases, cause a significant jump in the exposure time. Moreover, in one case for the SC ensemble, a lower evaporative resistance value resulted in a lower exposure time, which should not have been the case. These uncertainties are probably caused by the simplicity of the PHS model and should be taken into account when using this model in real-life situations. The PS ensembles insulation was relatively high and also contained multiple impermeable layers, meaning heat transfer between the skin and the environment was negligible and the corrections mentioned had almost no effect on the calculated evaporative resistance values, something that was supported by the results from the sensitivity analysis. As the impermeability of the clothing set has a significant impact on the PHS predictions, there were no differences in exposure time based on water loss criteria and the core temperature limitation was reached fairly quickly (at around 30 min) in all cases.

Results from this study show the need to correct for the pre-wetted skin temperature in the calculations of both methods in order for them to be physically correct. Other corrections should not be needed as they do not improve the results further although creating a larger clothing database would be advisable. However, the correction for the pre-wetted skin temperature can be omitted when impermeable and high insulated clothing is used. These results are in conformity with the conclusions by Wang et al. [33], who stated that the corrections should not be

needed for impermeable or high insulated clothing (>2.5 clo). Although our measurement on the PS set supports this statement, it was previously concluded on the basis of only one measurement [33]. Therefore, we recommend further tests with high insulated and impermeable clothing being carried out for verification. Actually, although it might be interesting to pinpoint the exact cut-off point in the thermal insulation range from which corrections are no longer necessary. The corrections have minimal impact when high insulated and impermeable clothing is used, and therefore they can be used in all cases.

The same clothing ensembles were also used in the study presented on the 12i3m – 12th International Meeting on Thermal Manikins and Modeling, Empa, St. Gallen, Switzerland [46].

Conclusion

Three clothing properties that are important for heat stress modelling – clothing area factor, thermal insulation, and evaporative resistance were measured for two clothing ensembles currently used by workers in sugarcane fields. First, for the thermal insulation measurements, we found that equation (32), a predictive equation from ISO 9920 standard is the most accurate for our ensembles; however, there is considerable confusion when determining the most suitable equation from this and other standards when protective clothing is used. Although, there was no significant difference in the resulting PHS predictions when using different equations for calculating the input thermal insulation, an advanced physiological model should be used to verify these results as differences in absolute values were significant in some cases. A new versatile equation for predicting resultant thermal insulation for various kinds of protective clothing should be developed in the future to avoid confusion when choosing from multiple equations. Second, both the mass loss and the heat loss methods for calculating evaporative resistance were used and some proposed corrections for the heat loss method were included. Even when there is no significant difference between the values calculated by the heat loss method and the mass loss method using the manikin's surface temperature, these calculations should not be used because they cannot accurately represent realistic physical conditions. The correction for the pre-wetted skin temperature should be used instead, especially in cases where there are no impermeable layers and low insulated clothing is being considered. Results of the PHS sensitivity analyses showed that using the manikin's surface temperature with such clothing can cause inaccurate predictions and is potentially dangerous when used in real-life situations. Usage of other corrections depends largely on the type of clothing being measured, and more investigation involving a more extensive set of data is needed.

Authors' note

Kalev Kuklane is now affiliated with Institute for Safety (IKV), Zoetermeer, Netherlands.

Declaration of conflicting interests

The author(s) declared no potential conflicts of interest with respect to the research, authorship, and/or publication of this article.

Funding

The author(s) disclosed receipt of the following financial support for the research, authorship, and/or publication of this article: This research was supported by two projects (RV9080000301, FSI-S-17_4444) at the Brno University of Technology, Czech Republic.

ORCID iD

Róbert Toma https://orcid.org/0000-0003-1521-0142

References

[1] Parsons K. *Human thermal environments: the effects of hot, moderate, and cold environments on human health, comfort, and performance*. Boca Raton, FL, USA: CRC Press, Inc., 2014.
[2] ISO 15265. *Ergonomics of the thermal environment – risk assessment strategy for the prevention of stress or discomfort in thermal working conditions*. Geneva, Switzerland: Author, 2014.
[3] Malchaire J, Kampmann B, Mehnert P, et al. Assessment of the risk of heat disorders encountered during work in hot conditions. *Int Arch Occup Environ Health* 2002; 75: 153–162.
[4] Holmer I. Protective clothing in hot environments. *Ind Health* 2006; 44: 404–413.
[5] Holmer I. Protective clothing and heat-stress. *Ergonomics* 1995; 38: 166–182.
[6] Wesseling C, Aragón A, González M, et al. Kidney function in sugarcane cutters in Nicaragua – a longitudinal study of workers at risk of mesoamerican nephropathy. *Environ Res* 2016; 147: 125–132.
[7] Roncal-Jimenez C, García-Trabanino R, Barregard L, et al. Heat stress nephropathy from exercise-induced uric acid crystalluria: a perspective on Mesoamerican nephropathy. *Am J Kidney Dis* 2016; 67: 20–30.
[8] Flouris AD, Dinas PC, Ioannou LG, et al. Workers' health and productivity under occupational heat strain: a systematic review and meta-analysis. *Lancet Planet Heal* 2018; 2: e521–e531.
[9] Malchaire J, Piette A, Kampmann B, et al. Development and validation of the predicted heat strain model. *Ann Occup Hyg* 2001; 45: 123–135.
[10] Fiala D, Lomas KJ and Stohrer M. A computer model of human thermoregulation for a wide range of environmental conditions: the passive system. *J Appl Physiol* 1999; 87: 1957–1972.
[11] Pokorný J, Fišer J, Fojtlín M, et al. Verification of Fiala-Based human thermophysiological model and its application to protective clothing under high metabolic rates. *Build. Environ* 2017; 126: 13–26.
[12] Fojtlín M, Psikuta A, Fišer J, et al. Local clothing properties for thermo-physiological modelling: comparison of methods and body positions. *Build Environ* 2019; 155: 376–388.

[13] Veselá S, Psikuta A and Frijns AJH. Local clothing thermal properties of typical office ensembles under realistic static and dynamic conditions. *Int J Biometeorol* 2018; 62: 2215–2229.
[14] Veselá S, Kingma BRM and Frijns AJH. Local thermal sensation modeling – a review on the necessity and availability of local clothing properties and local metabolic heat production. *Indoor Air* 2017; 27: 261–272.
[15] Vitousek PM. Beyond global warming – ecology and global change. *Ecology* 1994; 75: 1861–1876.
[16] McMichael AJ, Woodruff RE and Hales S. Climate change and human health: present and future risks. *Lancet* 2006; 367: 859–869.
[17] Psikuta A, Allegrini J, Koelblen B, et al. Thermal manikins controlled by human thermoregulation models for energy efficiency and thermal comfort research – a review. *Renew Sustain Energy Rev* 2017; 78: 1315–1330.
[18] Holmer I. Thermal manikin history and applications. *Eur J Appl Physiol* 2004; 92: 614–618.
[19] McCullough EA. The use of thermal manikins to evaluate clothing and environmental factors. *Elsevier Ergonom Book Ser* 2005; 3: 403–407.
[20] McCullough EA and Kenney WL. Thermal insulation and evaporative resistance of football uniforms. *Med Sci Sports Exerc* 2003; 35: 832–837.
[21] ISO 9920. *Ergonomics of the thermal environment – estimation of thermal insulation and water vapour resistance of a clothing ensemble*. Geneva, Switzerland: Author, 2007.
[22] EN 342. *Protective clothing – ensembles and garments for protection against cold*. Brussels, Belgium: Author, 2004.
[23] ASTM F2370 – 10. *Standard test method for measuring the evaporative resistance of clothing using a sweating manikin*. West Conshohocken, PA: Author, 2010.
[24] ASTM F2370-16. *Standard test method for measuring the evaporative resistance of clothing using a sweating manikin*. West Conshohocken, PA: Author, 2016.
[25] Richards MGM and McCullough EA. Revised interlaboratory study of sweating thermal manikins including results from the sweating agile thermal manikin. *Journal of ASTM International* 2005; 2(4): 27–39.
[26] Wang FM, Lai DD, Shi W, et al. Effects of fabric thickness and material on apparent 'wet' conductive thermal resistance of knitted fabric 'skin' on sweating manikins. *J Therm Biol* 2017; 70: 69–76.
[27] Xiaohong Z, Chunqin Z, Yingming Q, et al. The thermal insulation difference of clothing ensembles on the dry and perspiration manikins. *Meas Sci Technol* 2010; 21: 85203.
[28] Chen YS, Fan JT and Zhang W. Clothing thermal insulation during sweating. *Text Res J* 2003; 73: 152–157.
[29] Wang FM, Kuklane K, Gao CS, et al. Effect of temperature difference between manikin and wet fabric skin surfaces on clothing evaporative resistance: how much error is there? *Int J Biometeorol* 2012; 56: 177–182.
[30] Wang FM, Gao CS, Kuklane K, et al. A study on evaporative resistances of two skins designed for thermal manikin tore under different environmental conditions. *Text Bioeng Inform Symp Proc* 2009; 1: 211–215.
[31] Wang FM, Kuklane K, Gao C, et al. Development and validity of a universal empirical equation to predict skin surface temperature on thermal manikins. *J Therm Biol* 2010; 35: 197–203.
[32] Wang FM, Shi W, Lu YH, et al. Effects of moisture content and clothing fit on clothing apparent 'wet' thermal insulation: a thermal manikin study. *Text Res J* 2016; 86: 57–63.

[33] Wang FM, Zhang CJ and Lu YH. Correction of the heat loss method for calculating clothing real evaporative resistance. *J Therm Biol* 2015; 52: 45–51.
[34] Ueno S and Sawada S. Correction of the evaporative resistance of clothing by the temperature of skin fabric on a sweating and walking thermal manikin. *Text Res J* 2012; 82: 1143–1156.
[35] Koelblen B, Psikuta A, Bogdan A, et al. Comparison of fabric skins for the simulation of sweating on thermal manikins. *Int J Biometeorol* 2017; 61: 1519–1529.
[36] Havenith G, den Hartog E and Martini S. Heat stress in chemical protective clothing: porosity and vapour resistance. *Ergonomics* 2011; 54: 497–507.
[37] Bernard T, Ashley C, Trentacosta J, et al. Critical heat stress evaluation of clothing ensembles with different levels of porosity. *Ergonomics* 2010; 53: 1048–1058.
[38] Kuklane K, Heidmets S and Johansson T. *Improving thermal comfort in an orthopaedic aid: better Boston brace for scoliosis patients*. Hong Kong SAR: The Hong Kong Polytechnic University, 2006, pp. 343–351.
[39] Psikuta A, Frackiewicz-Kaczmarek J, Mert E, et al. Validation of a novel 3D scanning method for determination of the air gap in clothing. *Meas J Int Meas Confed* 2015; 67: 61–70.
[40] Havenith G, Kuklane K, Fan J, et al. A database of static clothing thermal insulation and vapor permeability values of Non-Western ensembles for use in ASHRAE standard 55, ISO 7730 and ISO 9920. *ASHRAE Trans* 2015; 121: 197–215.
[41] Wang FM, Ji EL, Zhou XH, et al. Empirical equations for intrinsic and effective evaporative resistance of multi-layer clothing ensembles. *Ind Text* 2010; 61: 176–180.
[42] Havenith G, Richards MG, Wang XX, et al. Apparent latent heat of evaporation from clothing: attenuation and 'heat pipe' effects. *J Appl Physiol* 2008; 104: 142–149.
[43] Wang FM. Measurements of clothing evaporative resistance using a sweating thermal manikin: an overview. *Ind Health* 2017; 55: 473–484.
[44] Pokorny J, Fiser J, Fojtlin M, et al. Verification of Fiala-Based human thermophysiological model and its application to protective clothing under high metabolic rates. *Build Environ* 2017; 126: 13–26.
[45] Havenith G, Fiala D, Blazejczyk K, et al. The UTCI-Clothing model. *Int J Biometeorol* 2012; 56: 461–470.
[46] Kuklane K. Regional and total insulation and evaporative resistance values of clothing for sugarcane harvesters and chemical sprayers in Latin America. In: *12th international meeting on thermal manikins and modeling*, Empa, St. Gallen, Switzerland, 29–31 August 2018.

International Journal of Environmental Research and Public Health

MDPI

Article

Insulation and Evaporative Resistance of Clothing for Sugarcane Harvesters and Chemical Sprayers, and their Application in PHS Model-Based Exposure Predictions

Kalev Kuklane [1,2,*], Róbert Toma [3] and Rebekah A.I. Lucas [4,5]

[1] Thermal Environment Laboratory, Division of Ergonomics and Aerosol Technology, Department of Design Sciences, Lund University, Box 118, SE-22100 Lund, Sweden
[2] Institute for Safety (IFV), P.O. Box 7112, 2701 AC Zoetermeer, The Netherlands
[3] Energy Institute, Brno University of Technology, 601 90 Brno, Czech Republic; 145743@vutbr.cz
[4] School of Sport, Exercise and Rehabilitation Sciences, University of Birmingham, Birmingham B15 2TT, UK; R.A.I.Lucas@bham.ac.uk
[5] La Isla Network, Washington, P.O. Box 816, MI 49301, District of Columbia, USA
* Correspondence: kalev.kuklane@ifv.nl; Tel.: +31-640-640-125

Received: 29 February 2020; Accepted: 25 April 2020; Published: 28 April 2020

Abstract: Many workers are exposed to heat stress that can be exacerbated by the type of clothing they wear. The resulted heat strain can lead to short or long-term heat-related disorders. This study aimed to measure clothing properties of sugarcane field workers and evaluate the heat strain by an international standard, predicted heat strain model (PHS). The clothing thermal insulation and evaporative resistance values of sugarcane cutter and chemical sprayer outfits were acquired for the whole body, body regions and specific body parts via thermal manikin measurements. The detailed clothing insulation values of body parts can be utilized in advanced thermo-physiological models, while in this study, the values for the whole body together with weather data were used in PHS. Estimated duration limited exposure times (DLE) for an hour-by-hour prediction over a workday and for a range of high humidity scenarios were calculated. Such evaluation tools can be used for risk assessment and management to support organizational measures and prepare equipment and materials in the case of hot weather events in order to avoid dehydration and other heat-related disorders.

Keywords: heat stress; dehydration; protective clothing; sugarcane field workers; prevention; clothing insulation; evaporative resistance; predicted heat strain; exposure evaluation; human thermal modeling

1. Introduction

Agricultural jobs are very much dictated by season and climate. This type of work needs to be done at specific times of the year and often these jobs are connected with warm or warm and wet seasons. Jobs related to sugarcane production are no exception. Sugarcane production in some parts of the world still requires heavy manual labor in a hot environment. Repeated heat exposure together with insufficient water replacement has been related to chronic kidney disease of unknown etiology (CKDu) [1,2]. CKDu is associated with a high mortality rate and has reached epidemic levels in several tropical countries, including Latin America, e.g., Nicaragua, El Salvador, etc. According to Moran and Gaffin [3] with reference to Knochel [4] and Knochel and Reed [5], heatstroke results in a 25% higher risk of kidney failure. If heatstroke does indeed increase the risk of kidney failure, then

long-term exposure that is close to heat tolerance limits may do so as well. Industrial sugarcane workers perform difficult, strenuous work under hot environmental conditions. All measures to reduce heat stress and improve the situation for these agricultural workers are needed. It is possible that clothing and protective gear further exacerbate worker's heat exposure, as clothing has a strong thermal impact on humans. The insulation and evaporative resistance can have opposing effects on thermal balance: the insulation effect can limit the radiant heat load, while the evaporative resistance impairs sweat evaporation and thereby promotes heat storage. Additionally, body motion creating a pumping effect in clothing at approximately similar workloads may allow lower thermal stress than in more static tasks due to enhanced evaporation. In connection to the changing climate, the human thermo-physiological and clothing models would allow making long-term impact predictions on humans based on climate change models. In order to reduce protective clothing-induced stress, we need to know the thermal performance of the available clothing items and other protective gear. The objectives of this study were to:

a) measure the insulation and evaporative resistance of the clothing used in the agricultural sector for the sugar industry for two tasks—sugarcane harvesting and chemical spraying and-
b) utilize the outcome in a predicted heat strain model (PHS) according to an international standard [6] for allowed exposure time prediction and recommendations.

2. Materials and Methods

In order to meet the objectives, the study was split into two sections. The first part dealt with measurements of clothing insulation and evaporative resistance. The second part utilized the acquired clothing properties and available information on the working conditions to predict the heat stress in selected conditions that may allow for preventive-measures planning.

2.1. Measurements of Clothing Properties

The thermal manikin Tore at Lund University, Sweden [7,8] was used for testing. Tested clothing ensembles were acquired from Ingenio San Antonio, the largest sugar mill in Nicaragua, and are currently worn by field workers (Figure 1). The sugarcane cutter (SC) outfit consisted of boxer shorts, socks, jeans, synthetic long-armed shirt, cap with textile for neck protection, protective boots, eye protection of metal mesh, glove on one hand and leg protection made of metal grid on one leg, with a total weight of 2.8 kg. The chemical (pesticide) sprayer (CP) outfit consisted of boxer shorts, socks, partially impermeable coveralls, impermeable apron covering front and back, protective gloves, cap, respirator and protective boots, with a total weight of 4.1 kg.

(**a**) (**b**) (**c**) (**d**)

Figure 1. Tested clothing: (**a**) underwear for both systems (provided by the laboratory), (**b**) sugarcane harvester's outfit (glove only on one hand and leg protector on one leg), (**c**) chemical sprayer's protective coveralls on top of underwear and (**d**) chemical sprayer's complete outfit with outer protective layers.

2.1.1. Clothing Insulation

The clothing insulation was measured following the methods described in standards ISO 15831 [9] and ISO 9920 [10] with some modifications. The tests were carried out at 20.0 ± 0.1 °C with 0.21 ± 0.08 m/s air velocity in static (I_T) and dynamic ($I_{T,r}$, walking 90 steps/min, corresponding to the speed of about 3.5 km/h) conditions. Clothing basic insulation (I_{cl}) for PHS predictions was calculated according to the standards, considering air layer insulation (I_a) and clothing area factor (f_{cl}). The latter was acquired from a photographic method taking pictures of the garment ensembles and the nude manikin from front and from the side [11]. For basic information for evaporative resistance calculations, the insulation of the textile, simulated sweaty skin was also measured but only in static conditions. Air layer insulation around the human body shape was measured with a nude manikin. Insulation was measured with hair (wig) on the manikin's head.

2.1.2. Evaporative Resistance

Total evaporative resistance (R_{et}) of the clothing sets and the wet textile skin was measured following ASTM F2370-15 [12] at so-called isothermal conditions with the manikin surface and air temperature being set to 34 °C and utilizing the heat-loss method for evaporative resistance calculations. Evaporative resistances were measured without using a wig on the manikin's head, and the air velocity was kept at 0.54 ± 0.09 m/s in order to avoid build-up of water vapor pressure in the air near the manikin surface that could affect the evaporation. The evaporative resistance values were corrected for differences in the manikin surface and textile skin based on heat loss according to Wang et al. [13].

2.1.3. Data Presentation

Each condition was tested twice. In order to utilize the insulation and evaporative resistance values in advanced thermal models, insulation or evaporative resistance of individual body areas are needed, as thermoregulatory responses (i.e., blood flow and sweating) are heterogeneous across the body and not uniformed. Therefore, an average value for a clothing set does not allow proper evaluation of localized discomfort, though simple and low-cost models, including the PHS, utilize an average whole-body value for a complete clothing set. Therefore, the results are presented as average values for individual zones, regional areas and an average whole-body value.

The insulation results are sorted by the percentage differences of air layer insulation in static as compared to dynamic conditions. The evaporative resistance results are sorted by the magnitude of difference between measured and corrected wet textile skin total evaporative resistance values.

2.2. Exposure Evaluation according to Predicted Heat Strain Model (PHS)

In spite of criticism on the PHS model [14–16], we considered that the PHS model is easily available for everybody, has a low cost and has been validated in a wide range of hot conditions. If to consider the limitations related to heavily insulating clothing [16] and repeated exposures [14,15], it still gives a reasonably good prediction, that is very useful for planning a workday in advance and preparing preventive measures against heat stress. Thus, a web tool based on PHS algorithms [6] at http://www.eat.lth.se/fileadmin/eat/Termisk_miljoe/PHS/PHS.html was utilized for the exposure evaluations. The programmer had access to ISO/FDIS 7933: 2004; however, it was verified that the DIS version and final standard [6] were the same. Exposure characteristics were calculated as the limit values based on the core temperature and water loss based on an hour-by-hour approach for one hot day weather conditions (Ta = 18.6–36.4 °C, T_g = 20.5–52.1 °C; see Figure 2) for several activity level combinations. Predictions were made for each hour conditions and did not reflect the physiological status of the previous hour. Thus, the predictions for the morning period may overestimate the duration limited exposure (DLE), while afternoon periods may underestimate it.

Additionally, a range of temperature conditions (Ta = 28–36 °C) was selected as a fictive pedagogical example where each selected workload, in combination with the tested clothing, would show some DLE for the core temperature. Thus, in this simulation, the selected temperatures were combined with the same high constant relative humidity (70%). The whole range of set conditions would not be relevant for specific agricultural activities. Instead, some of these may be relevant for specific process industries; for example, the paper industry, where some urgent tasks have to be carried out at high temperatures and humidity, or the glass industry, where similar clothing (except for specific leg and hand protections) may be used. The selected conditions with high temperatures and humidity may also resemble the conditions in restaurant kitchens and laundries in warm countries [17].

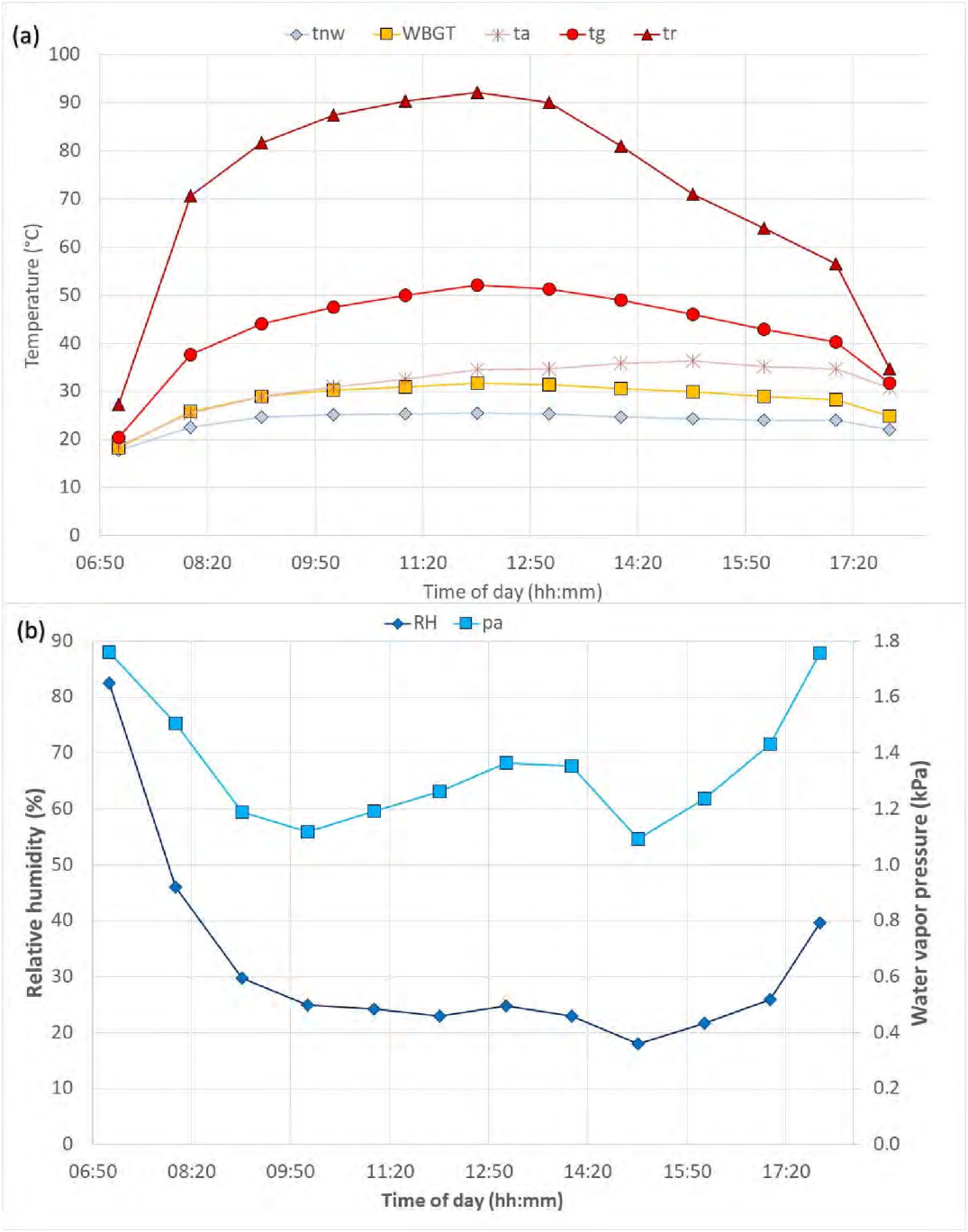

Figure 2. Environmental parameters for one day (14 January 2015) in a sugarcane field in Nicaragua. (**a**) Temperatures (°C): t_{nw}—natural wet bulb temperature, WBGT—wet bulb globe temperature index; t_a—air temperature, t_g—temperature of a globe thermometer and t_r—mean radiant temperature; (**b**) humidity: RH—relative humidity (%) and p_a—absolute humidity expressed as water vapor pressure in the air (kPa). Average wind speed over the day was relatively stable around 2 m/s.

From manikin tests, the clothing properties (basic insulation and evaporative resistance; for methods, see section 2.1) for both sets were were close to the limits of PHS requirements ($I_{cl,SC}$ = 0.107 m² K/W, $I_{cl,CP}$ = 0.177 m² K/W; $R_{ed,SC}$ = 13.2 m² Pa/W, $R_{ed,CP}$ = 74 m² Pa/W). Clothing properties and hourly sugarcane field weather data were used in the PHS tool to evaluate the heat stress in the present

conditions for one day (Figure 2). For the high humidity scenario, the wind speed (v_a) was kept 2 m/s as measured in the field today, while relative humidity (RH) was set to 70%, allowing water vapor pressure in the air (p_a) to change depending on air temperature. Additionally, the mean radiant temperature (t_r) 70 °C and alt. globe temperature (t_g) 44 °C were kept constant for this scenario. Estimated activity levels (200–300 W for CP and 250–350 W for SC) and other required parameters were also entered into the PHS model. Activity levels were based on heart rate measures taken from sugarcane workers in the field and estimated according to ISO 8996 [18], as well as from previous measurements and estimations in the field [17]. The workers were assumed to be acclimated, and drink was freely available. For predictions, some anthropometric parameters were taken as estimated averages. It was also assumed that workers were frequently in a standing posture with an average walking velocity (v_w) of 0.5 m/s. Table 1 lists most of the input parameters; however, some parameters are not listed, as they are mentioned in the text above or did change depending on other input data; for example, water vapor pressure in the air was calculated by air humidity and air temperature.

Table 1. Input to predicted heat strain model (PHS) for the high humidity (RH = 70%) scenario.

Parameter	SC	CP
Acclimatization	1	1
Drink freely available	1	1
Body height	1.75	1.75
Body mass	70	70
Body surface area (calculated from mass and height, m^2)	1.84	1.84
Posture: (1 = sitting, 2 = standing, 3 = crouching)	2	2
Air temperature	34 (28–36)	34 (28–36)
Air velocity	2.0	2.0
Metabolic energy production	250, 300, 350	200, 250, 300
Clothing basic insulation (1 clo = 0.155 m^2 K/W)	0.69	1.14
Static moisture permeability index (calculated from insulation and evaporative resistance)	0.55	0.19
Fraction covered by reflective clothing	0	0
Angle between wind and walking direction	not used	not used
Walking speed	0.5	0.5
Mechanical power	0	0

Note: SC—sugarcane cutter and CP—chemical sprayer outfits, respectively.

3. Results

3.1. Manikin Tests

Clothing area factors from the photographic method for SC and CP were 1.26 and 1.41, respectively. Clothing total and total resultant insulation for different body parts, body regions and for the whole ensembles (marked as "total") values for the air layer, sweating skin and tested ensembles are given in Table 2. Clothing total evaporative resistance for body parts, body regions and for the whole ensembles are given in Table 3.

Table 2. Total and total resultant insulation of the whole body, body regions and individual zones (m^2 K/W) with percentual differences between static (I_T) and dynamic (I_{Tr}) values.

	Air Layer			Textile skin	Sugarcane Cutters				Chemical Sprayers			
Body Parts	I_T (=I_a)	I_{Tr} (=I_{ar})	**Diff (%)**	I_T	I_T	I_{Tr}	I_{Tr}/I_T	**Diff (%)**	I_T	I_{Tr}	I_{Tr}/I_T	**Diff (%)**
L.Hand	0.108	0.055	−48.7	0.135	0.180	0.114	0.63	−36.5	0.181	0.123	0.68	−32.1
Hands	0.100	0.053	−47.5	0.132	0.137	0.077	0.56	−44.0	0.172	0.115	0.67	−33.3
R.Hand	0.093	0.050	−46.5	0.129	0.109	0.057	0.52	−47.9	0.165	0.108	0.65	−34.8
Feet	0.103	0.057	−44.7	0.122	0.181	0.144	0.80	−20.0	0.208	0.149	0.72	−28.1
Lower Arms	0.101	0.056	−44.2	0.142	0.172	0.105	0.61	−39.3	0.259	0.165	0.64	−36.1
L.Lower leg	0.082	0.051	−38.3	0.111	0.168	0.128	0.76	−24.0	0.269	0.205	0.76	−23.8
Arms	0.104	0.069	−33.4	0.147	0.194	0.115	0.59	−40.5	0.258	0.160	0.62	−38.1
Upper arms	0.105	0.078	−25.8	0.149	0.209	0.122	0.59	−41.4	0.259	0.158	0.61	−39.3
Lower legs	0.082	0.063	−23.2	0.116	0.181	0.147	0.81	−18.9	0.255	0.212	0.83	−16.9
Total	*0.098*	*0.076*	*−22.0*	*0.131*	*0.191*	*0.143*	*0.75*	*−25.3*	*0.257*	*0.188*	*0.73*	*−26.8*
Legs	0.089	0.071	−19.8	0.118	0.206	0.154	0.74	−25.6	0.287	0.205	0.71	−28.6
Head, hands & feet excluded	0.093	0.076	−18.4	0.131	0.195	0.146	0.75	−25.3	0.278	0.200	0.72	−28.3
Belly	0.093	0.078	−16.2	0.121	0.331	0.261	0.79	−21.1	0.457	0.322	0.70	−29.6
Thighs	0.095	0.080	−15.2	0.121	0.229	0.160	0.70	−29.9	0.316	0.202	0.64	−35.9
R.Lower leg	0.082	0.075	−8.1	0.121	0.194	0.166	0.86	−14.4	0.241	0.219	0.91	−9.2
Buttocks	0.070	0.064	−7.9	0.107	0.253	0.220	0.87	−13.1	0.396	0.281	0.71	−29.1
Torso	0.092	0.086	−6.3	0.135	0.187	0.163	0.87	−12.8	0.283	0.226	0.80	−20.2
Back	0.093	0.090	−4.0	0.146	0.158	0.141	0.89	−11.3	0.228	0.190	0.83	−16.7
Chest	0.105	0.104	−0.6	0.152	0.160	0.141	0.88	−11.8	0.262	0.216	0.82	−17.7
Head	0.174	0.184	5.9	0.144	0.208	0.208	1.00	0.1	0.198	0.193	0.98	−2.2

Note: L—left, R.—right.

Table 3. Corrected total evaporative resistance of the whole body, body regions and individual zones (m^2 Pa/W).

Body Parts	Textile Skin	Sugarcane Cutters	Chemical Sprayers
R.Hand	4.6	6.0	446.6
Hands	5.8	9.2	305.3
L.Lower leg	7.8	32.6	132.4
Legs	7.8	28.1	65.7
Thighs	7.4	27.7	56.7
L.Hand	7.7	16.1	245.8
Lower Arms	8.1	14.7	87.0
Belly	6.9	43.7	585.3
Lower legs	9.1	29.4	99.5
Total	*8.2*	*20.9*	*81.0*
Head, hands & feet excluded	8.3	21.2	92.2
Hands & feet excluded	8.4	20.6	73.7
Hands excluded	8.4	22.2	78.1
Feet	7.4	65.6	188.8
Arms	8.7	18.4	73.9
R.Lower leg	10.3	26.3	66.5
Torso	8.7	18.2	180.9
Back	9.0	13.8	165.1
Upper arms	9.1	21.2	70.4
Buttocks	9.2	32.3	98.6
Chest	9.2	14.6	203.1
Head	9.9	16.0	20.4

Note: L.—left, R.—right.

3.2. Evaluation of Heat Strain with PHS

Figures 3 and 4 show the duration limited exposure (DLE) based on core temperature and water loss criteria, respectively, during one day hour-by-hour in sugarcane cutter and chemical sprayer outfits. Although, outdoor work has a changing environment and PHS cannot really accommodate that, still the example here, reflected in Figures 3 and 4, is an attempt to show a possibility to manage that shortcoming with hour-by-hour calculations based on the environmental data given in Figure 2.

Figure 5 shows the DLE based on the core temperature depending on the air temperature (air humidity was always set to 70% independent of the temperature) and workload for SC and CP, respectively. Figure 6 shows the DLE based on water loss for SC. For CP, the core temperature was always the major limiting parameter, and the water loss limit stayed commonly the same for almost all conditions around 250 min. Here, it has to be pointed out that, for a practical application, the lowest DLE value has to be selected as an allowed work limit.

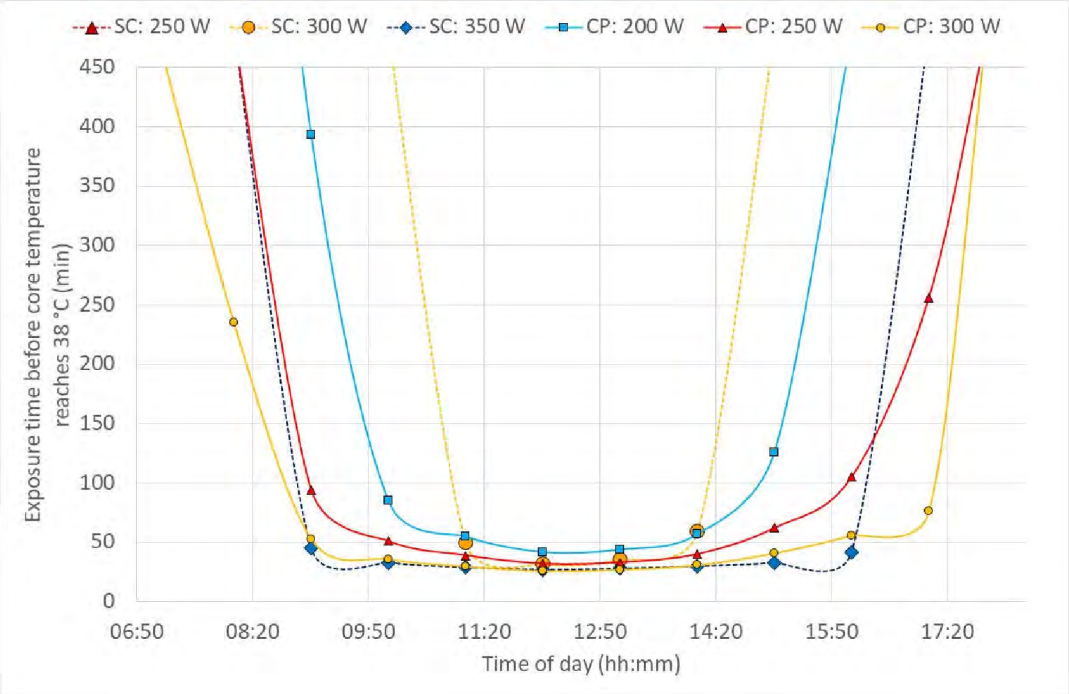

Figure 3. Expected daily duration limited exposure (DLE) for sugarcane cutters (SC) and chemical sprayers (CP) at various activity levels based on core temperature (criterion $T_{rec} < 38$ °C). At the lowest activity for sugarcane cutters (SC: 250 W), DLE was above 8 h (480 min), and therefore, the line cannot be seen in this diagram.

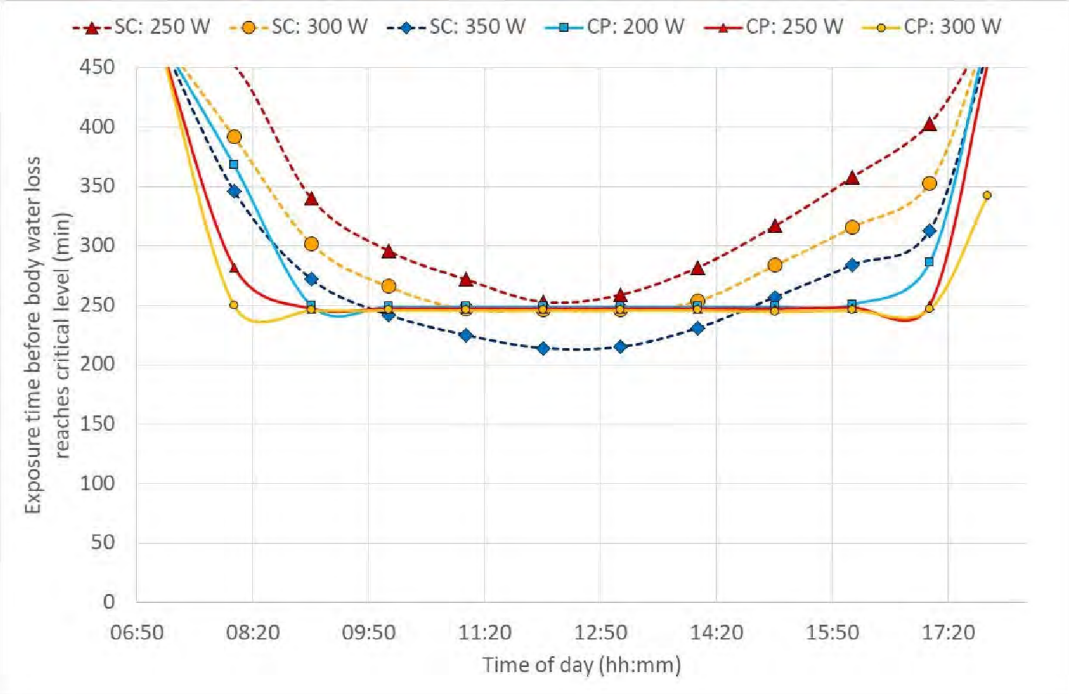

Figure 4. Expected daily duration limited exposure for sugarcane cutters (SC) and chemical sprayers (CP) at various activity levels based on water loss (criterion $D_{wl,lim} < 5\%$).

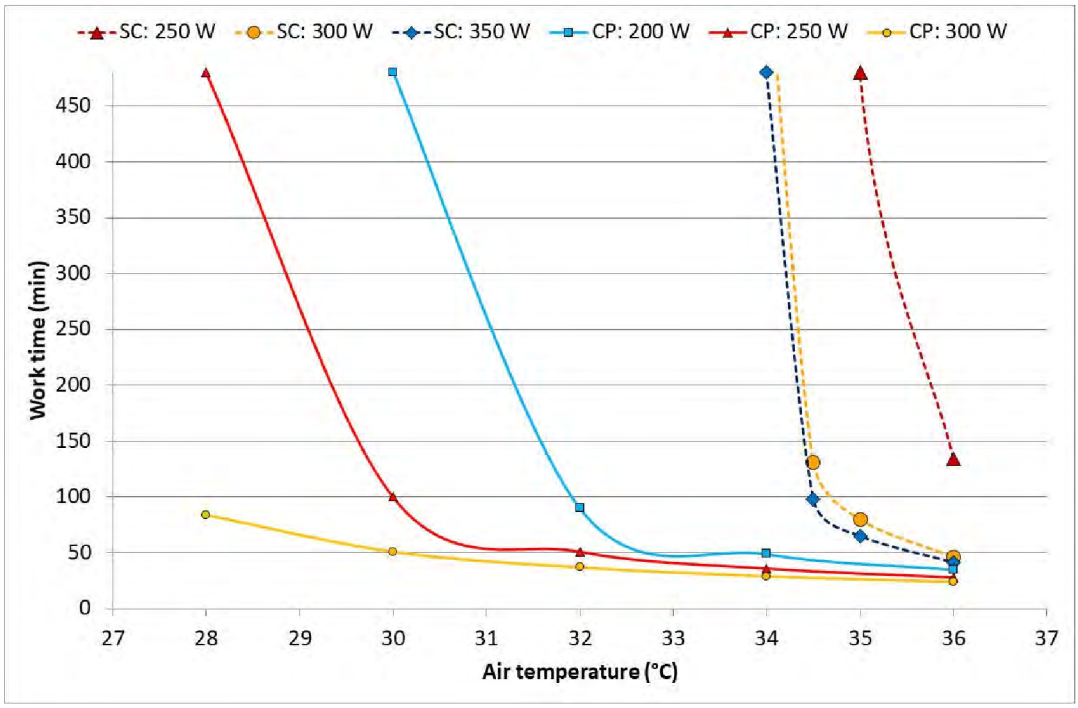

Figure 5. Expected duration limited exposure for sugarcane cutters (SC) and chemical sprayers (CP) at various activity levels based on core temperature (criterion $T_{rec} > 38$ °C) in a fictive high humidity scenario.

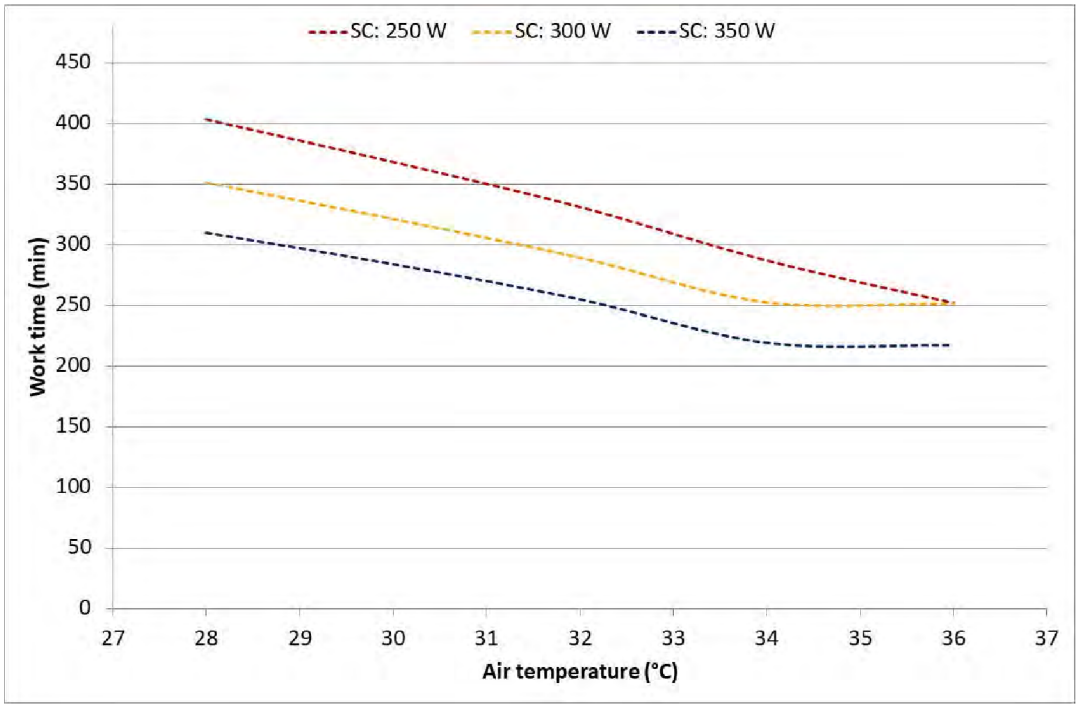

Figure 6. Expected duration limited exposure for sugarcane cutters at various activity levels based on water loss (criterion $D_{wl,lim} < 5\%$) in a fictive high humidity scenario.

4. Discussion

4.1. Manikin Tests

Total and total resultant clothing insulation for the air layer (AL), sugarcane cutters (SC) and chemical sprayers (CP) were 0.098 and 0.076, 0.191 and 0.143 and 0.257 and 0.188 m^2 K/W, respectively. This means a reduction in total insulation due to defined body motion by 22.0%, 25.3% and 26.8%, respectively. Considering the I_{Tr} to I_T ratio (I_{Tr}/I_T) of the complete garment ensembles (SC and CP), and the values drawn in ISO 9920 (Equation 32 and Figure 4 of [10]), then these values were comparable and stayed somewhat above 0.7.

However, insulation in different body parts could change from +6% (Head in AL) to −49% (Left Hand in AL). In SC and CP, the changes were from 0% (Head) to −48% (Right Hand) and from −2% (Head) to −39% (Upper arms), respectively. The results, especially from AL, show clearly the effect of body parts' swinging radius or being rigidly fixed in the walking manikin tests. The biggest change is for hands and feet followed by arms and legs, then torso zones and, finally, the head. Variation with clothing is modified by body area coverage, e.g., asymmetrical protection of hand and lower leg in SC (Figure 1b), and air permeability of the layers in CP (Figure 1c,d). Part of the difference could be also related to a variation in local air velocity at specific zones. Total thermal insulation of the textile skin (TS; complete coverage of the body, including hands feet and head) was 0.131 m^2 K/W.

For technical measurements and various model evaluations, we need to consider what differences between the zones or changes do not match the reality. This may be built in the established correction equations, e.g., for walking. We may need to consider applying wind during testing in order to compensate for that. For example, walking at 3.5 km/h with a manikin may require 1 m/s wind to simulate the realistic influence of the motion. The same question may be raised to some extent for validation of the manikin results by humans walking on a treadmill.

The corrected total evaporative resistance of TS, SC and CP was 8.2, 20.9 and 81.0 m^2 Pa/W (SC and CP include the skin and air layer resistance). Regional total evaporative resistance of TS shifted from 4.6 (right hand, thinner cotton glove was used) to 10.3 (right lower leg) m^2 Pa/W. As mentioned above, some effect could be related to a variation in local air velocity around specific zones, but in this case, also to thickness of the skin and some overlap of separate layers (gloves at hands and socks on feet for skin simulation). Values for different parts of SC varied from 6.0 (right hand, almost nude, but with slight coverage of the end of the sleeve) to 65.6 (feet with boots) m^2 Pa/W. Variation in CP was from 20.4 (head with some parts uncovered) to above 500 (belly, two tight layers above each other). There has been a discussion among manikin testers on how potential exclusion of the zones not covered by wet textile skin may affect the total evaporative resistance. Here, the total; total excluding the head, hands and feet; total excluding the hands and feet and total excluding the hands were calculated. The difference from the total was, on average, 2.0% (8.3–8.4 m^2 Pa/W), 2.2% (20.6–22.2 m^2 Pa/W) and 0.0% (73.7–92.2 m^2 Pa/W) for TS, SC and CP, respectively, showing the influence of even or uneven evaporative resistance distribution; i.e., depending on tested clothing, the elimination of some body parts may influence increasing or decreasing the total insulation and thus, point to the importance of full-body coverage with wet skin.

In spite of these shortcomings, the current study managed to collect detailed data on real protective clothing used by workers in sugarcane fields. This study utilized only the values for the complete ensemble in a standard occupational heat strain model. However, the reported detailed data could be used in advanced human thermoregulatory models [19]. Additionally, detailed information on different body regions may allow improving the clothing for better ventilation and heat dissipation. This may be difficult in the case of chemical protection, while some new ideas may be generated for specific solutions, for example, using cooling systems in clothing [20–22].

4.2. Evaluation of Heat Strain with PHS

According to the model predictions, the heat exposure in chemical protective clothing was strongly limited by the increasing core temperature (Figure 3) and would be so under any (worse-case) high humidity scenario (Figure 5), too. Simultaneously, cane cutters' core temperatures reached

above 38 °C only at the highest activities and hottest periods of the hot day (Figure 3). In these cases, the continuous exposure should not exceed 50 min, and regular rest and drinking breaks are needed. The outcome clearly supports a known recommendation to have a long recovery/lunch breaks (>2 h) in well-ventilated areas in the shade and sufficient fluid replacements during the hottest period of the day. For the scenarios with high air humidity but lower solar loads, air temperatures above 34 °C may become a problem (Figure 5). In most of the evaluated conditions, dehydration can be a stronger limitation (Figures 4 and 6): core temperature rises may trigger rest breaks, and during breaks, people drink. Alternatively, as the thirst sensation is not as strong a factor as core temperature rise, dehydration is harder to notice subconsciously [23]. The results from the current study strongly recommended that, depending on the weather conditions, more or less frequent drinking rest breaks should be enforced by the organization. As the PHS model calculates water loss, then advice for quantities and the frequency of drinking may be estimated. The PHS data also provides estimations of exposure time and rest break frequency based on core temperature calculations. This enables the evaluation of work situations, risk assessments and of the work/rest schedules. Lundgren et al. [15] has pointed out that the predictions for females have larger discrepancies from actual measurements; thus, the larger safety margins have to be applied for females and possibly for other specific population groups. Still, knowing the weather forecast or climate change predictions in addition to knowledge on clothing properties and workloads allows organizations to prepare for harsh conditions in advance and organize work practices that reduce negative health impacts with minimal losses in productivity. It is also important that risk assessments of work tasks are conducted regularly and in good time before any casualties occur, for example, according to the SOBANE strategy [24,25].

5. Conclusions

This study measured the properties of clothing used in sugarcane fields and utilized them in a standard tool for heat strain prediction. In spite of criticism on the PHS model, it allows a rough estimation of heat strain in the working population, as well as the preparation of countermeasures under hot conditions. This study also showed that weather data can effectively be utilized as input into the prediction models, and such automated inputs into a webtool or app can make a complex model into an easy-to-handle tool for practitioners, e.g., ClimApp [26]. The detailed clothing insulation and evaporative resistance values collected in the current study could be used in more advanced thermo-physiological models and, in combination with local weather data, could be used to support workplace policies and decision-making processes during hot weather or heatwaves. However, it must be considered that any model outcome must be utilized with care, as no model is perfect. Furthermore, the data used in model validations needs to be selected carefully, as test conditions may not always reflect real-world situations.

Author Contributions: K.K. (K. Kuklane) did the major planning of the laboratory study, carried out the PHS analysis and did the major writing of the article. K.K. and R.T. (R. Toma) carried out the manikin testing together. R.T did clothing area factor measurements, a large part of the evaporative resistance-related calculations and analysis and contributed with discussion and commenting on the paper. R.A.I.L. (R.A.I. Lucas) organized the clothing for testing, did any data collecting in the field that was used in the analysis and made inputs on the physiological evaluations of the conditions in discussing and commenting on the paper. All authors have read and agreed to the published version of the manuscript.

Funding: This research was performed within the framework of the ClimApp project. Project ClimApp is part of ERA4CS, an ERA-NET initiated by JPI Climate, and funded by FORMAS (SE), IFD (DK) and NWO (NL), with co-funding by the European Union (Grant 690462).

Acknowledgments: The work was partly carried out as a method evaluation for the ERA4CS project ClimApp—Translating climate service information into personalized adaptation strategies to cope with thermal climate stress (http://www.jpi-climate.eu/nl/25223441-ClimApp.html).

Conflicts of Interest: The authors declare no conflicts of interest.

References

1. Roncal-Jiménez, C.; García-Trabanino, R.; Barregard, L.; Lanaspa, M.A.; Wesseling, C.; Harra, T.; Aragón, A.; Grases, F.; Jarquin, E.R.; González, M.; et al. Heat stress nephropathy from exercise-induced uric acid crystalluria: A perspective on mesoamerican nephropathy. *Am. J. Kidney Dis.* **2016**, *67*, 20–30, doi:10.1053/j.ajkd.2015.08.021
2. Wesseling, C.; Aragón, A.; González, M.; Weiss, I.; Glaser, J.; Bobadilla, N.A.; Roncal-Jiménez, C.; Correa-Rotter, R.; Johnson, R.J.; Barregard, L. Kidney function in sugarcane cutters in Nicaragua—A longitudinal study of workers at risk of Mesoamerican nephropathy. *Environ. Res.* **2016**, *147*, 125–132, doi:10.1016/j.envres.2016.02.002
3. Moran, D.S.; Gaffin, S.L. Clinical Management of Heat-Related Illnesses. Chapter 11. In *Wilderness Medicine*, 5th ed.; Auerbach, P.S., Ed.; Mosby Elsevier: Maryland Heights, MO, USA, 2007; pp. 268–283.
4. Knochel, J.P. Environmental heat illness: An eclectic review. *Arch. Intern. Med.* **1974**, *133*, 841–864
5. Knochel, J.P.; Reed, G. Disorders of heat regulation. In *Clinical Disorders of Fluid and Electrolyte Metabolism*; Kleeman, C.R., Maxwell, M.H., Narin, R.G., Eds.; McGraw-Hill: New York, NY, USA, 1987; pp. 1197–1232
6. ISO 7933:2004. *Ergonomics of the Thermal Environment—Analytical Determination and Interpretation of Heat Stress Using Calculation of the Predicted Heat Strain*; The International Organisation for Standardisation: Geneva, Switzerland, 2004.
7. Hänel, S.E. A joint Nordic project to develop an improved thermal manikin for modeling and measuring human heat exchange. In *Paper Presented at the Medical and Biophysical Aspects on Protective Clothing*; Centre de Recherches du Service de Santk des Armks: Lyon, France, 1983; pp. 280–282.
8. Kuklane, K.; Heidmets, S.; Johansson, T. Improving thermal comfort in an orthopaedic aid: Better Boston Brace for scoliosis patients. In Proceedings of the Paper Presented at the 6th International Meeting on Manikins and Modelling (6I3M), The Hong Kong Polytechnic University, Hong Kong, China, 16–18 October 2006; pp. 343–351.
9. ISO 15831:2004. *Clothing—Physiological Effects—Measurement of Thermal Insulation by Means of a Thermal Manikin*; International Organisation for Standardisation: Geneva, Switzerland, 2004.
10. ISO 9920:2007. *Ergonomics of the Thermal Environment—Estimation of Thermal Insulation and Water Vapour Resistance of a Clothing Ensemble*; International Organisation for Standardisation: Geneva, Switzerland, 2007.
11. Havenith, G.; Kuklane, K.; Fan, J.; Hodder, S.; Ouzzahra, Y.; Lundgren, K.; Au, Y.; Loveday, D. A Database of Static Clothing Thermal Insulation and Vapor Permeability Values of Non-Western Ensembles for Use in ASHRAE Standard 55, ISO 7730, and ISO 9920. *ASHRAE Trans.* **2015**, *121*, 197–215
12. ASTM F2370-15. *Standard Test Method for Measuring the Evaporative Resistance of Clothing Using a Sweating Manikin*; [Standard] American Society of Testing and Materials International (ASTM): Philadelphia, PA, USA, 2015.
13. Wang, F.; Kuklane, K.; Gao, C.; Holmér, I. Development and validity of a universal empirical equation to predict skin surface temperature on thermal manikins. *J. Biol.* **2010**, *35*, 197–203
14. Bröde, P.; Fiala, D.; Lemke, B.; Kjellström, T. Estimated work ability in outdoor warm environments depends on the chosen heat stress assessment metric. *Int. J. Biometerol.* **2017**, doi:10.1007/s00484-017-1346-9.
15. Lundgren-Kownacki, K.; Martínez, N.; Johansson, B.; Psikuta, A.; Annaheim, S.; Kuklane, K. Human responses in heat—Comparison of the Predicted Heat Strain and the Fiala multi-node model for a case of intermittent work. *J. Therm. Biol.* **2017**, *70*, 45–52, doi:10.1016/j.jtherbio.2017.05.006
16. Wang, F.; Gao, C.; Kuklane, K.; Holmér, I. Effects of various protective clothing and thermal environments on heat strain of unacclimated men: The PHS (predicted heat strain) model revisited. *Ind. Health* **2013**, *51*, 266–274
17. Lundgren, K.; Kuklane, K.; Venugopal, V. Occupational heat stress and associated productivity loss estimation using the PHS model (ISO 7933): A case study from workplaces in Chennai, India. *Glob Health Action* **2014**, *7*, doi:10.3402/gha.v7.25283
18. ISO 8996:2004. *Ergonomics of the Thermal Environment—Determination of Metabolic Rate*; International Organisation for Standardisation: Geneva, Switzerland, 2004.
19. Fiala, D.; Havenith, G. Modelling Human Heat Transfer and Temperature Regulation. In *Studies in Mechanobiology, Tissue Engineering and Biomaterials*; Gefen, A., Ed.; Springer: New York, NY, USA, 2015; pp. 1–38

20. Gao, C.; Kuklane, K.; Holmér, I. Cooling vests with phase change materials: The effects of melting temperature on heat strain alleviation in an extremely hot environment. *Eur. J. Appl. Physiol.* **2011**, *111*, 1207–1216
21. Kuklane, K.; Gao, C.; Holmér, I. Ventilation solutions in clothing. In Proceedings of the 10th Joint International Scientific Conference CLOTECH 2012: Innovations in Textile Materials & Protective Clothing, 20–21 September 2012, Warsaw, Poland; pp. 205–212
22. Zhao, M.; Kuklane, K.; Lundgren, K.; Gao, C.; Wang, F. A ventilation cooling shirt worn during office work in a hot climate: Cool or not? *Int. J. Occup. Saf. Ergon.* **2015**, *21*, 457–463, doi:10.1080/10803548.2015.1087730
23. Parsons, K. *Human Thermal Environments*, 3rd ed.; CRC Press, Taylor & Francis Group: Boca Raton, FL, USA, 2014.
24. ISO 15265:2004. *Ergonomics of Thermal Environments—Strategy of Evaluation of the Risk for the Prevention of Constraints or Discomfort under Thermal Working Conditions*; International Organization for Standardization: Geneva, Switzerland, 2004.
25. Malchaire, J.; Kampmann, B.; Mehnert, P.; Gebhardt, H.; Piette, A.; Havenith, G.; Holmér, I.; Parsons, K.; Alfano, G.; Griefahn, B. Assessment of the risk of heat disorders encountered during work in hot conditions. *Int. Arch. Occup. Environ. Health* **2002**, *75*, 153–162, doi:10.1007/s004200100287.
26. Petersson, J.; Kuklane, K.; Gao, C. Is there a need to integrate human thermal models with weather forecasts to predict thermal stress? *Int. J. Environ. Res. Public Health* **2019**, *16*, 4586, doi:10.3390/ijerph16224586.